Comparison Study of Liquid CO2 and Water as a Fracturing Fluid for Improved Gas Production in Tight Reservoirs

A Thesis

In Partial Fulfillment of the Requirements

For the Degree of

Master of Applied Science

in

Petroleum Systems Engineering

University of Regina

by

Birzhan Alimbekov

Regina, Saskatchewan

December, 2018

UNIVERSITY OF REGINA

FACULTY OF GRADUATE STUDIES AND RESEARCH

SUPERVISORY AND EXAMINING COMMITTEE

Birzhan Alimbekov, candidate for the degree of Master of Applied Science in Petroleum Systems Engineering**,** has presented a thesis titled, ***Comparison Study of Liquid CO_2 and Water as a Fracturing Fluid for Improved Gas Production in Tight Reservoirs,*** in an oral examination held on September 5, 2018. The following committee members have found the thesis acceptable in form and content, and that the candidate demonstrated satisfactory knowledge of the subject material.

External Examiner:	Dr. Amr Henni, Industrial Systems Engineering
Supervisor:	Dr. Fanhua Zeng, Petroleum Systems Engineering
Committee Member:	*Dr. Farshid Torabi, Petroleum Systems Engineering
Committee Member:	Dr. Saman Azadbakht, Petroleum Systems Engineering
Chair of Defense:	Dr. Helen Huang, Faculty of Business Administration

*Not present at defense

Abstract

Nowadays, Western Canadian Sedimentary Basin's unconventional tight reservoirs are enjoying technology development like horizontal drilling and hydraulic fracturing. Hydraulic fracturing substantially improves production however it is crucial to understand how fracture growth and production comparison when different fluid systems like water and CO_2 based systems are being used.

In this thesis, based on tight reservoir model in WCSB, firstly we have reviewed how conventional water based hydraulic fracturing damages formation and affects recovery of the fracturing fluid back to surface. Then reservoir simulation software GOHFER coupled with rock geomechanics has been employed to perform dynamic hydraulic fracturing for predicting hydraulic fracture dimensions and simulating fracturing liquid distribution. Models with slickwater, hybrid slickwater and pure CO_2 models were created in order to compare effect of CO_2 on fracture propagation.

Results showed that using liquid CO_2 as a fracturing fluid gave the longest fracture width, but due to low viscosity CO_2 has low proppant carrying capacity. As a result propped fracture length was shorter than slickwater case. Also, different amount of proppant was pumped for pure CO_2 case in order to see how that affects fracture geometry. The higher proppant amount the larger was maximum fracture width and slight increase in average fracture width.

Once accurate GOHFER models were generated, they were imported to create a CMG models in order to predict gas production and compare all three models. Pure CO_2 case gave the best production performance, hybrid the second best and base

slickwater case gave the least amount of gas production. Tight low permeability reservoirs have high capillary pressure and due to that factor water is trapped in pores. Trapped water was very hard to produce and prevented gas to travel towards the fracture which was investigated in this research.

This research delivers new understanding on utilization of liquid CO2 as a fracturing fluid and can be reference for CO2 fracturing in unconventional tight reservoirs.

Acknowledgements

I would like to thank my supervisor Dr. Bill (Fanhua) Zeng for his guidance, patience and support during my master study at the University of Regina. I would also like to thank my respectable committee members: Committee members for reviewing my thesis and giving insightful comments.

I would like to acknowledge the support from the Computer Modeling Group (CMG) and Halliburton.

In addition, I would like to extend the gratitude to my colleagues and all my great friends for making the experience at University of Regina wonderful. Last but not the least, I appreciate the love, encouragement and support from my family and my wife.

Dedication

I dedicate this thesis to my loving wife Aigerim Nurkayeva who loves and supports me.

Table of Contents:

List of Tables

List of Figures

List of Abbreviations, Symbols and Nomenclature

ς_{min}	Fracture minimum horizontal stress
v	Poisson's ratio
ς_{1}	overburden stress
α	Biot's constant
p_p	Pore pressure
ς_{ext}	Tectonic stress
k_f	Proppant pack permeability
w_f	Hydraulic fracture width
k_e	Permeability of pseudoized fracture block in simulation model
w_{block}	Width of pseudoized fracture block in simulation model
WCSB	Western Canadian Sedimentary Basin
LGR	Linear Grid Refinement

CHAPTER 1: Introduction

1.1 Background

1.1.1 Tight Resource in Western Canadian Sedimentary Basin

Canada's main source of oil and natural gas is Western Canadian Sedimentary basin which includes southwest corner of the Northwest Territories, northeastern British Columbia, Alberta, southern Saskatchewan and southwestern Manitoba. (AER, 2015)

WCSB has enormous reserves of oil and gas which includes oil sands, conventional and unconventional resources. According to Alberta Energy Regulator unconventional resources of WCSB are tight oil whereas oil is found in low-permeability rock like sandstone, siltstone, shale and carbonates; tight gas whereas natural gas is found in low-permeability rock like sandstone, siltstone and carbonates; and shale gas whereas natural gas is locked in fine-grained, organic rich rock. Since oil and gas are locked in these tight and low-permeable rocks, it was possible to extract these resources only through combination of horizontal drilling and hydraulic fracturing techniques. Since 2013, 80% of all oil and gas wells drilled in Alberta were horizontal wells and more than 10,000 wells were completed using multi-stage hydraulic fracturing. (AER, 2015)

Figure 1-1. Geological view of theF WCSB (Canadian Society of Western Exploration Geophysicists)

Moreover, according to National Energy Board tight oil production grew from 0 to 350,000 bbl/day for the period of 2005-2013 and tight gas production grew from 3 billion cubic feet to 7 billion cubic feet a day for the period of 2000-2013 which can be noted in Figure 1-2. In 2005, Bakken formation of southeast Saskatchewan and southwest Manitoba was first tight oil play in WCSB and by 2010 it spread to Cardium, Viking, Lower Shaunavon, Montney/Doig, Duvernay/Muskwa, Beaverhill Lake and Lower Amaranth formations. Figure 1-3 shows the locations of those plays in WCSB.

Since 2014, 51% of total Canadian natural gas production accounted for tight and shale gas and it is estimated that by 2035 80% of natural gas production of Canada will come from tight and shale gas reservoirs.

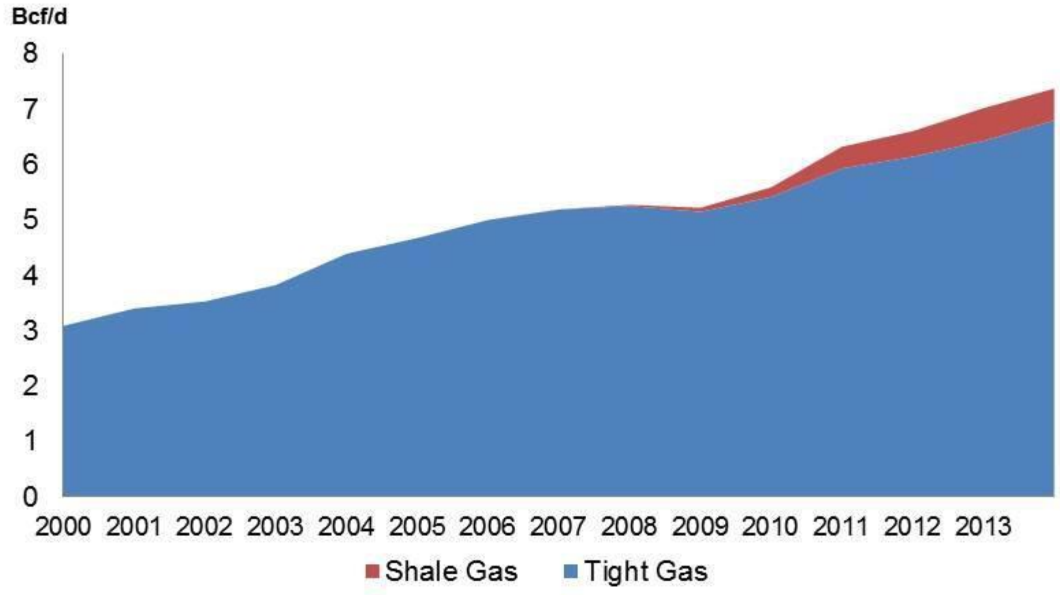

a). Canadian shale and tight gas production

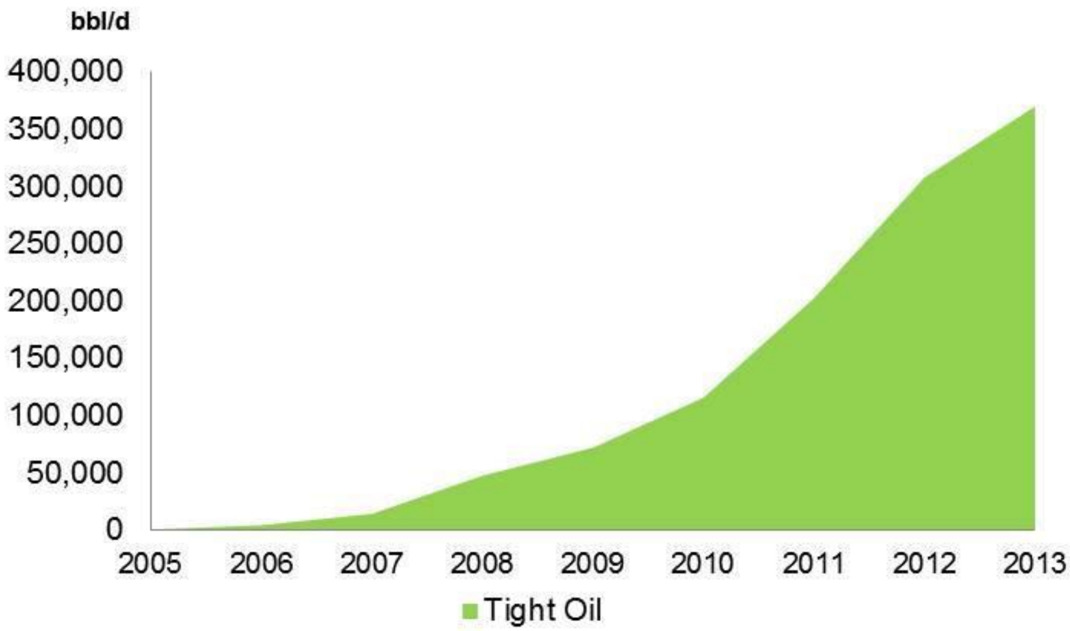

b). Canadian tight oil production

Figure 1-2. Canadian production from tight resources (NEB, 2015)

First type of natural gas produced in WCSB is dry gas and it is mostly consisted of methane. When heavier hydrocarbons like hexane, octane, etc. and non-hydrocarbon like helium, nitrogen, etc. are removed from stream and remained gas is called dry gas according to U.S. Energy Information. The only liquid produced with dry gas is water. Another type of gas is wet gas which contains heavier hydrocarbons like ethane, butane and methane content has to be less than 85%. When raw natural gas is produced, heavy hydrocarbons will separate from as state as liquids. The gas is called “liquid rich”, if liquid amount is more than 10 barrels for every MMscf.

Since production of natural gas from tight and shale reservoirs is increasing, our thesis will focus on these formations. Figure 1-4 illustrates tight gas resources in Canada. Among these shale gas plays, Duvernay/Muskwa formation has rapidly evolved into one of the hottest natural gas plays in recent years. It has a potential of producing total of 542 million m3 of crude oil, 2.17 trillion m3 of natural gas and 995 million m3 of natural gas liquids (AER, 2017). Duvernay covers130, 000 square km of Alberta which accounts for 20% of Alberta province. This formation attracts a lot of companies due to its rich NGL content including condensate which is needed for bitumen mixing so bitumen will be thinner and shipped in oil pipelines.

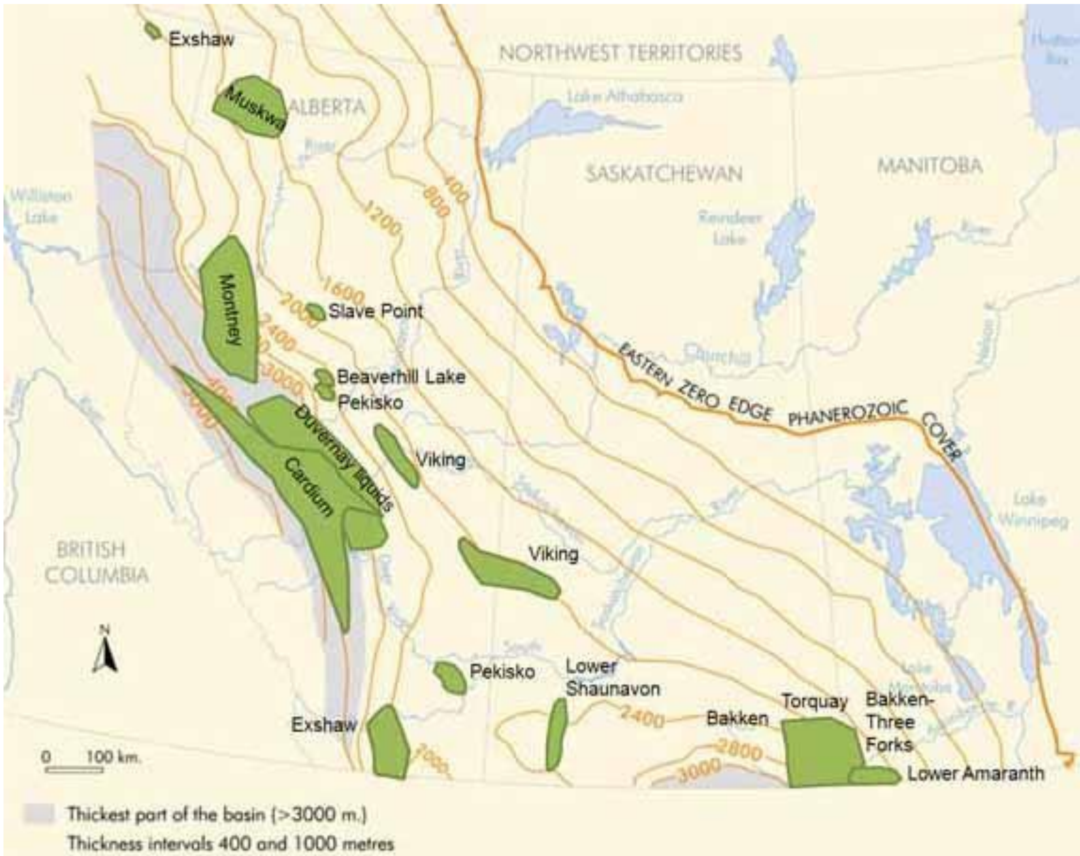

Figure 1-3. Location of tight oil and gas activity in the WC SB (NEB, 2011)

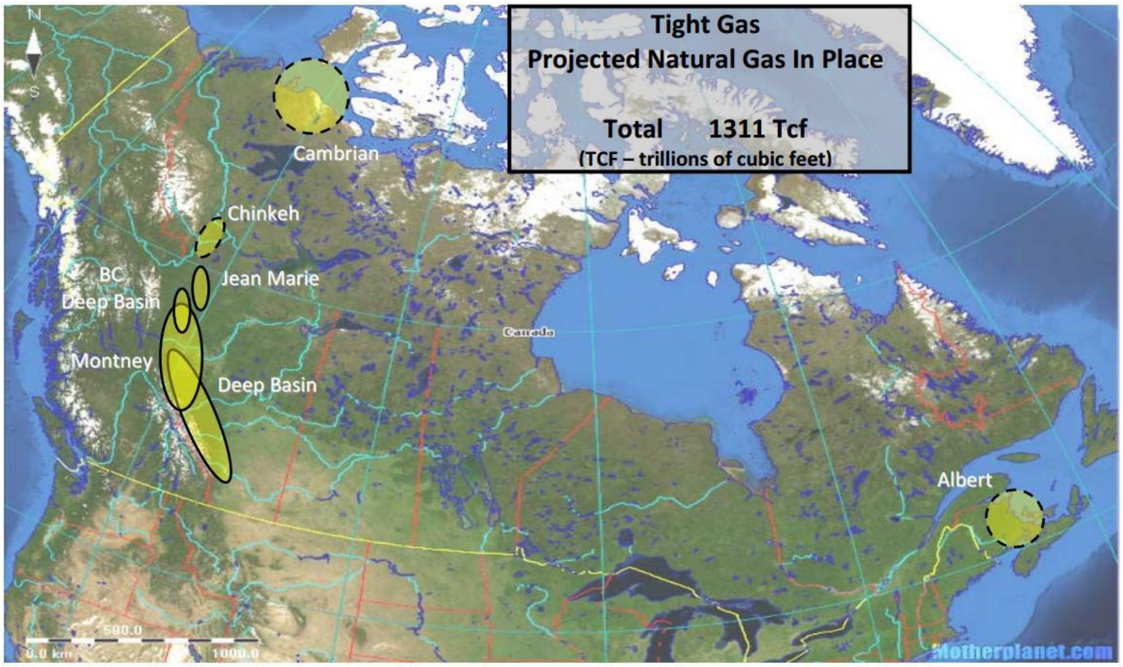

Figure 1-4. Distribution of tight gas resources (Heffernan, 2010)

This formation was buried 372 million years ago during the Upper Devonian Period and oil and gas was created due to heat and pressure. (Rokosh, 2012)Some oil and gas migrated to Leduc Formation reefs which has some of the largest conventional plays in Alberta. Duvernay is at 1000 m depth but it gets deeper closer to Alberta's foothills up to 5000 m. It is divided into 2 basins West Shale Basin which Fox Creek play and East Shale Basin which Innisfail play and they are divided by Leduc-Rimbey-Meadhowbrook reef which can be seen in Figure 1-5. There is calcareous mudstone and carbonate in both plays but higher content in Innisfail which has only oil where Fox creek has both gas and oil.

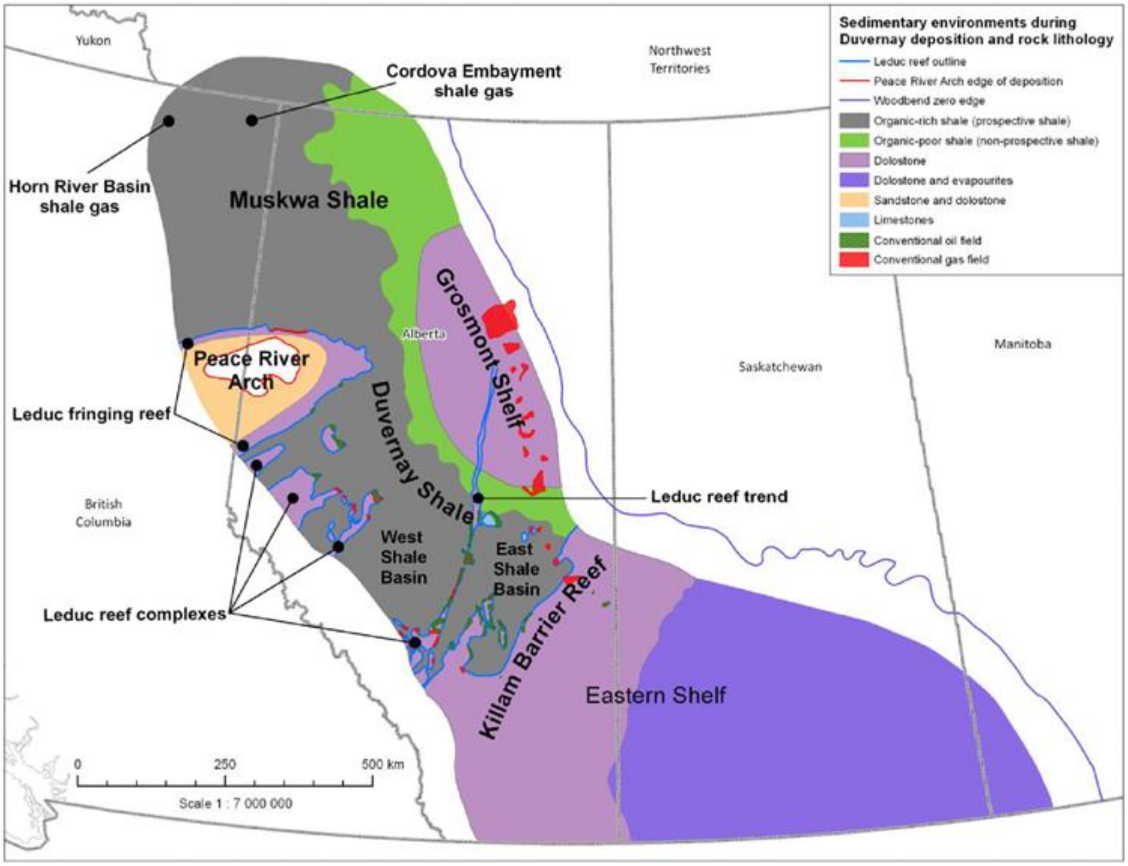

Figure 1-5. Duvernay shale play (ERCB, 2012)

1.1.2 Hydraulic Fracturing in Tight Reservoirs

Tight and shale reservoirs have very low permeability and when well is drilled and perforated reservoir fluids will not flow without hydraulic fracturing. In 1947 first experimental hydraulic fracturing was performed and in 1949 first commercially successful stimulation was performed. Massive hydraulic fracturing started in 1970s and quickly spread to Canada, Germany and Netherlands. In 1980s when horizontal drilling technology was developed, Texas started massive multistage hydraulic fracturing operations on horizontal wells. Hydraulic fracturing is fracturing of various rock layers by pressurized liquid. (King, 2012) It is formed when fracturing fluid like water, gas, and oil pumped into the wellbore at appropriate rate so downhole pressure s more than rock fracture gradient. Once fracture created and necessary width and length is attained, proppant like sand, ceramic or other particulates are injected in order to keep fracture open which is shown on Figure 1-6. After pumping is finished reservoir fluids flow through permeable propped fracture to the wellbore which is shown on Figure 1-7. During selection of proppant, it is needed to consider strength of proppant since it might fail at greater depth where pressure and stresses are higher.

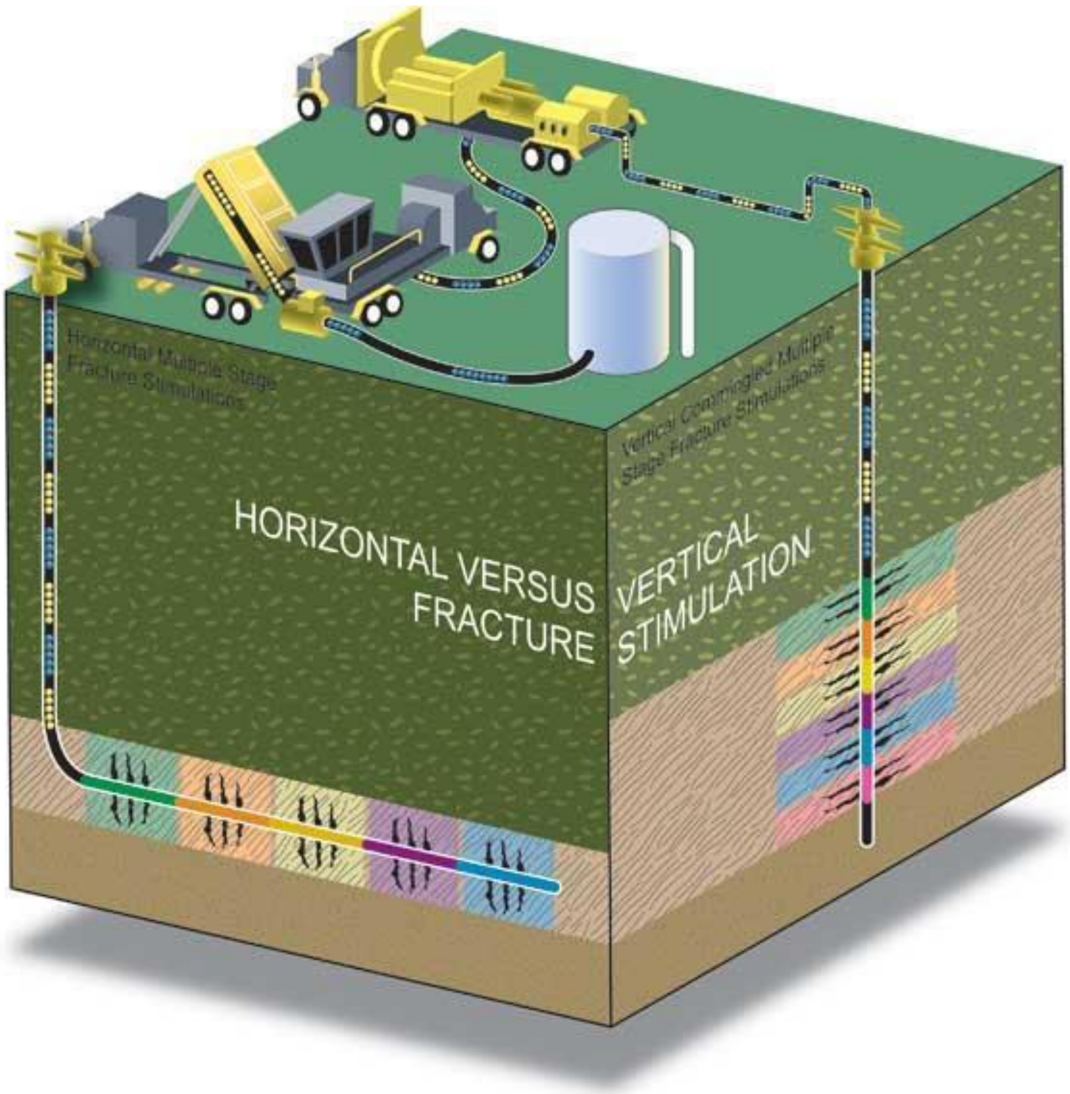

Figure 1-6. Schematic of hydraulic fractured wells (NEB, 2015)

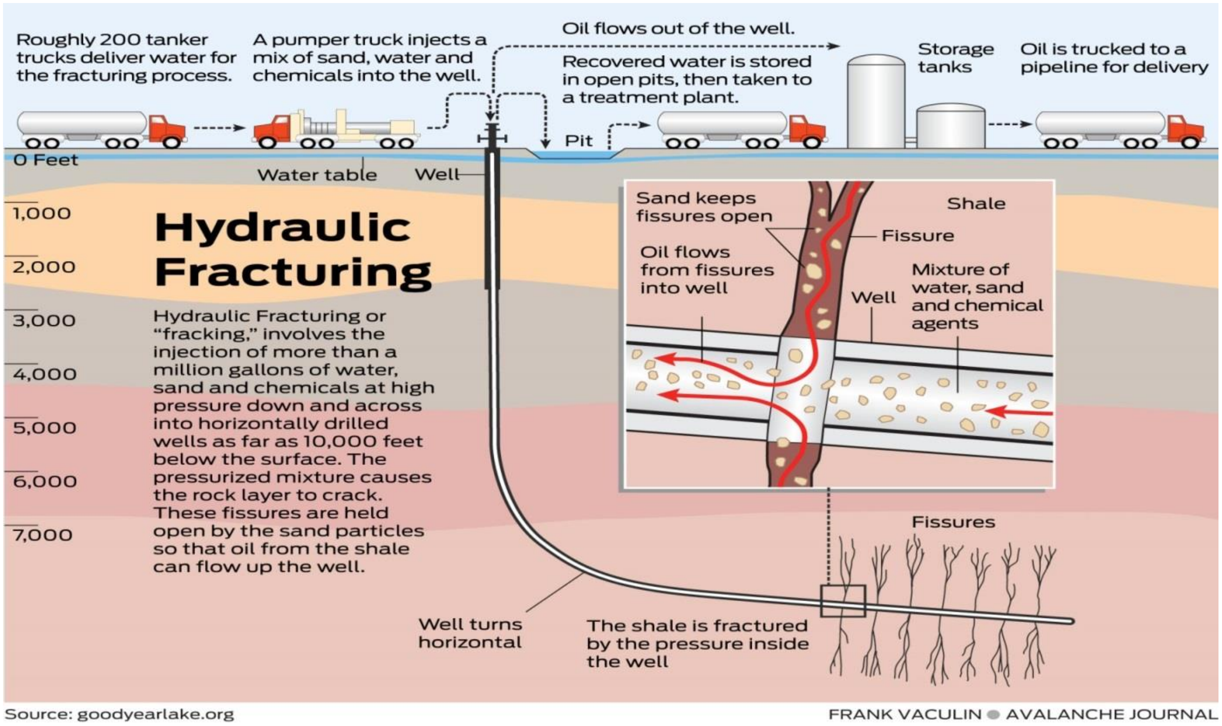

Figure 1-7. How fractures are created. (Schmidt, 2008)

Another factor affecting successful fracturing is leak off. If loss of fracturing fluid from fracture channel into surrounding permeable rock not controlled, more than 70% of fracturing fluid may leak to formation which leads to matrix damage and altered fracture geometry. Due to that factor fluid can be high viscous and usually high-viscosity fluid creates causes large main fracture. Fluid can be less viscous but high-rate where fracture cases small spread-out micro-fractures. Typically fluid consists of water, proppants, and chemical additives like gel, foams, and gases like nitrogen, carbon dioxide and air.

It also important to predict parameters like length, width and height of the fracture that's mainly affected by rock properties like Young's modulus of elasticity, Poisson's ratio, Biot's number, overburden stress etc. Young's modulus of elasticity is a material property which describes stiffness or ratio of the stress to the strain and Biot's number is the efficiency with which internal pore pressure offsets the externally applied vertical total stress. A high modulus rock requires more applied stress to yield a given strain, so it appears to be stiffer and also as Biot's number declines, net intergranular tress increases and ore pressure variations have less impact on net stress. Poisson's Ratio is defined as the ratio of lateral to axial strain under conditions of axial loading. In order predict length, height and width of fracture 2D, pseudo-3D and full 3D modeling methods were developed over the years of research. Perkins-Kern-Nordgren (PKN) and Khristianovic-Geerstma-de Klerk (KGD) are widely used 2D modeling methods (Geertsma, 1979). The first model is used when fracture length is considerably longer than the fracture height and second one is used when the fracture height is considerably larger than fracture length. The fracture length is shown in Figure 1-7.

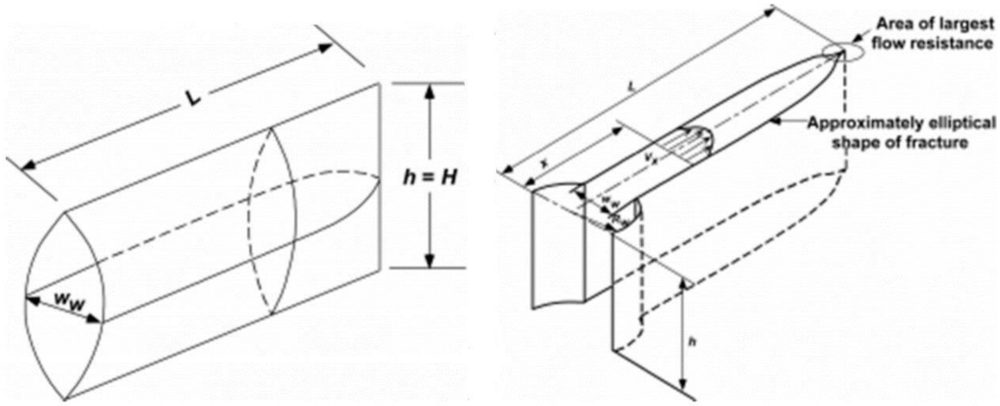

(a) PKN geometry for a 2D fracture (b) KGD geometry for a 2D fracture

Figure 1-8. Two dimensional models (Gidley et al. 1989)

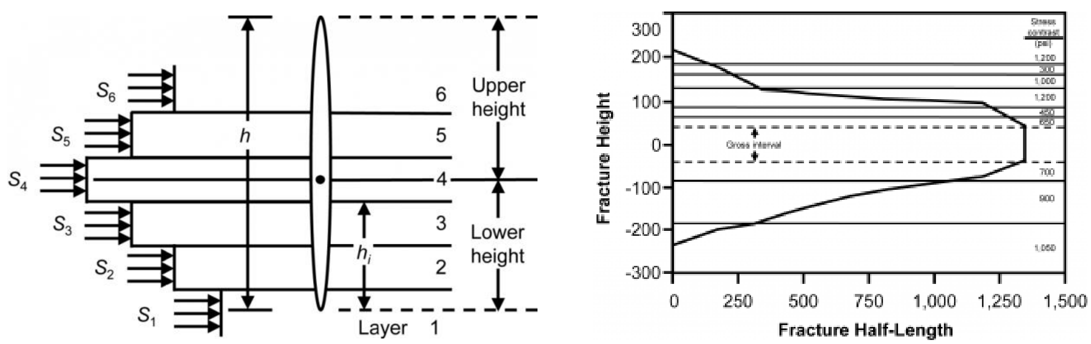

(a) Width and height from P3D model (b) Length and height distribution from P3D model

Figure 1-9. Two dimensional models (Gidley et al. 1989)

Once computers started to develop and computer processing became faster pseudo-three-dimensional models started to be used by the most fracture design engineers. P3D model fracture propagation theory and equation derivations for programming 3D models were explained by Clifton in Figure 1-8. This model gives more accurate fracture geometry and dimensions since it utilizes complete data about layer of formation and also layers above and below.

1.2 Problem Statement

Large volumes of water are injected during hydraulic fracturing operations and it might become significant problem in water scarce places. Small volume hydraulic fracturing operations require 500-2000 m3 of, moderate volume hydraulic fracturing operations might require 10000-50000 m3 and high volume hydraulic fracturing operations will require 50,000 – 100,000 m3 of water. Moreover, due to tight nature of the reservoir fracturing fluid as water may get trapped and formation may not have enough energy to push water back to the wellbore. It might take decades to produce fracturing water back to surface.

Moreover, water can be unsuitable to water-sensitive formations due clay-swelling. After hydraulic fracturing water saturation increases around fracture and water flows to matrix and leads to clay swelling. (Hewitt, 1963) This will block gas to flow from matrix to fracture and decreases production of gas.

Also high capillary pressure makes water to imbibe into the matrix pores which prevents counter-current gas flow. (Agrawal, 2013) Hydraulic fracturing can create complex fracture network around one perforation and water will fill the fractures without proppant. This effect will lead to low water flowback from those micro fractures. (Fan, L., 2010)

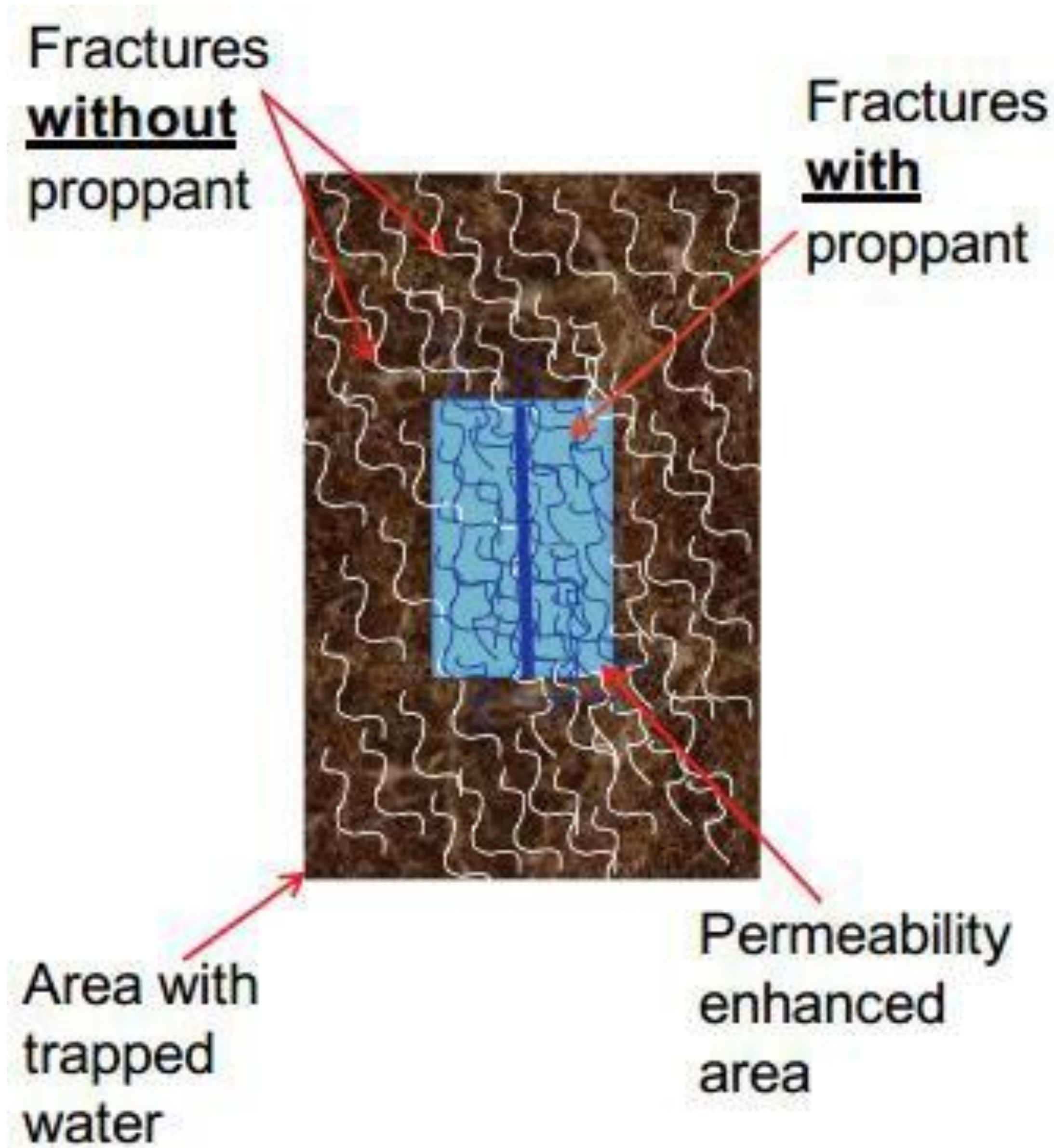

Figure 1-10. Illustration of water distribution in fracture network (Fan, L ., 2010)

1.3 Objectives

This study focuses on enhancing hydrocarbon recovery by utilizing and comparing fracturing fluid based on water and CO_2 in the tight gas reservoir. A geological model which contains a horizontal well is built with CMG and there are 10 stages of hydraulic fractures, in a tight gas reservoir which were modeled and imported from GOHFER. The aim is to develop a simulation study to enhance gas and oil recovery by using CO_2 as a fracturing fluid rather than conventional water.

The detailed objectives are:

(1)To build comprehensive hydraulic fracturing models on GOHFER that uses water and CO_2 as a fracturing fluid based on proprietary field data collected from a company and publicly available SPE papers and validate such model by the production data

(2)To build comprehensive numeric model on CMG that uses GOHFER model in order accurately investigate effect of water and CO_2 as a fracturing fluid and future performance of reservoir

1.4 Outline

A summary of the content of Chapters Two to Four follows:

(1) Chapter Two delivers a detailed literature review related to the topic of hydraulic fracturing using water and its effect on reservoir, numeric simulation using GOHFER and CMG IMEX in order to prove damaging effect of water

(2) Chapter Three focuses on literature review on hydraulic fracturing using CO_2 and

its effect on reservoir, numeric simulation using GOHFER and CMG IMEX in order to show effect on reservoir performance

(3) Chapter Four lists the conclusions and future recommendations resulting from this study.

CHAPTER 2: Water based hydraulic fracture modeling with GOHFER and CMG

2.1 Introduction

This chapter presents an extensive numerical study on water based hydraulic fracturing and how it damages the reservoir due to high capillary pressure and gel filtercake. First part of chapter discusses about building accurate fracture model in Duvernay formation using GOHFER simulator. Second part of chapter talks about how modeled fractures have been imported into numeric simulator in order to estimate gas and water production using CMG. Moreover, water saturation distribution in and around fracture was investigated too.

2.2 Literature review

2.2.1 Slickwater

The most widespread fluid system used for hydraulic fracturing system is slickwater fluid system. In recent decades it was applied for unconventional shale gas reservoirs quite a lot. (Cheng, 2012) This fluid consists of water, proppant and specific chemicals like friction reducers, clay stabilizers, surfactants, breakers. Friction reducer is a chemical additive based on polyacrylamide or mineral oil which reduces friction between fluid and a pipe by changing rheological properties of fluid.

In order to have a maximized access to reservoir, complex fracture system and maximum surface area is needed to be created using water. Also for carrying sand and placement of sand into formation rate and pressure is another factor to consider. Name “slickwater” comes from chemical additive friction reducer. Without friction reducer pipe friction will cause friction to increase and it will be not possible to reach necessary rate. Slickwater doesn’t necessarily mean fresh water, but flowback water is also can be used. Depending on formation in some cases it’s better to use produced water since it has already compatible minerals with formation.

Slickwater is very suitable for brittle shale since it will enlarge natural micro fractures in shale bed. (King, 2010) Since viscosity of slickwater is not high, sand carrying capacity is not that high. High rate is enough to carry sand into fracture system so that fractures do not lose much width and leak off is low too.

Since slickwater has viscosity limitations, polymer based gels are also very popular as a fracturing fluid. Moreover, polymer based gel could be cross-linked with boron and transition metals like aluminum, antimony, chromium etc. Molecular weight of base-polymer is increased by crosslinking which lead to increase in viscosity and temperature tolerance. Design of fracturing fluid and specifics of formation usually decides how many and which chemicals are needed to be added. (Ketler, 2006) Generally, chemical additives volume will vary from 0.5% to 2%. Figure 2-1 shows percentages of chemical additives:

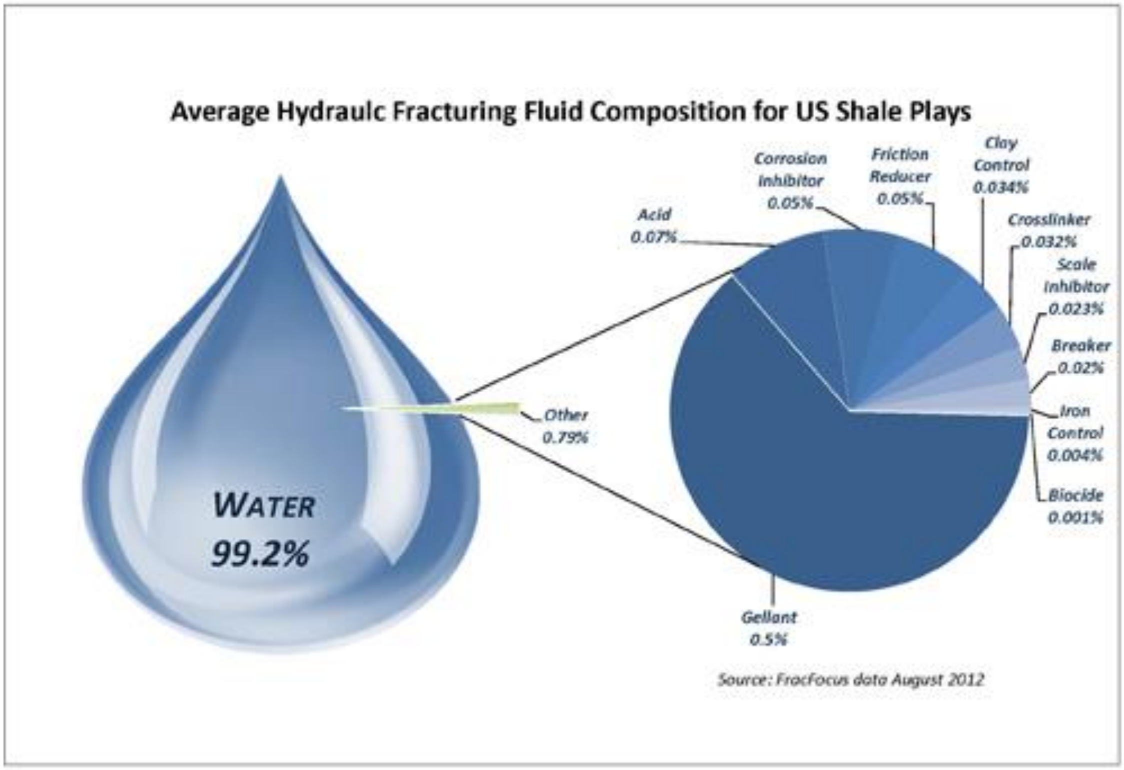

Figure 2-1. Average hydraulic fracturing fluid composition for US Shale plays (Chemical disclosure registry, 2012)

2.2.2 Chemical additives

Chemical additives in the figure above are the major components of the most hydraulic fracturing jobs of shale reservoirs. Of course, not all of those chemicals are added due to specifics of formation and fluid is being used. Each chemical additive has specific purpose like eliminating bacteria or preventing clay swelling. Table 2-1 shows several chemical additives and its purpose. (Arthur, 2008)

2.2.3 Damage from hydraulic fracturing fluid

Once well is hydraulically fractured, it needs to flow back before put on production. There are several factors which affect flowback. First, hydraulic fracture needs an injection of large volume of water and there will be invasion of water into matrix. Invaded water into matrix will eventually flow until residual water saturation and the rest of water will stay in the matrix. Difference in capillary pressure of matrix and fracture faces makes water get trapped at the efflux face of matrix adjacent to fracture. These two factors will result in permanent water blockage which his illustrated in Figure 2-2. (Hadley and Handy, 1956)

Table 2-1. Fracturing Fluid Additives (Makhanov, 2013)

Additive Type	Main Compounds	Purpose
Diluted Acid (15%)	Hydrochloric acid or muriatic acid	Help dissolve minerals and initiate cracks in the rock
Biocide	Glutaraldehyde	Eliminates bacteria in the water that produce corrosive byproducts
Breaker	Ammonium persulfate	Allows a delayed break down of the gel polymer chains
Corrosion Inhibitor	N,n-dimethylformamide	Prevents the corrosion of the pipe
Crosslinker	Borate salts	Maintains fluid viscosity as temperature increases
Friction Reducer	Polyacrylamide Mineral oil	Minimizes friction between the fluid and the pipe
Gel	Guar gum or hydroxyethyl cellulose	Thickens the water in order to suspend the sand
Iron Control	Citric acid	Prevents precipitation of metal oxides
KCl	Potassium chloride	Creates a brine carrier fluid
Oxygen Scavenger	Ammonium bisulfite	Removes oxygen from the water to protect the pipe from corrosion
pH Adjusting Agent	Sodium or potassium carbonate	Maintains the effectiveness of other components, such as crosslinkers
Proppant	Silica, quartz sand	Allows the fractures to remain open so the gas can escape
Scale Inhibitor	Ethylene glycol	Prevents scale deposits in the pipe
Surfactant	Isopropanol	Used to increase the emulsifying properties of the fracturing fluid

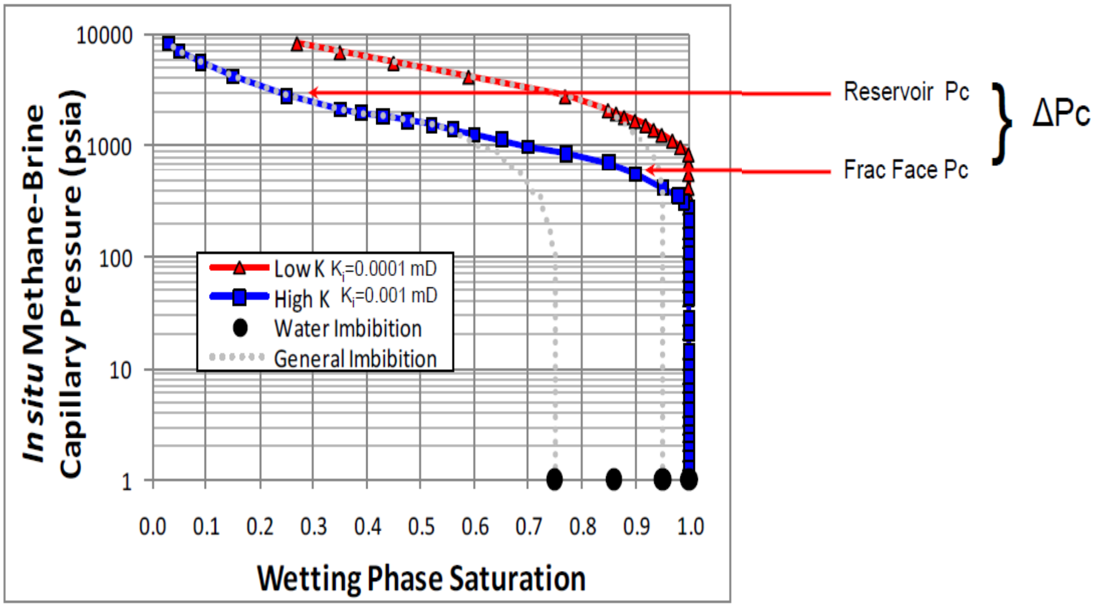

Figure 2-2. Effect of water blockage due to capillary pressure and relative permeability (Byrnes, 2012)

Another factor affecting water flowback is polymer damage. In order to control leak-off of fracturing fluid into formation polymers are purposed to create filter cake illustrated in Figure 2-3. (Mayerhofer, 1991) Once fracturing fluid starts to leak-off to formation filter cake will be created but it will stick to fracture face and block the conductivity and matrix permeability. Decreased matrix permeability and conductivity will prevent water flowback.

Bad design of fracturing fluid like may result in clay swelling and fines migration which will block certain pores by locking water in them. (Economides and Martin, 2008) Clay stabilizers like potassium chloride etc. are added to fluid to prevent clay swelling which his shown on figure 2-4.

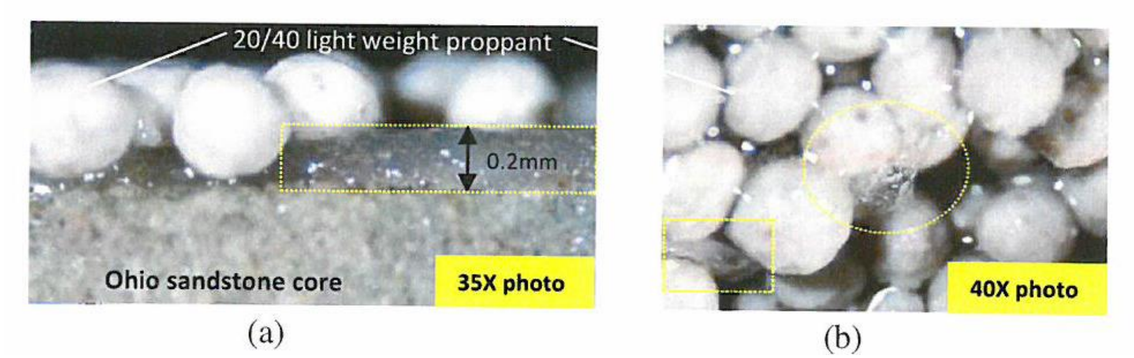

Figure 2-3. Filter cake buildup after hydraulic fracturing (STIM-LAB, 2003)

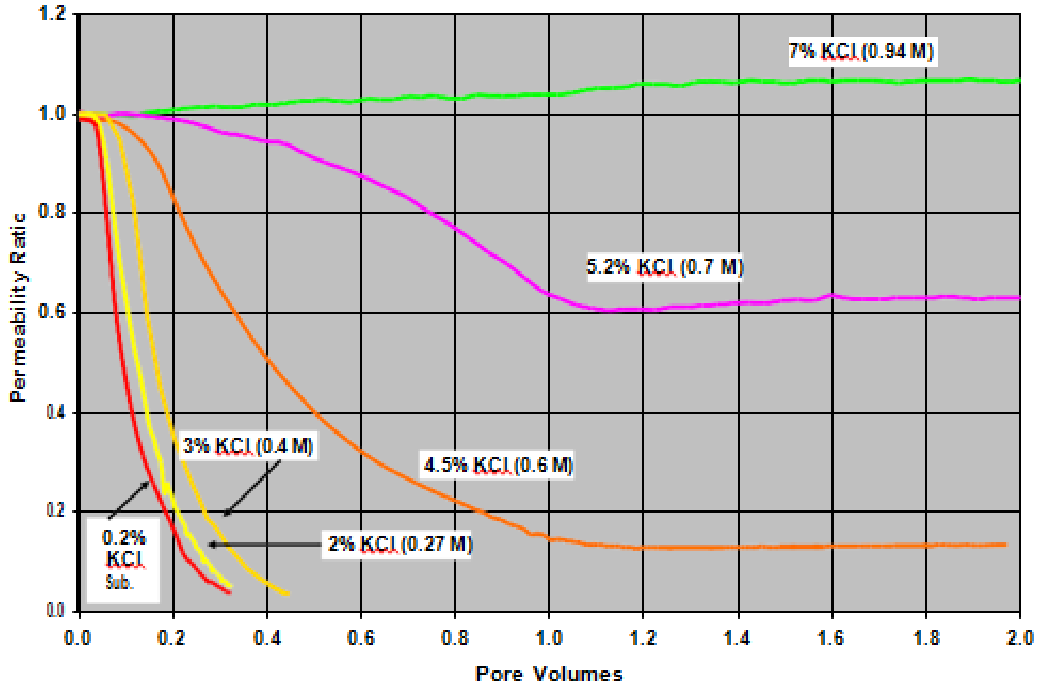

Figure 2-4. Clay control with KCL (Halliburton, 2006)

2.2.4 Methods of modeling hydraulic fractures

There are analytical, numerical and semi analytical/numerical types of hydraulic fracture modeling. For short term duration all three methods can be used: analytical, semi-analytical, and numerical; for mid-term prognosis semi-analytical and numerical can be used; and for long-term only numerical should be used in order to have accurate hydraulic fracturing model. (Akuanyionwu, 2012)

Analytical modeling uses assumptions like single phase flow, homogenous reservoir and ignoring gravity effects and has simplifications like equivalent wellbore radius and negative skin factor. So, physics of flow between matrix and fracture are ignored. Next upgrade in modeling is two phase flow and semi-analytical model can perform two phase flow calculations while modeling. Still there are basic assumptions and simplifications like in analytical model in order to have fast simulations. Last improvement in modeling is physics of the fluid flow between matrix and fracture which can be handled with numerical modeling method. Basic technique is to refine gridblocks towards wellbore and permeability of the gridblocks are changed to accurately represent hydraulic fracture. This technique is called local grid refinement (LGR).

2.2.5 Hydraulic fracture modeling in the past

Hydraulic fracturing is way more effective in horizontal wells rather than vertical wells. Productivity index of the horizontal well is 2-5 times better than vertical in the same homogenous medium. Moreover, when horizontal well had crossed natural vertical fracture network, production was 10 times more. (Karcher, 1986) Hegre stated that hydraulic fracture modeling depends on the objectives of the model. In explicit modeling, it is recommended fracture width to be increased and permeability decreased in order to keep the same conductivity without causing numerical error. Also, equivalent wellbore radius method can be used for modeling hydraulic fractures, if the fractured horizontal well is inside of one areal grid cell. (Hegre, 1996)

Soehlingen field horizontal well hydraulic fracture modeling using fully coupled local grid refinement was studied and LGR method was good for long term production and analytical model was good for short term production. (Ehrl, 2000) Development of faster computers made possible to model hydraulic fractures in 3D multiphase simulator explicitly. Modeling became faster and simulator was integrated with fracture simulator to create LGR. (Shaoul, 2005) Comparison of analytical hydraulic fracture modeling versus explicit numerical modeling was performed and analytical model oversimplified by not considering fracture geometry and reservoir boundary conditions of Dunbar field. (Sadrpanah, 2006)

Also, infinite-conductivity line source method was used to model hydraulic fractures in tight gas formations. There was an issue modeling shut-in pressures, so wellbore cross-flow must be included for the coarse grid field scale. (Abacioglu, 2009) A lot of tight reservoirs have natural fractures and microseismic data helped to estimate extent of hydraulic fractured area within natural fracture network. This method called volumetric fracture modeling approach assisted to calculate drainage volume of shale gas reservoirs. (Harikesvanallur, 2010)

Mathematical model of hydraulic fracture that includes non-Darcy flow with inertial effects, non-Newtonian fluid behavior, adsorption, rock deformation and other reaction effects was developed. Later model was added to generic simulator and hydraulic fractures modelled successfully. (Wu, 2011) LGR technique was modified by lowering grid size to the dimensions of fracture without decreasing calculation time and this technique used multiple LGR's. Traditional LGR would have used 116856 grid cells more where amalgam LGR used 7000 more grids. (Moneim, 2012)

2.3 GOHFER Fracture design

In order to build accurate fracture propagation model commercial fracture simulator GOHFER is used to simulate fluid, proppant and fracture propagation design. Calculations performed by software are assumed to characterize actual, quantitative fracture propagation. Fracture growth equations were all calculated using high speed computer. Design mode of the simulator was used to model fracture which was closely matched to field pumping schedule. In the end, simulator output was fracture geometry and properties.

2.3.1 Reservoir properties

The more reservoir rock property information is available is better to accurately design fracture. First step in designing and optimizing fracture starts with evaluation of reservoir properties and those properties will affect production performance of fracture design. Reservoir parameters like reservoir fluid compressibility, reservoir fluid viscosity, pay zone thickness, initial reservoir pressure, reservoir temperature, porosity, effective permeability of pay zone, fluid saturations are needed for fracture design. Table 2-2 shows summarized table of reservoir properties.

Table 2-2. Reservoir data used for fracture design (Dunn, 2012 & Field data)

Reservoir Parameters	
Initial reservoir pressure, kpa	55000
Static reservoir temperature, ^{o}C	110
Porosity, %	0.06
Net sand thickness, m	40
Layer formation depth, m	3100
Permeability, md	0.0001
Gas viscosity, cp	0.07
Water saturation, %	0.1
Gas gravity , dimensionless	0.63
Compressibility, kpa^{-1}	0.00000911

Table 2-3. Geophysical properties used for fracture design. (Taylor, 2014 and Field Data)

Geophysical Parameters	
Poisson's ratio, dimensionless	0.28
Young's modulus, psi	4,000,000
Biot's number	0.47
Closure gradient, kPa/m	.0133
Average fracture gradient, kPa/m	24.54

Second step is to define petrophysical properties of the rock which defines lithology formation. It is important to know petrophysical properties of the rock since it will impact calculation of rock stress analysis, deformation behavior of rock and fracture geometry and orientation. Those properties are Poisson's ratio, Young's modulus, Biots number and closure gradient. Table 2-3 summarizes averaged petrophysical property data.GOHFER has log analysis tool which utilizes LAS logging data files that conform to the standard for version 2 certification. LAS file from a company was acquired and imported into software. By combining TVD, overburden gradient, pore pressure, tectonic stresses with mechanical properties and Biot's poroelastic coefficient software computes minimum horizontal stress curve.

$$\sigma_{\min} \cong \frac{v}{1-v}(\sigma_1 - \alpha p_p) + \alpha p_p + \sigma_{\text{ext}},$$

… Equation 1 (Hubert, 1957)

Also lithological model was generated from logs based on 6 components: volume fraction of shale, sand(quartz, feldspars, mica), lime, dolomite, anhydrite(including other heavy minerals) and coal. Figure 2-5 shows lithology model and other logging data.

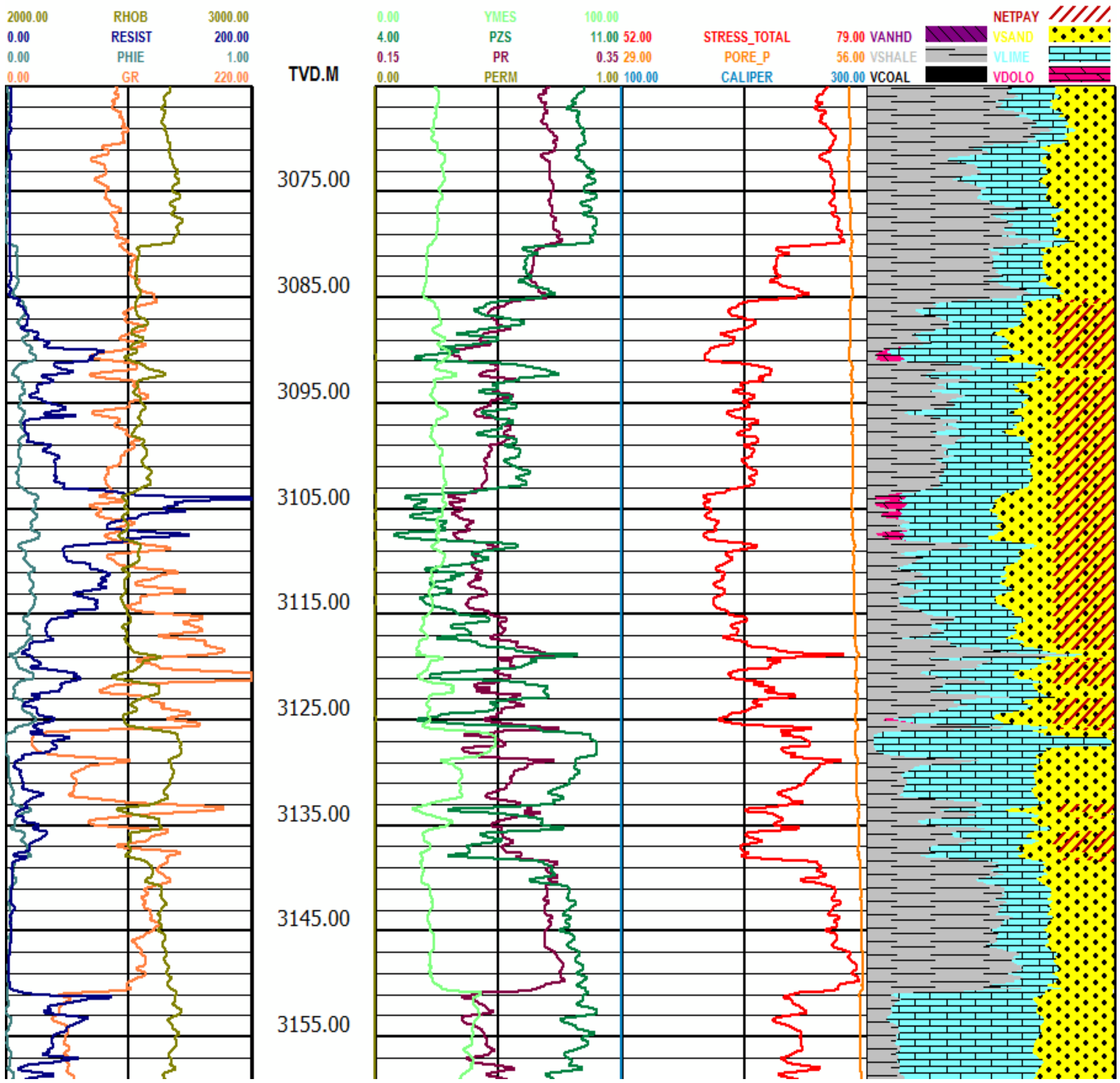

Figure 2-5. Lithology model from logging data.

Another feature of the software is net-pay curve generation based on effective porosity, resistivity and shale fraction logs. This quick look method helped us to find potential pay targets. Figure 2-6 shows effective porosity was mapped from LAS file.

2.3.2 Grid system

Grid oriented feature of the software allowed to build a grid structure in horizontal and transverse directions which is used to describe the entire reservoir similar to reservoir simulators. Grid system was used to calculate elastic rock displacement and planar finite difference grid for fluid flow solutions. Each node or grid has specific fluid composition, proppant concentration, shear, leakoff, width, pressure, viscosity, and other variables (Baree , 2018) Figure 2-7 shows permeability was assigned for each node.

Moreover well directional survey was imported and displayed in 3D view and well breakdown conditions were evaluated on any point of the wellbore trajectory. Tangential stress distribution can be changing at any point around the wellbore along the directional survey. Those rapid changes in stress happen due to rock type changes when well is drilled. Well were drilled in angle upwards to decrease fracture growth tortuosity. Figure 2-8 shows breakdown profile.

.

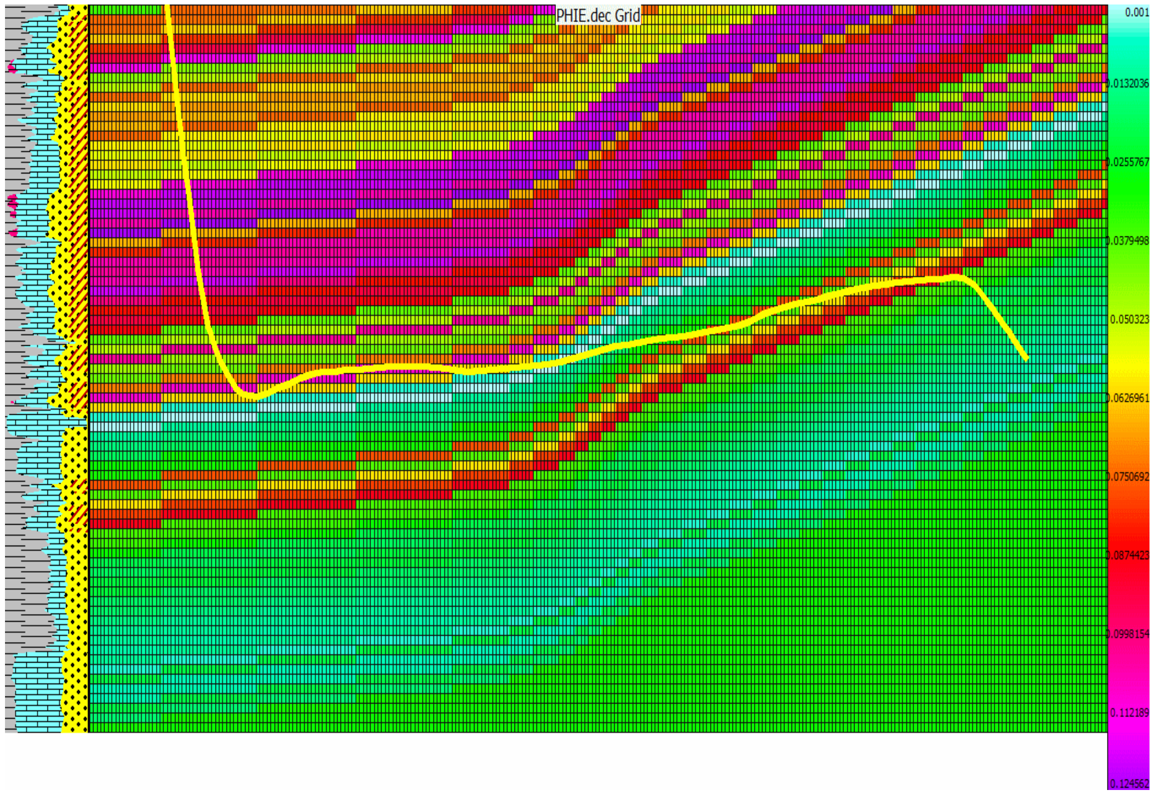

Figure 2-6. Effective porosity distribution in GOHFER model

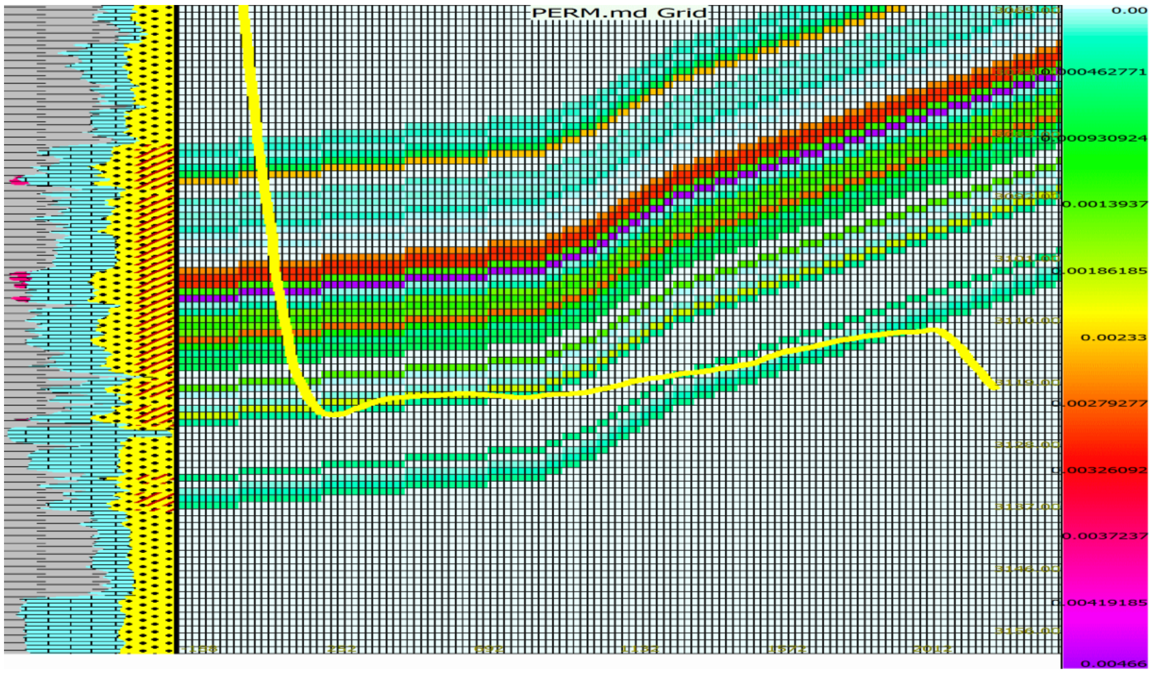

Figure 2-7. Permeability distribution in GOHFER model

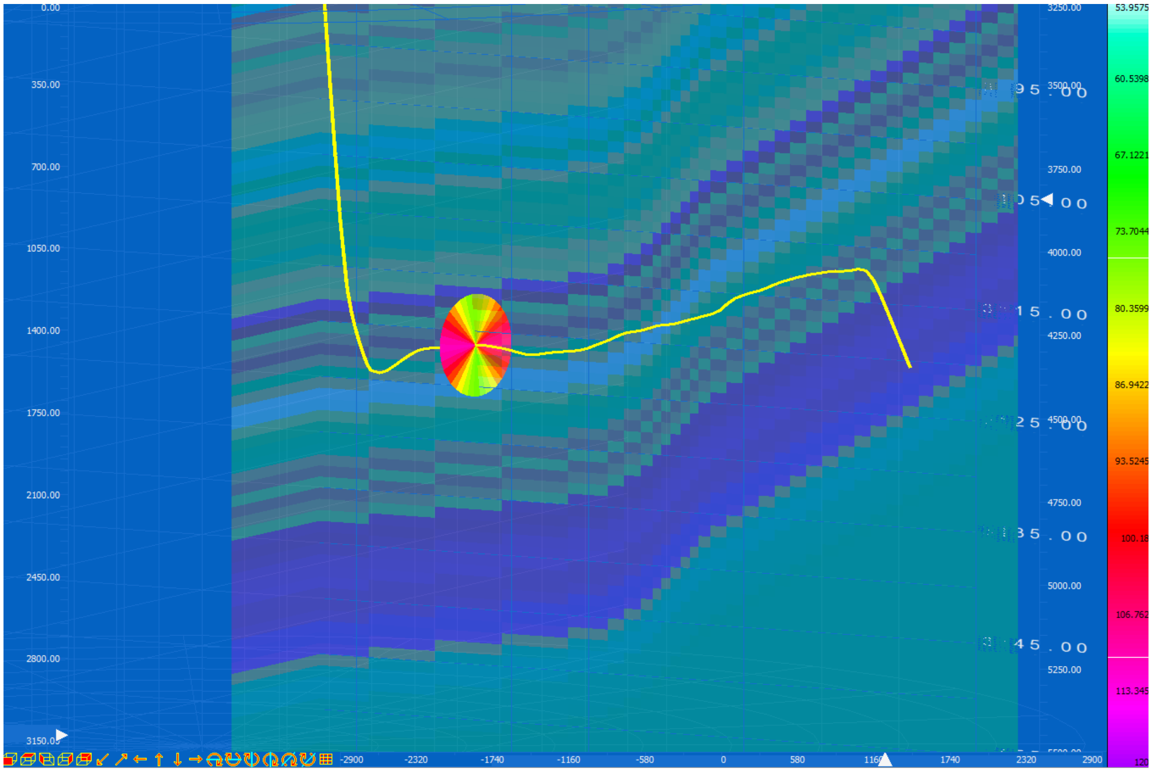

Figure 2-8. Breakdown profile

2.3.3 Fluid and proppant selection

The fluid and proppant type was modeled according to Kaybob area Duvernay formation hydraulic fracturing modeling study. (Taylor, 2013) According to Taylor the recommended maximum sand concentration for slickwater was 200kg/m3 and depends on the rate. Common practice is having acid spearhead to assist the breakdown and remove near-wellbore damage from perforating the casing and cement behind the casing. (Broacha, 2009) After acid stage, there is slickwater pad followed by 100 mesh proppant laden fluid. 100 mesh proppant is used to mitigate fracture downward growth and especially when fracture initiation rate is low. Moreover, it helps it helps to bridge off natural fractures that may lead to screen out. (King, 2008) After 100 mesh stages which have concentrations at 50-125 kg m3, main proppant 40/70 is pumped at 125-225 kg/m3 concentrations. Larger size proppants in shales are tend to give conductivity, but also tend to grow fracture downwards. (King, 2010) At last proppant stages curable resin coated proppant 40/70 was used at concentrations 100-150 kg/m3. Having resin coated proppant at tail is effective method of controlling proppant flowback. (Pope, 1987) Table 2-5 shows detailed pumping schedule:

Table 2-4. Slick water pumping schedule

Stage #	Elapsed Time hh:mm:ss	Stage time mm:ss	Fluid	Proppant	Stage volume m3	Cum. Volume m3	Rate m3/min	Prop. Conc. kg/m3	Cum. Prop. Kg
1	0:00	10:00	HCL 15%	None	30	30	3	0	0
2	10:00	23:20	Slickwater	None	70	100	3	0	0
3	33:20	3:13	Slickwater	None	45	145	14	0	0
4	36:33	2:55	Slickwater	100 Mesh	40	185	14	50	2000
5	39:28	4:02	Slickwater	100 Mesh	55	240	14	75	6125
6	43:30	4:27	Slickwater	100 Mesh	60	300	14	100	12125
7	47:57	4:43	Slickwater	100 Mesh	63	363	14	125	20000
8	52:40	7:21	Slickwater	40/70 Badger	100	463	14	75	27500
9	1:00:00	9:16	Slickwater	40/70 Badger	125	588	14	100	40000
10	1:09:17	9:08	Slickwater	40/70 Badger	122	710	14	125	55250
11	1:18:24	9:04	Slickwater	40/70 Badger	120	830	14	150	73250
12	1:27:28	8:23	Slickwater	40/70 Badger	110	940	14	175	92500
13	1:35:51	7:41	Slickwater	40/70 Badger	100	1040	14	200	112500
14	1:43:32	7:45	Slickwater	40/70 Badger	100	1140	14	225	135000
15	1:51:17	3:43	Slickwater	40/70 CRC	50	1190	14	100	140000
16	1:55:00	2:51	Slickwater	40/70 CRC	38	1228	14	125	144750
17	1:57:51	2:39	Slickwater	40/70 CRC	35	1263	14	150	150000
18	2:00:30	4:09	Slickwater	None	58.08	1321	14	0	150000
19	2:04:38	10:00	Slickwater	None	0	1321	0	0	150000

2.2.4 Pressure match and fracture parameters

Once all 10 sets of perforations were entered all of them were run according to pumping schedule from table 2-5 to match simulated pressure curve with the actual pressure curve. Obtaining all necessary field information in order to build an accurate hydraulic fracturing model reduced amount of assumptions to be made. In order to match pressure some parameters like Pressure dependent modulus factor, pressure dependent leakoff, relative permeability ratio, and transverse storage coefficient and tortuosity factor had to be modified. As an example pumping stage 1 can be seen in Figure 2-9, simulation run shows pipe friction, bottomhole pressure, injection rate, well pressure, and surface and bottomhole proppant concentrations. These parameters helped to design fracture so it is operationally possible to execute regarding friction pressure and wellhead pressure limitations. In this case maximum wellhead pressure was 90 MPa. Also Figure 2-9 shows treating pressure was matched by pressure field data in order to validate our model.

After all 10 stage engine runs were performed, 10 hydraulic fractures were obtained. Summary of fracture is shown in table 2-6 where there are length, proppant cutoff length, fracture height and fracture width. Gross fracture length is 1114 m, average width is 3 mm and average proppant cutoff length is 126 m.

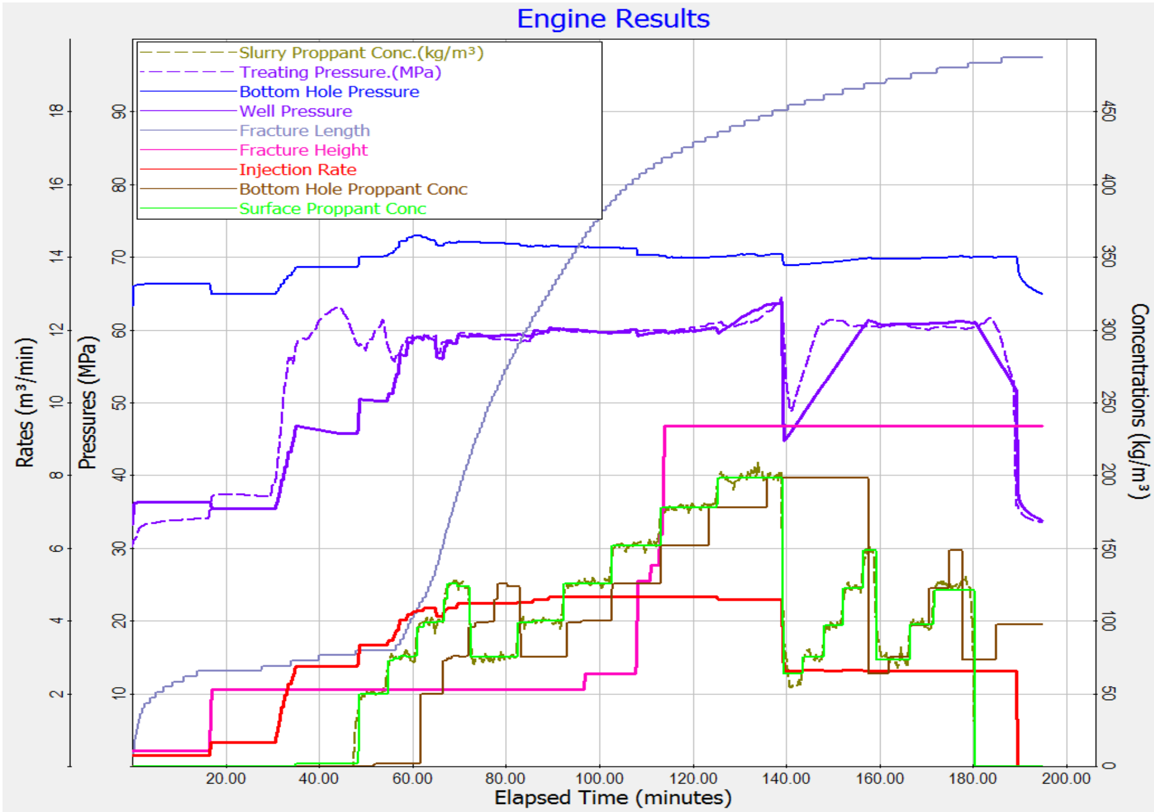

Figure 2-9. GOHFER pressure match

Table 2-5. Summary of slick water fracture parameters

Fracture		Gross Frac Length.M	Fracture Height.M	Average Proppant Conc.kg/m²	Average Fracture Width. mm	Max Fracture Width.mm
1	Transverse 6	1959.1	24.00	2.68	4.29	9.80
	Transverse 5	850.2	12.00	0.81	2.29	4.91
	Transverse 4	1460.1	16.00	1.88	3.30	6.08
	Transverse 3	166.3	12.00	0.06	1.21	3.59
	Transverse 2	1737.3	20.00	2.39	3.89	6.96
	Transverse 1	18.5	4.00	0.16	1.32	1.30
2	Transverse 6	1718.8	12.00	2.77	3.90	6.12
	Transverse 5	942.6	12.00	1.13	2.55	3.57
	Transverse 4	1090.4	12.00	1.94	2.81	5.03
	Transverse 3	998.0	12.00	1.11	2.55	3.59
	Transverse 2	1072.0	12.00	1.84	2.72	4.98
	Transverse 1	1497.0	12.00	2.66	3.62	7.18
3	Transverse 6	1774.3	20.00	2.43	4.06	6.60
	Transverse 5	776.2	4.00	1.17	2.34	4.11
	Transverse 4	1256.8	20.00	1.70	2.96	5.10
	Transverse 3	794.7	4.00	1.04	2.32	3.64
	Transverse 2	1035.0	4.00	1.81	2.73	4.82
	Transverse 1	1626.4	4.00	2.48	3.87	6.25
4	Transverse 6	406.6	0.00	0.00	1.44	1.43
	Transverse 5	1737.3	20.00	2.35	3.89	6.51
	Transverse 4	1182.9	16.00	1.49	2.76	5.08
	Transverse 3	813.2	4.00	1.13	2.39	3.87
	Transverse 2	1182.9	16.00	1.42	2.81	5.14
	Transverse 1	1515.5	4.00	2.24	3.62	6.90
5	Transverse 6	2033.0	32.00	2.23	4.17	8.24
	Transverse 5	646.9	16.00	0.13	1.49	2.97
	Transverse 4	665.4	16.00	0.15	1.66	2.93
	Transverse 3	166.3	0.00	0.00	1.18	1.30
	Transverse 2	147.9	0.00	0.00	1.13	1.30
	Transverse 1	1940.6	4.00	1.96	4.13	6.51
6	Transverse 3	2217.9	40.00	1.26	3.99	6.69
	Transverse 2	757.8	24.00	0.06	1.43	2.48
	Transverse 1	1755.8	44.00	3.34	4.41	10.49
7	Transverse 6	1700.4	28.00	2.57	4.22	10.21
	Transverse 5	1182.9	24.00	1.97	3.55	11.26
	Transverse 4	961.1	12.00	1.61	2.60	6.49
	Transverse 3	1312.2	12.00	2.51	3.64	9.36
	Transverse 2	166.3	12.00	0.41	0.80	2.11
	Transverse 1	18.5	4.00	0.15	1.32	1.30
8	Transverse 6	1534.0	24.00	8.60	3.21	13.50
	Transverse 5	998.0	24.00	9.25	3.12	12.91
	Transverse 4	979.6	24.00	7.53	3.53	12.54
	Transverse 3	1090.4	28.00	9.05	4.02	15.42
	Transverse 2	924.1	24.00	3.76	3.37	7.63
	Transverse 1	1349.2	28.00	8.19	3.96	14.20
9	Transverse 6	1571.0	28.00	8.42	3.35	14.05
	Transverse 5	998.0	28.00	7.85	3.29	11.94
	Transverse 4	1182.9	28.00	5.18	3.59	13.46
	Transverse 3	942.6	24.00	8.14	3.07	11.89
	Transverse 2	924.1	28.00	5.01	4.07	8.39
	Transverse 1	1441.6	40.00	7.70	3.91	12.93
10	Transverse 6	1681.9	28.00	2.90	4.22	10.42
	Transverse 5	720.8	8.00	1.63	2.57	7.72
	Transverse 4	147.9	8.00	0.65	1.18	4.43
	Transverse 3	1275.3	8.00	2.22	3.11	8.18
	Transverse 2	905.6	8.00	1.84	2.65	7.05
	Transverse 1	1515.5	12.00	3.24	3.76	9.84
Average		**1113.5**	**16.56**	**2.78**	**2.97**	**7.06**

2.2.1 Production history matching and results

In order to validate our model cumulative gas and production, gas and water rates were used. There is no data available as microseismic to match fracture length and profile or net pressure data to validate results. Well X from Duvernay field has produced for 943 day with cumulative production of 5.8 million cubic meters of gas and 3.2 thousand cubic meters of water. Figure 2-10 shows gas production history match to field production data.

After cumulative gas production gas and water rates were matched and this can be seen in Figures 2-11 and 2-12. It can be seen from cumulative gas production and gas rate is higher in the beginning but equalizes in the end. This can be explained by simulator not accounting FR filter cake, but in the field it might be needed some time to clean up from residue and eventually reach necessary rate.

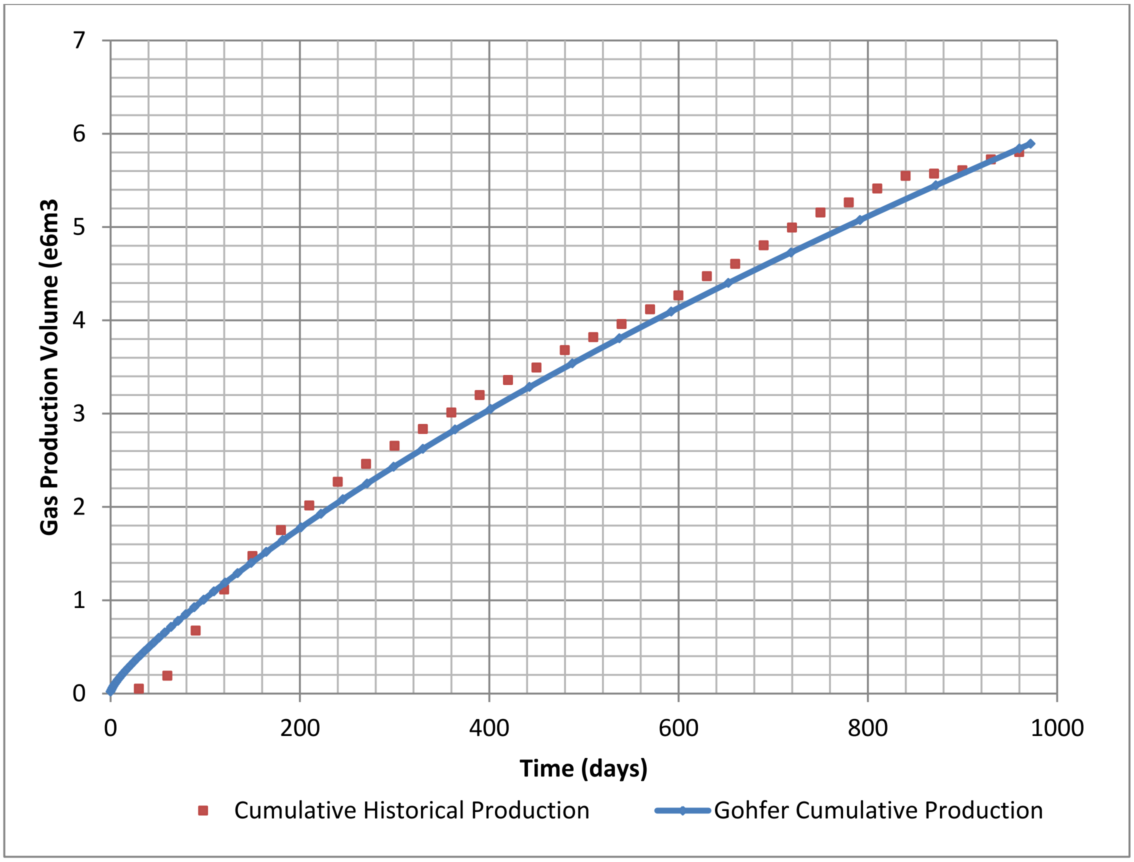

Figure 2-10. Gas production history match for GOH FER model

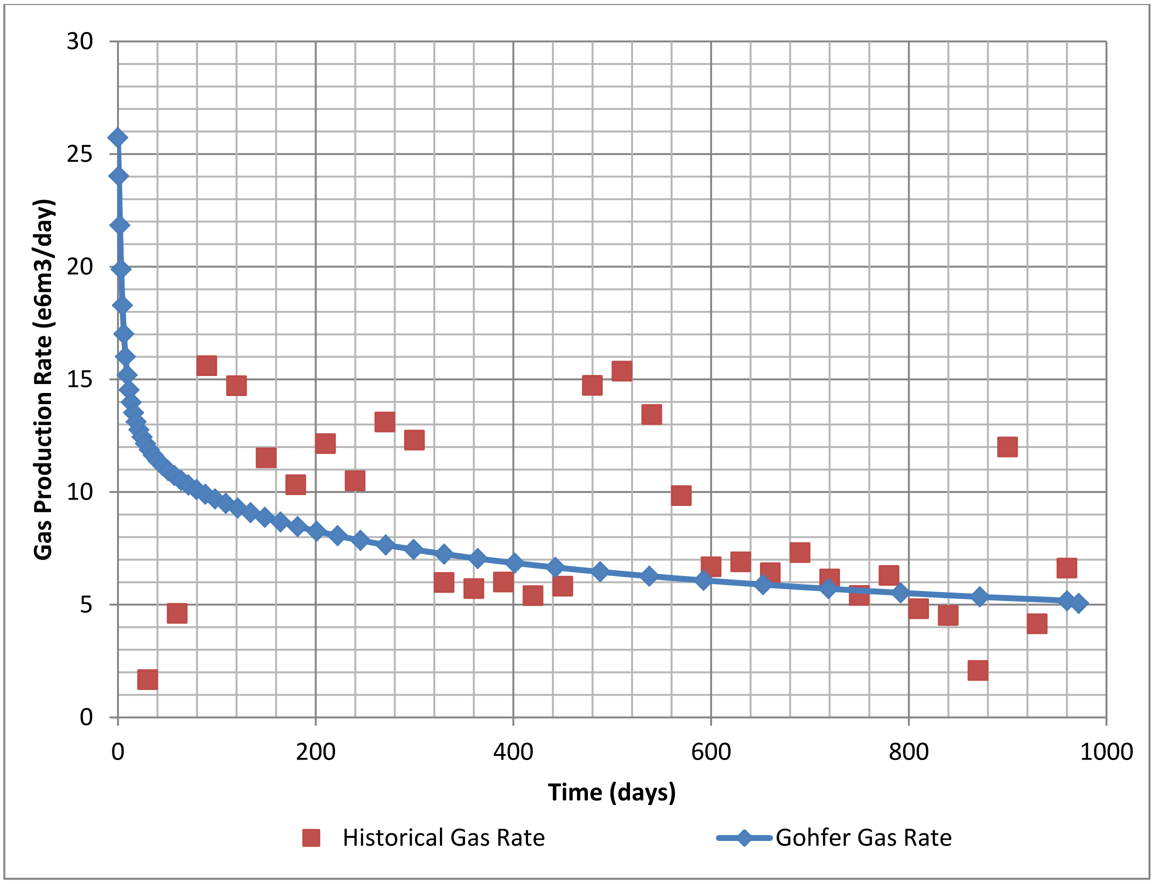

Figure 2-11. Gas rate history match for GOHFER model

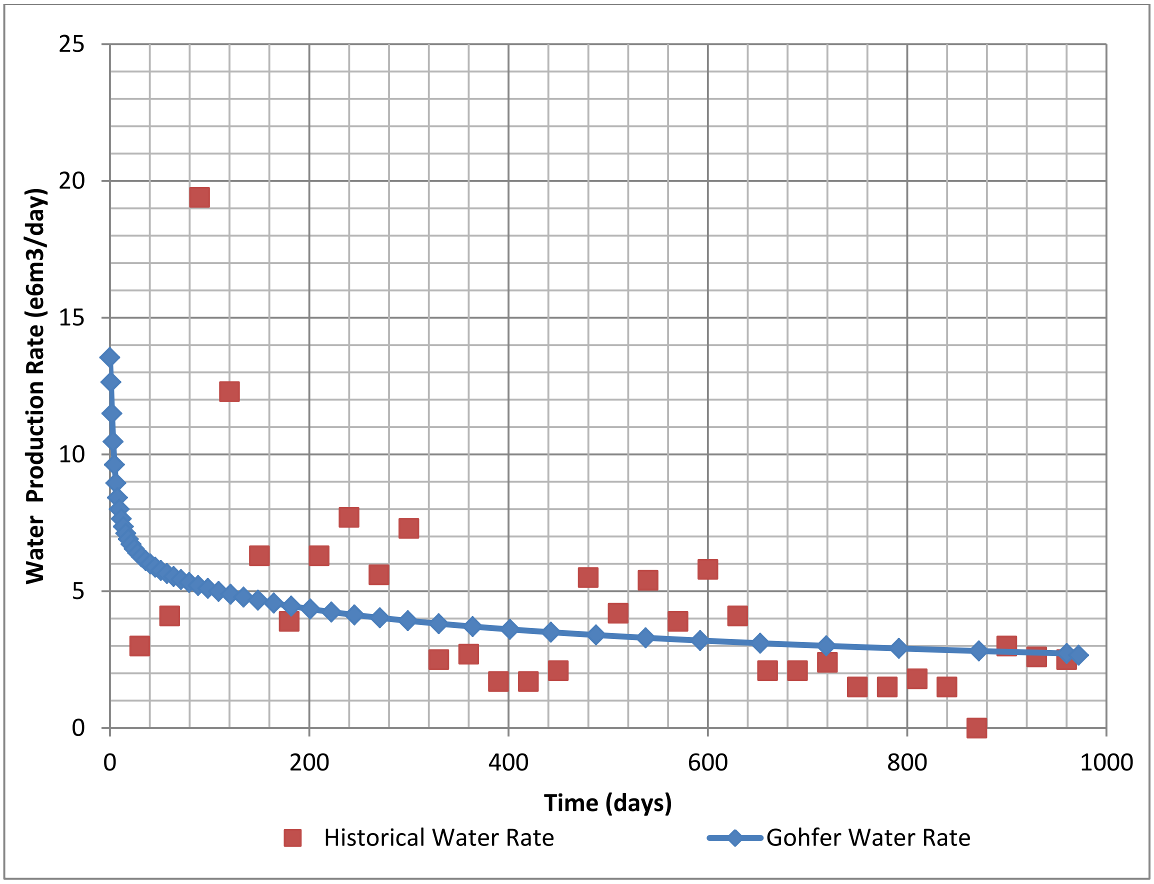

Figure 2-12. Water rate history match for GOHFER model

Each stage has 6 perforation clusters except stage 6 due to its low permeability. Net pay map shows that lower Duvernay is divided from middle Duvernay by impermeable clay layer and most of the stage 6 was drilled in impermeable zone. According to the table 2-6 most of the perforations had fracture growth but not all of them had proppant. This can be explained by fluid leak off to other perforations when there are pressure fluctuations. As an example, Figure 2-13 shows 2D view of one of traverse propped fractures, there is limitation in fracture height due to impermeable layers in the pay zone.

Finally, Figure 2-14 shows top view of the grid output of 57 tranvserse fractures. Toe and heel fractures have less width and height than stages in heel zones due to toe being separated in different low thickness pay zone, however fracture length is slightly higher than heel stage fractures.

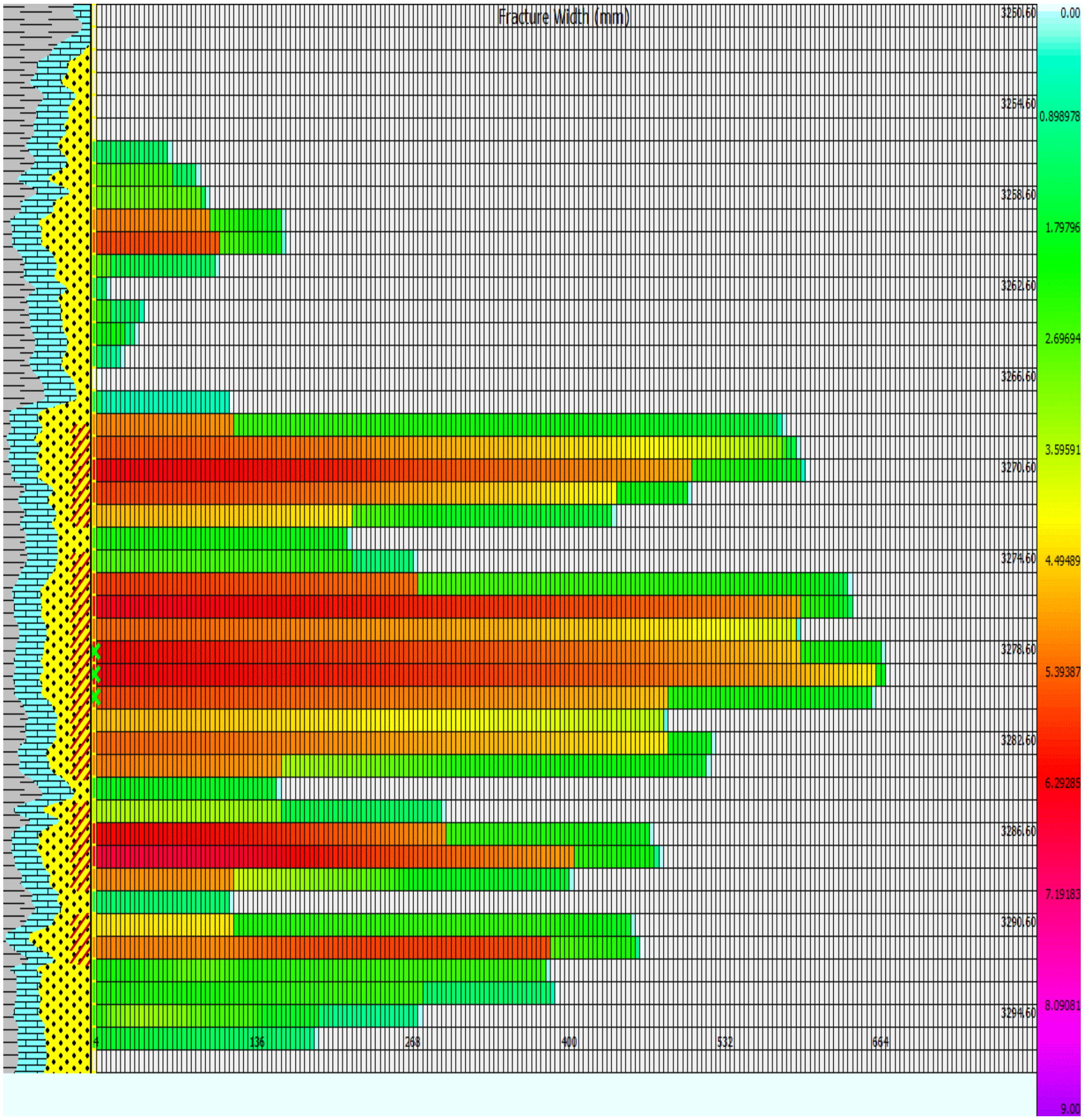

Figure 2-13. Slickwater transverse fracture 1

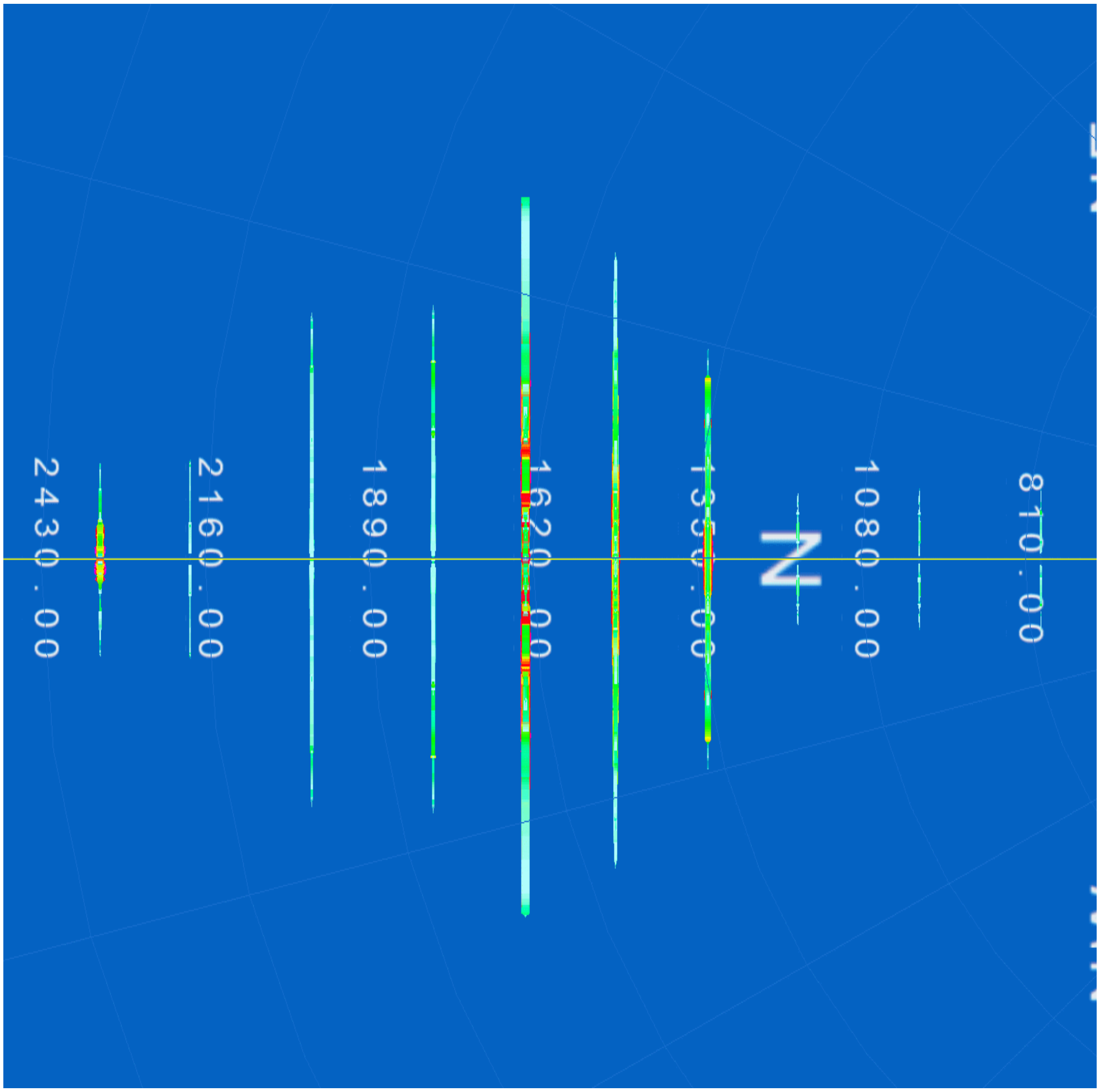

Figure 2-14. Top view of fracture profiles of all stages

2.3 Numerical simulation with CMG

Once GOHFER hydraulic fracture model was created, those models for each 10 stages were imported into the CMG IMEX black oil model. Detailed imported models were added to appendix section of the thesis. Model had 1 well with 10 stages and dimensions were 3050 x 1050 x 30 m. Reservoir properties were taken from table 2-2 from previous section. CMG model had regular Cartesian grid system which can be discretized into 61*50 m for I direction, 21*50 m for J direction and 1*30 m for K direction as shown in Figure 2-15. Two porosity regions consisting domain was used to encompass fracture network and matrix blocks called dual porosity model. Warren and Root developed analytical transfer function that accounted for communication of two domains matrix and fracture. (Warren, 1963)

Initial pressure and depth were acquired from Operator Company which summarized in table 2-2. There is no bottom water zone and due to that gas/water contact was outside of the reservoir boundary. The initial phase saturations are enacted as endpoint saturations in the relative permeability curves which can be seen in Figure 2-16. In simulation model rock is water wet and no transition zone is assumed in the model.

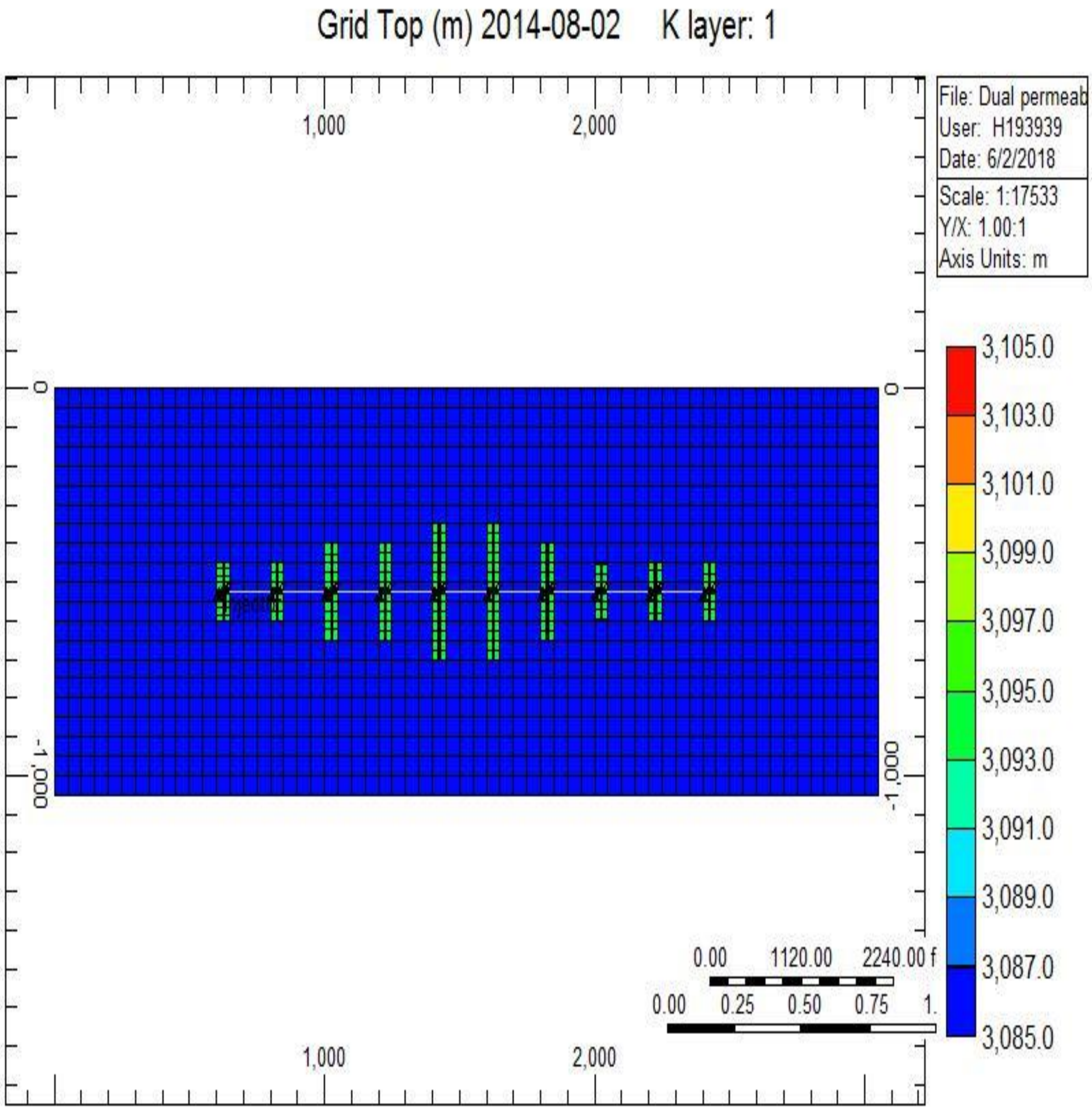

Figure 2-15. Top view of CMG 3D model

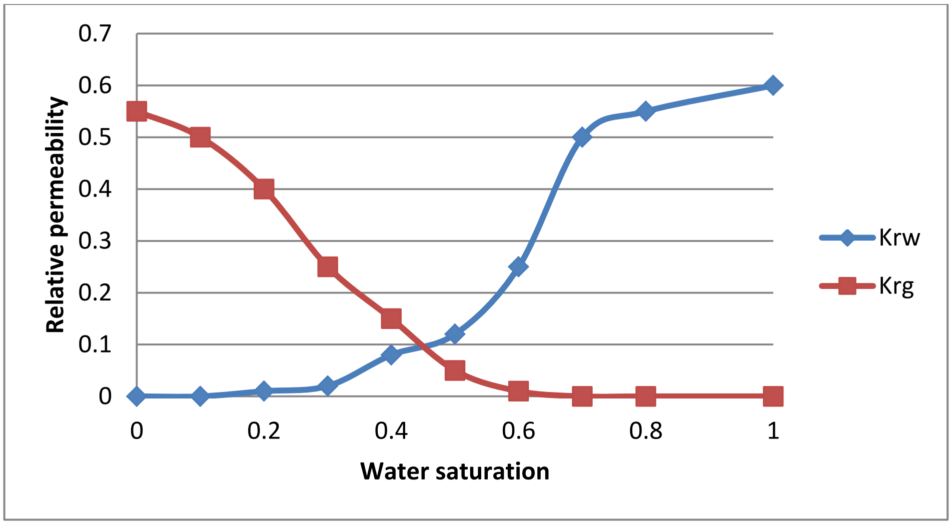

a) Matrix relative permeability

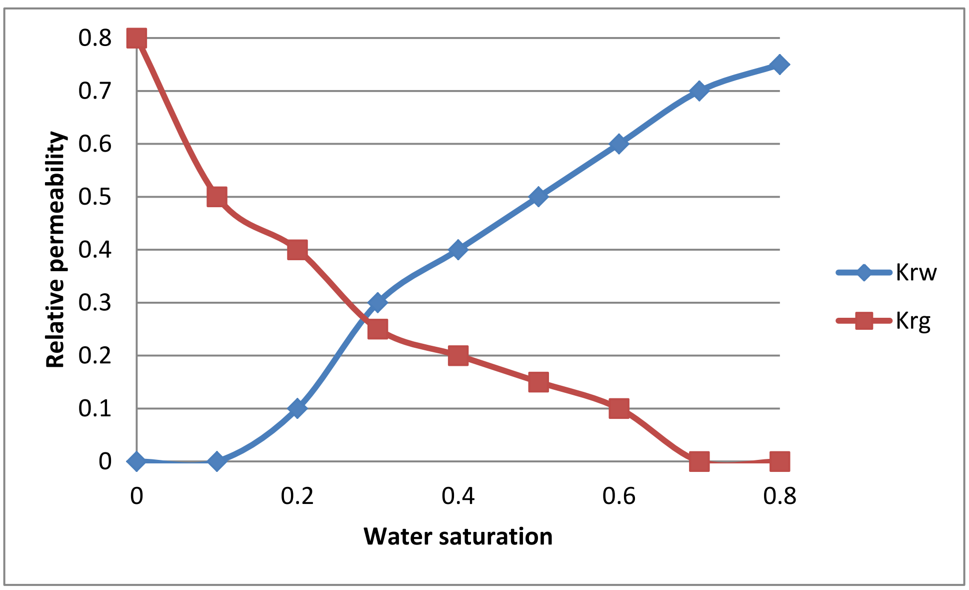

b) Fracture relative permeability

Figure 2-16. Matrix and Fracture relative permeability curves.

Due to low permeability capillary pressure can be high a 10000 psi in shale formations according to Byrnes. (Byrnes, 2011) For our simulation capillary pressure was provided from the company which can be seen in Figure 2-17. Due to high-frac face water saturation is not in equilibrium and capillary forces act to imbibe the fluid into the reservoir which can be proven in the simulation.

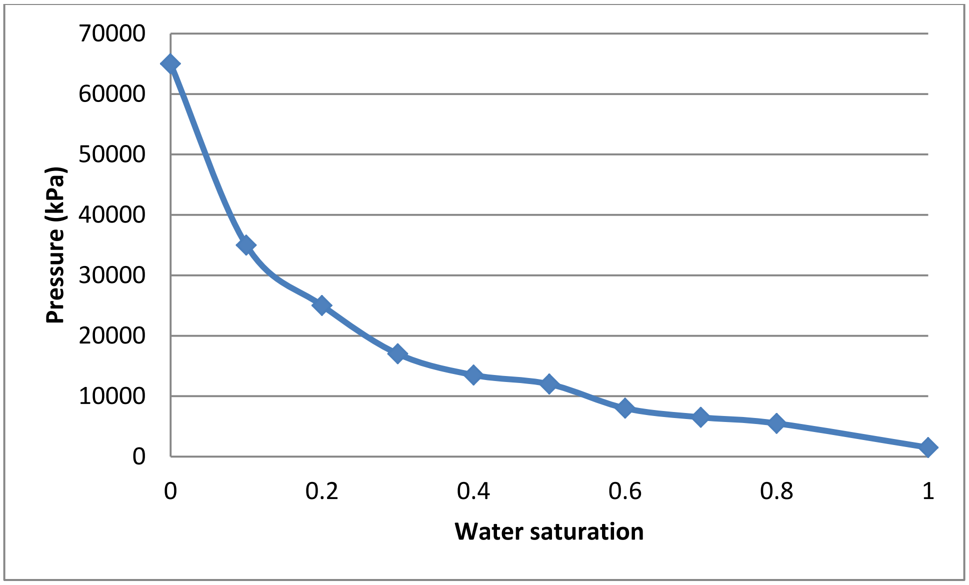

Figure 2-17. Capillary pressure curve

2.3.1 Grid refinement

CMG model is based on finite difference mathematical approximation where accuracy is of the approximation depends on the grid system. In order accurately predict fluid flow and nearby fracture, local grid refinement (LGR) technique was used. LGR technique models hydraulic fracture at its finest setting and grid size gradually becomes larger as it gets farther from fracture as shown in Figure 2-18.

Propped fracture length was different for each traverse and each stage roughly varying from 4m to 300 m. Fracture width were ranging from 1 to 7 mm, however CMG increased fracture width to 600 mm by decreasing the permeability due to CMG limitation. Following formula was used in grid refinement:

$$kf \times wf = ke \times wblock \qquad \text{… Equation 2 (CMG, 2017)}$$

For example, fracture with permeability of 10,000 md and 5 mm in width, can be converted to a fracture with permeability of 50 md but and 1m in width in CMG. Conductivity in both cases is equal to 50md-m.

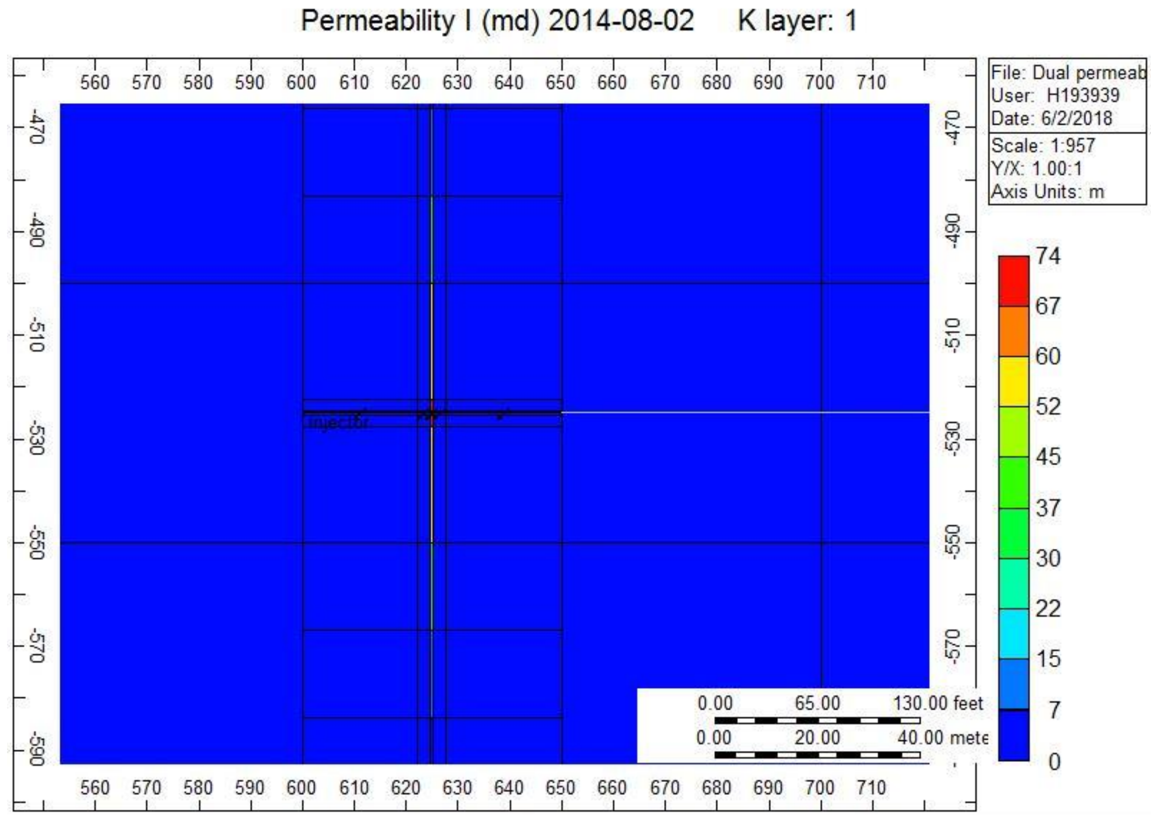

Figure 2-18. Grid refinement of stage 1.

In table 2-5 which shows pumping schedule that proppant concentration was stepped up at least after 1 pipe volume is pumped. This technique is used in hydraulic fracturing operations to prevent screen outs. Since proppant concentration is lowest in the beginning and highest in the end of the fracturing operations, fracture conductivity is lowest at the tip and highest near wellbore. Dividing of gridlock by changing conductivity will describe non-uniform fracture conductivity.

2.3.2 History matching

In Figure 2-19 water and gas production curves were matched as much as possible however there is slight discrepancy. Due to lack of pressure data, curves were matched as best as can. Gas production curve has lower production in the beginning in history and higher in the middle period, but eventually matches in the end.

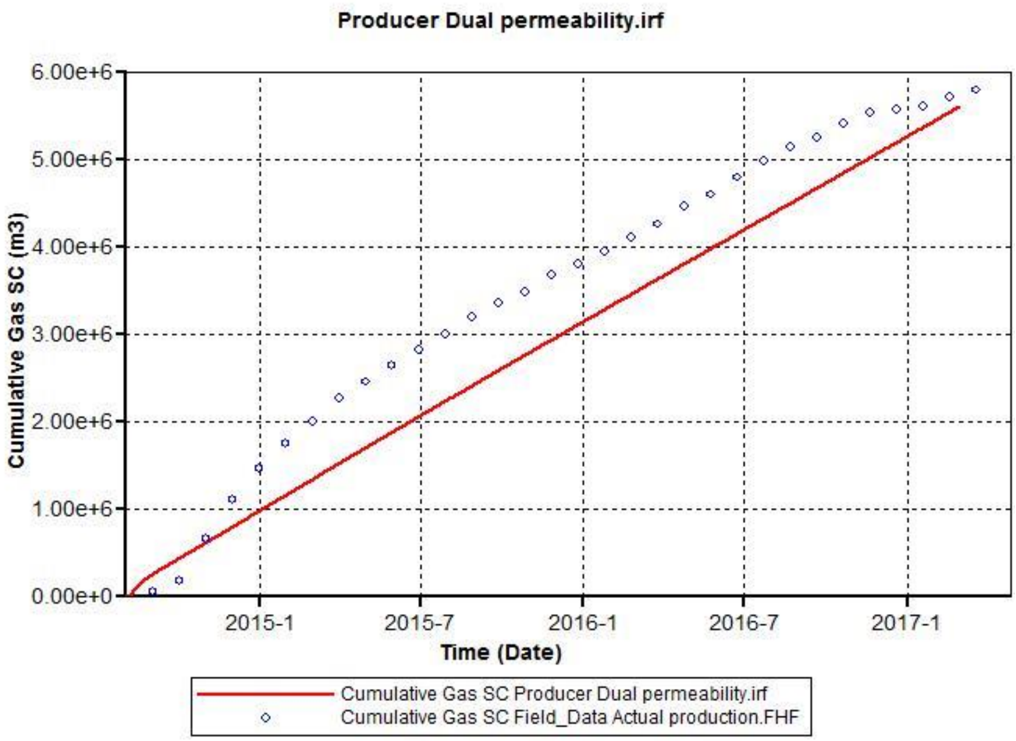

Figure 2-19. Gas production history match in CMG

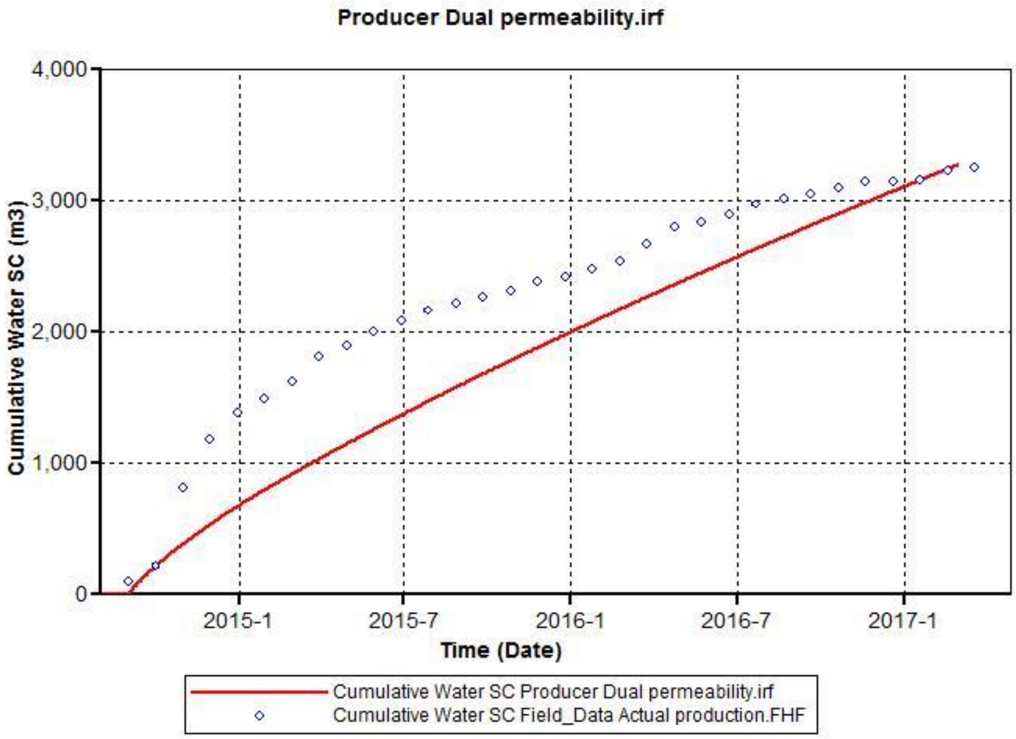

Figure 2-20. Water production history match in CMG

Figure 2-20 shows water production history. Also, history matching procedure was performed where the gas and water rates were matched. Water rate and gas rate trends were matched but gas rate drops sharper in simulation than field data due to some repairs to the well.

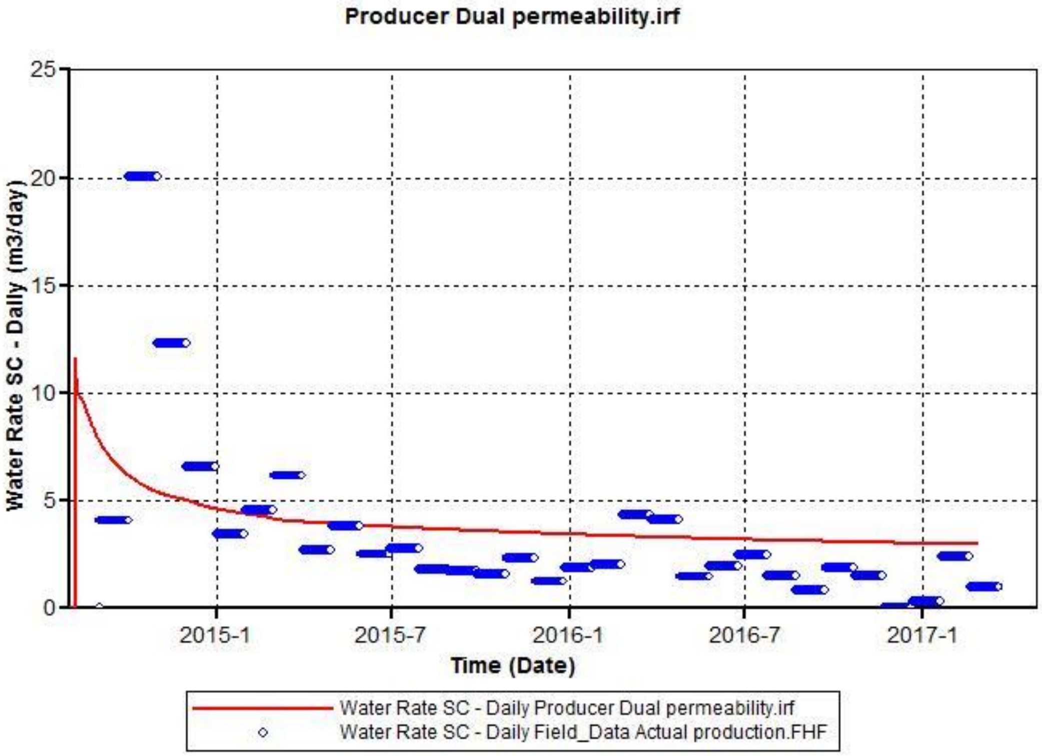

Figure 2-21. Gas production rate history match in CMG

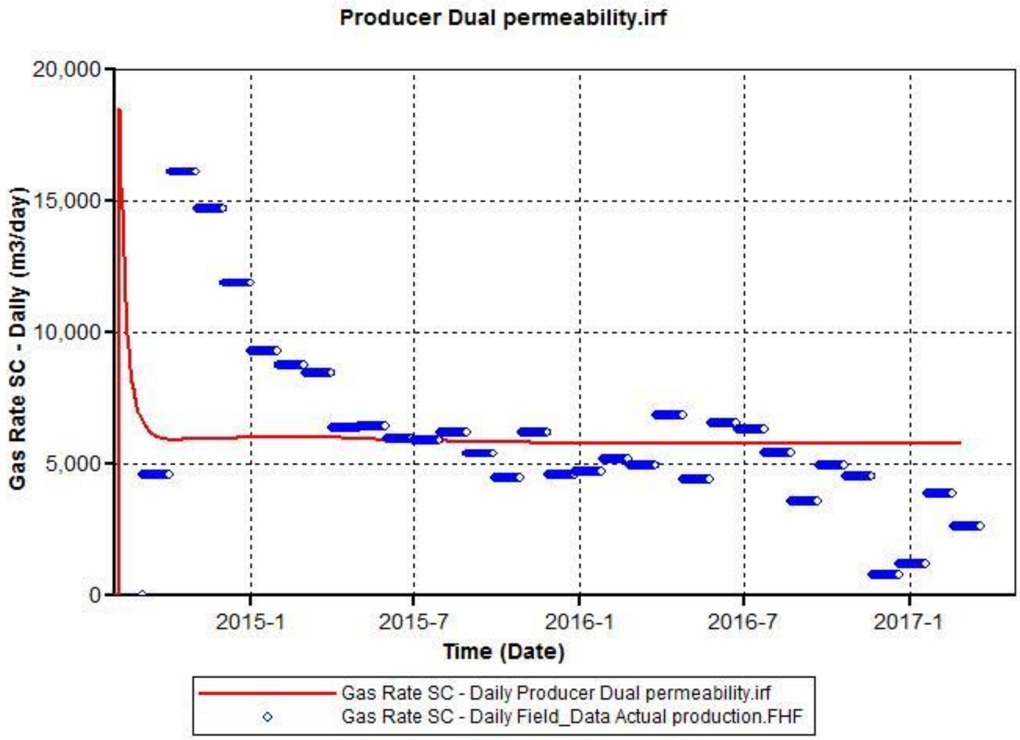

Figure 2-22. Water production rate history match in CMG

2.3.3 Results and discussion

Numerical model that was built in CMG incorporating GOHFER fracture model was a base model for water based hydraulic fracturing model. Incorporation of GOHFER model with CMG gave us accurate numerical model which considered geomechanical aspects of hydraulic fractures rather than using generic hydraulic fracture built in CMG.

Injection of 15,000 m3 of water was performed over 1 week rather than 2 days in order water soak into formation. That can be seen from Figure 2-23 that pressure in fracture and around it went up 70 Mpa whereas reservoir pressure is 55 Mpa. Figure 2-24 shows pressure distribution after 3000 days of production where reservoir dropped in and around fracture. Pressure dropped until 35000 Mpa in some fracture and 45000 around fracture.

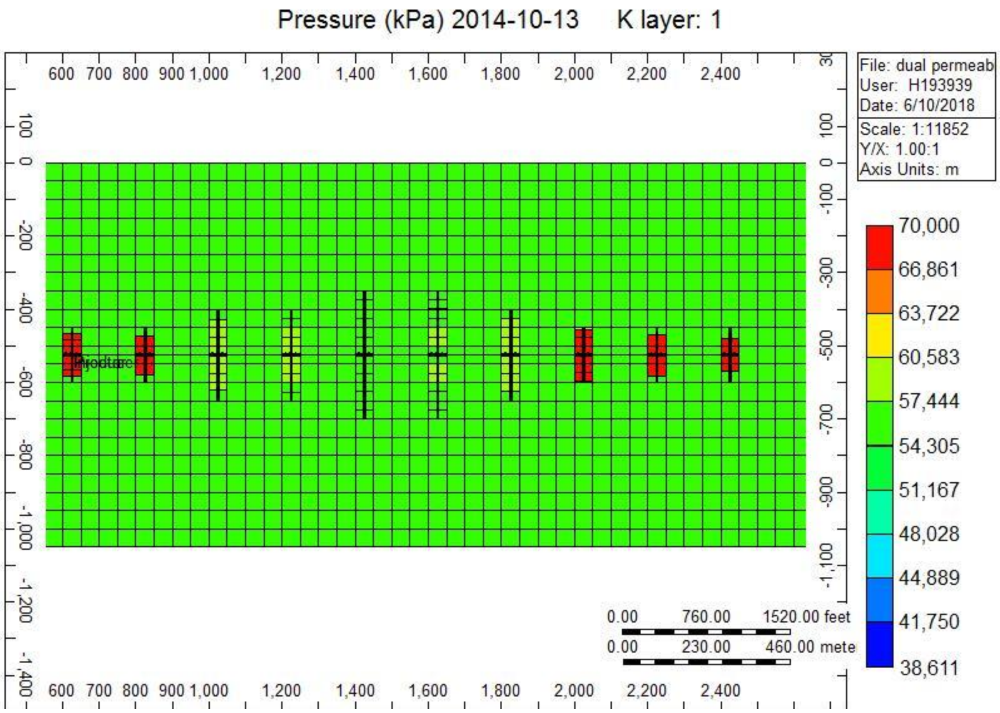

Figure 2-23. Pressure distribution after 2 months of production

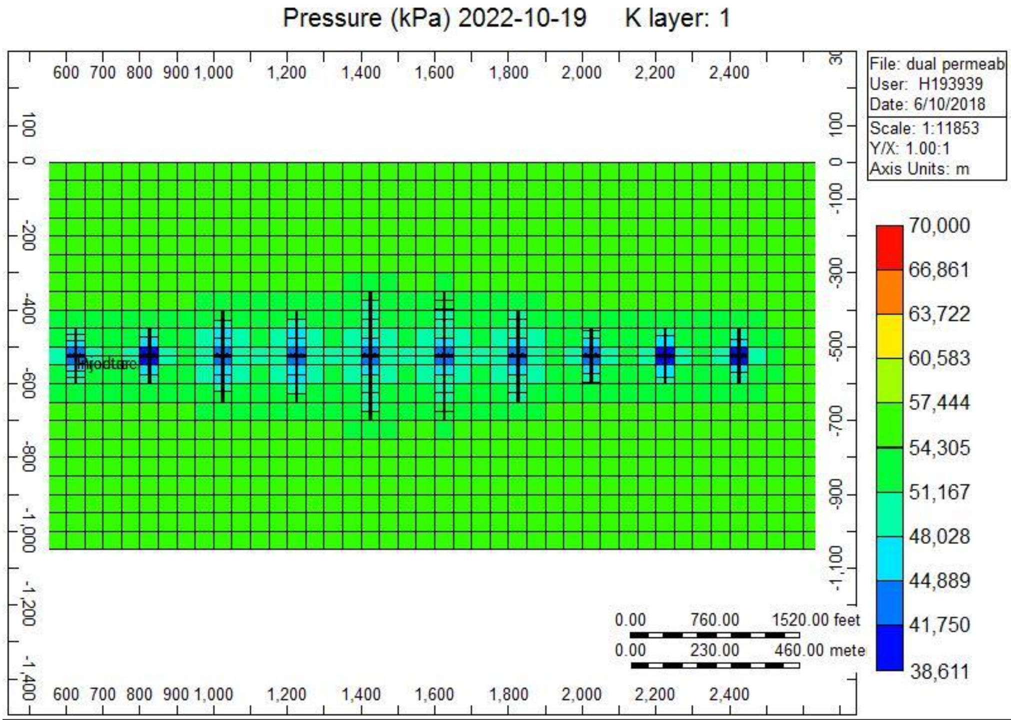

Figure 2-24. Pressure distribution after 3000 days of production

Lastly the main important finding of simulation is water saturation in and around hydraulic fractures. 3 zones were investigated: zone 1 is fracture, zone 2 is surrounding area up to 2m and zone 3 is up to 10 m. Figure 2-25 shows water saturation went up to 95% inside of fracture and ranges from 60% to 90% around the fracture (up to 2m) depending how far from the wellbore.

Figure 2-26 shows water saturation distribution in and around fracture after 943 days of production. High capillary forces pushed water from fracture deep into reservoir by increasing water saturation but decreasing water saturation inside of fracture. Fracture water saturation and surrounding area of the fracture up to 2m came to equilibrium by imbibing into formation which is 60%, however there was still saturation difference between fracture and surrounding area up to 10 m. Lastly, Figure 2-27 shows water saturation distribution in and around fracture after 3000 days. Water saturation is evenly distributed between fracture and water imbibing zone up to 10 m from fracture which was equal to 50%.

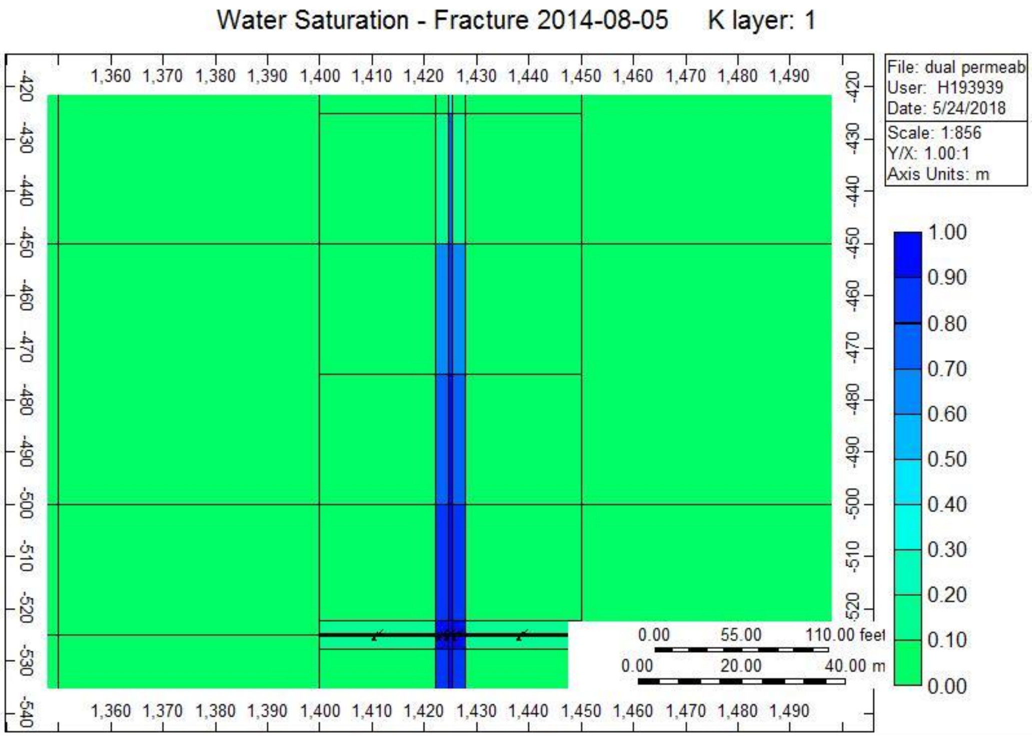

Figure 2-25. Water distribution in fracture after stimulation

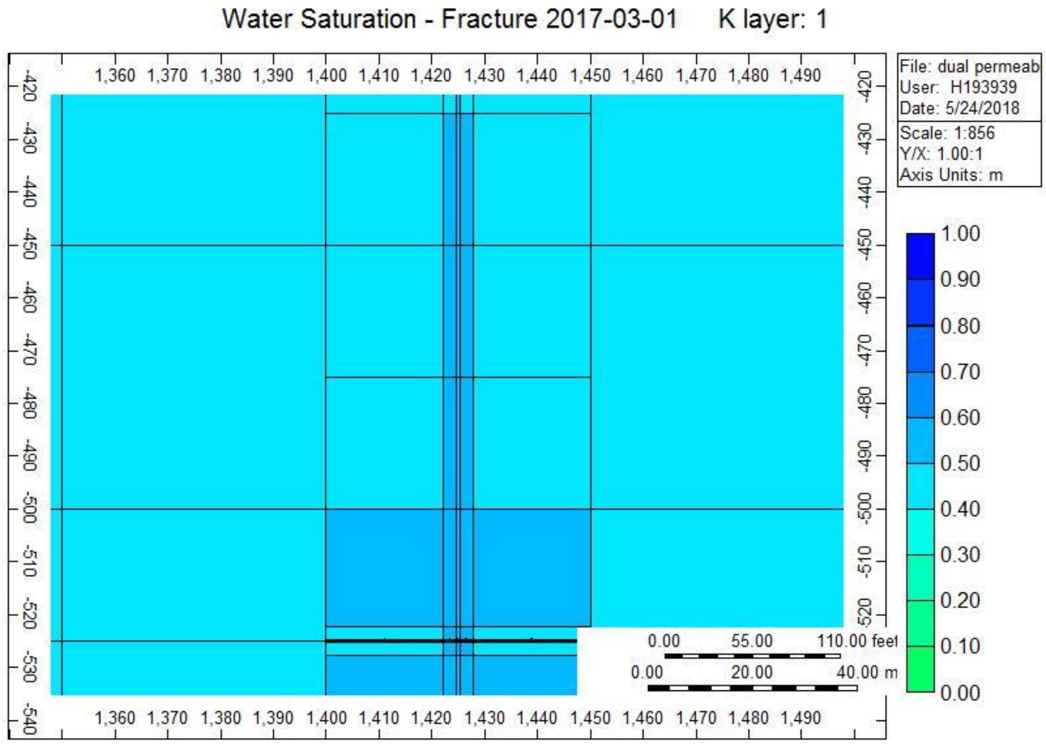

Figure 2-26. Water distribution in fracture after 943 days of production

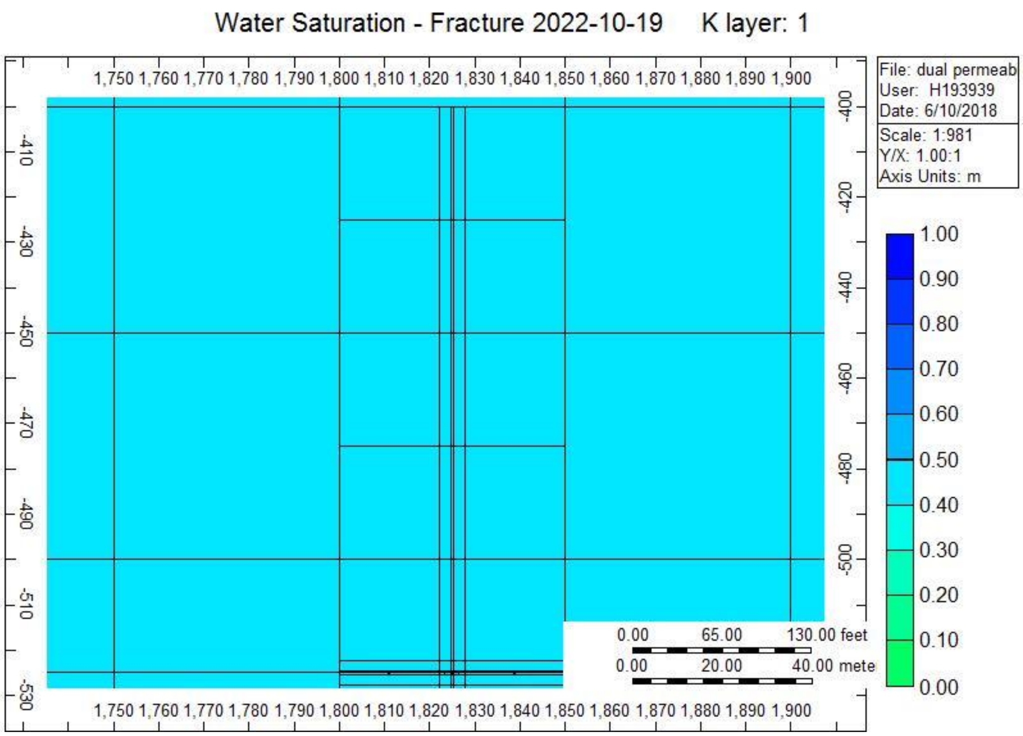

Figure 2-27. Water distribution in fracture after 3000 days of production

In the end, cumulative production of water and gas was analyzed, Figure 2-28 shows that after 3000 days 18.69 million m3 of gas was produced and this data later will be used to compare with CO_2 hydraulic fracturing gas production data. Figure 2-29 shows cumulative water production of 8000 m3 which is still only 53% of the injected water, assuming that all produced water is fracturing water. These base results generated using slickwater model will be compared to CO_2 hydraulic fracturing model in order investigate effect of CO_2 as a fracturing fluid on fracture properties and well production performance.

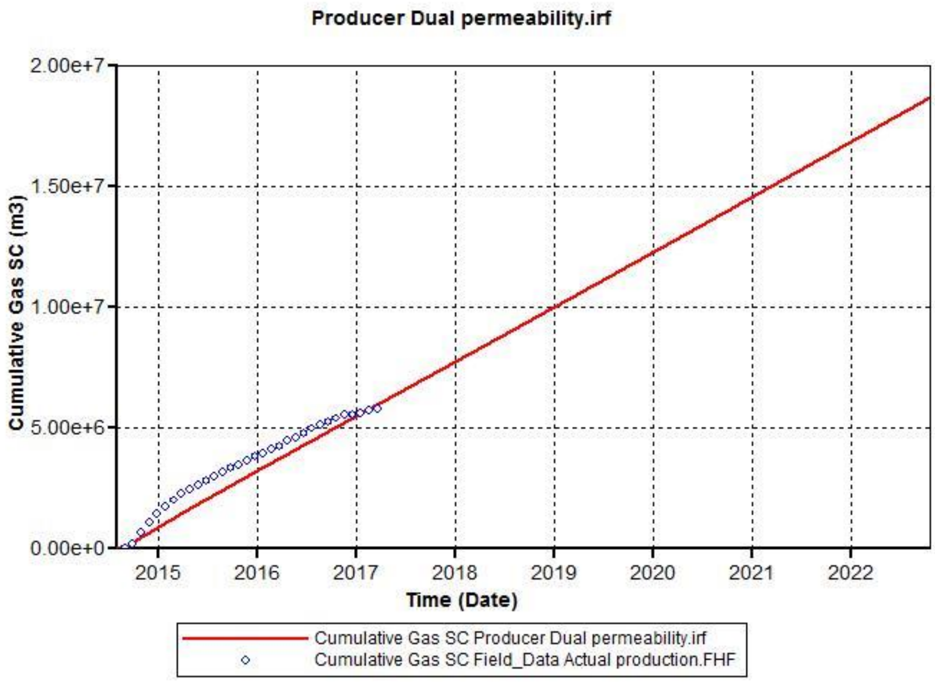

Figure 2-28. Gas Production after 3000 days

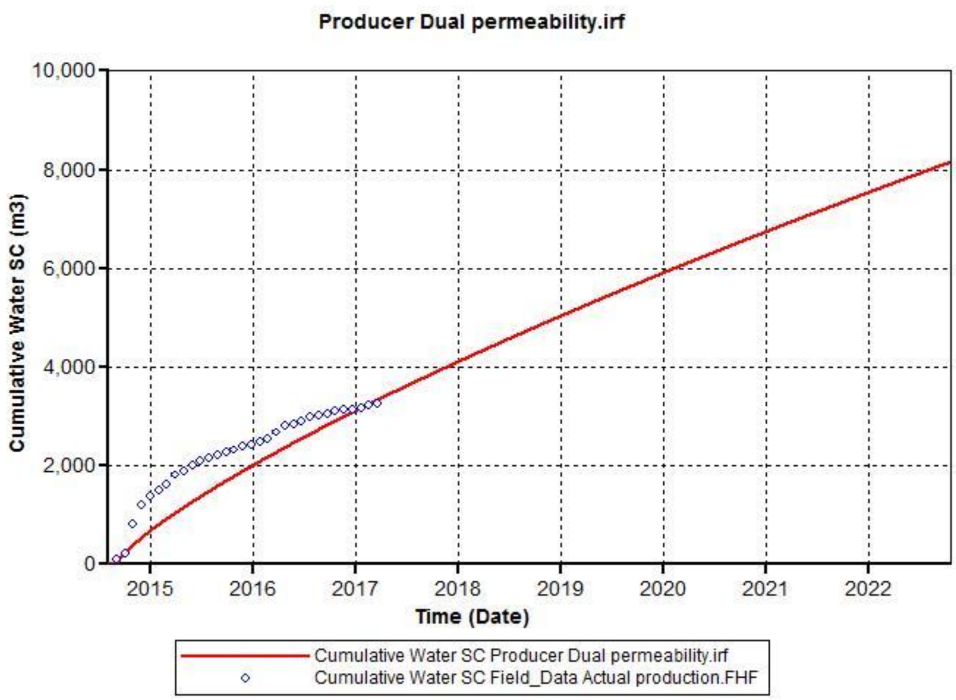

Figure 2-29. Water Production after 3000 days

CHAPTER 3: CO_2 based hydraulic fracturing

3.1 Introduction

In this chapter it is discussed about CO_2 based hydraulic fracturing. Since there is a problem with too much emission of CO_2 all over the world, CO_2 based hydraulic fracturing can solve several problems like permanently sequestering CO_2 underground, conservation of water and enhancement of oil production of well by being inert fluid and causing small damage to reservoir comparing to water. Base slickwater model designed in chapter 2 has been modified with CO_2 fracturing fluid in order to investigate effect of CO_2 to fracture parameters and effect on gas production.

3.2 Literature review

The first use of CO_2 as a fracturing fluid happened in 1970s and it was implemented as part of energized fluid system in North America. Most of the time it was used in depleted and water sensitive formations. 1980s liquid CO_2 became popular and effective hydraulic fracturing fluid in low permeability gas reservoirs. (Lillies, 1982) Moreover, CO_2 didn't affect relative permeability curves by changing saturations in invaded zone, however limited amount of proppant could be placed due to low viscosity. (Sinal, 1987) In 1990's densometers started to be used, this allowed to pump higher concentrations of the sand with CO_2. (Tudor, 1994) CO_2 based fracturing fluid was used in wells with different permeability ranging from 0.1 mD to 10 Darcies, different temperatures ranging from 10 to 100 degrees Celsius an experimented over 1000 wells. (Gupta, 1998) Also, CO_2 was compared with N_2 as a waterless fracturing fluid in shale gas formation and CO_2 showed significant improvement in gas production comparing to N2. (Mazza, 2001) CO2 foam based fracturing fluids are more common rather than pure CO2 since foams can carry more proppant into fracture. Good and economically viable CO2 viscosifier is still a challenge of pure CO2 hydraulic fracturing. (Enick, 2012)

According to the above references, for the past 40 years there are a lot of CO2 hydraulic fracturing performed on vertical wells, but there are not much information about fracturing with CO2 in horizontal wells except water sensitive Montney shale in Canada. (Reynolds, 2014) CO2 fracturing was only 2.4% of all US stimulation treatments for the period of 2011-2013 and approximately 30% of treatments in Canada according to FracFocus report. (Ribeiro 2013, Patel 2014)

Simulation studies with CO2 hydraulic fracturing started since 1979 when first CO2 hydraulic fracturing operations were attempted. Settari tried to simulate fracturing model low-viscosity fluid similar to CO2 and tried to match CO2 frac field data. (Settari, 1987) Due to low viscosity of CO2 proppant transport in hydraulic fractures was modeled and investigated with UTFRAC-3D by Gadde. (Gadde, 2004) In 2005 Li modeled tool erosion in gravel-pack and frack-pack applications using computational fluid dynamics simulator. (Li, 2005) 3D planar fracture simulator was used to model horizontal fracture growth based on vertical transverse isotropic model in the Haynesville shale formation by Farinas in 2013. (Farinas, 2013) Lastly, Fang simulated pressurized cracks and hydraulic fracturing in with super critical carbon dioxide using Universal Distinct Element Code. (Fang, 2014)

3.2.1 Properties of CO_2

CO_2 is very unique fluid due its physical properties. It exists in liquid, gas, solid or supercritical form depending on pressure and temperature. Usually when its brought to field CO_2 is stored in vessel at 2 MPa and -35 degrees Celsius. Once it mixed with sand at surface and pumped through high pressure pumps it will go up to 35-40 MPa but at surface temperature. Then it will go downhole and enter into formation where temperature will increase up to bottomhole temperature and pressure will equalize wit reservoir pressure. Lastly, during flow back pressure will decrease. For usual fracturing operations density of CO_2 is 1-1.2 g/cm3 and viscosity is 0.02--.16 cp. (Gupta, 1998)

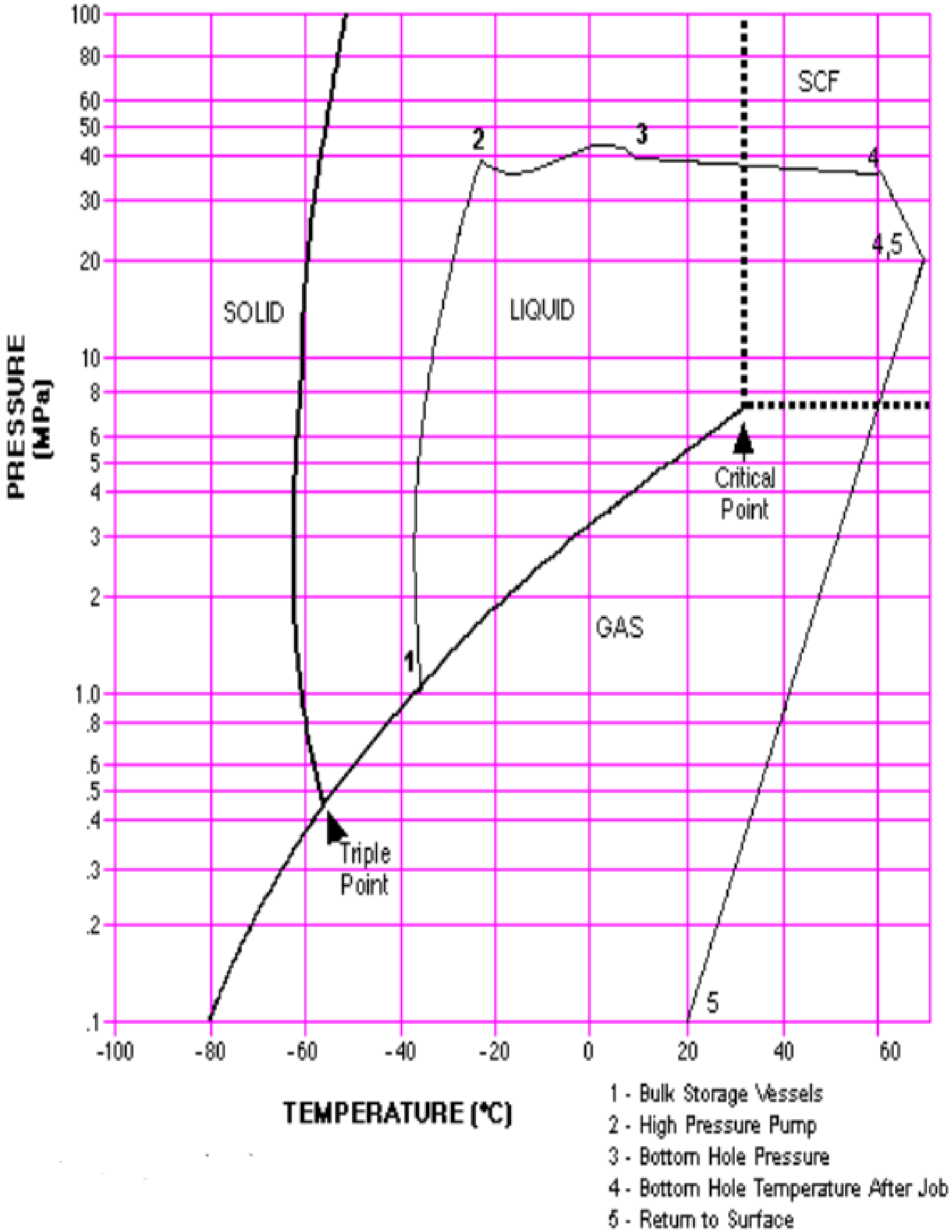

Figure 3-1. CO2 pressure vs Temperature (Gupta, 1998)

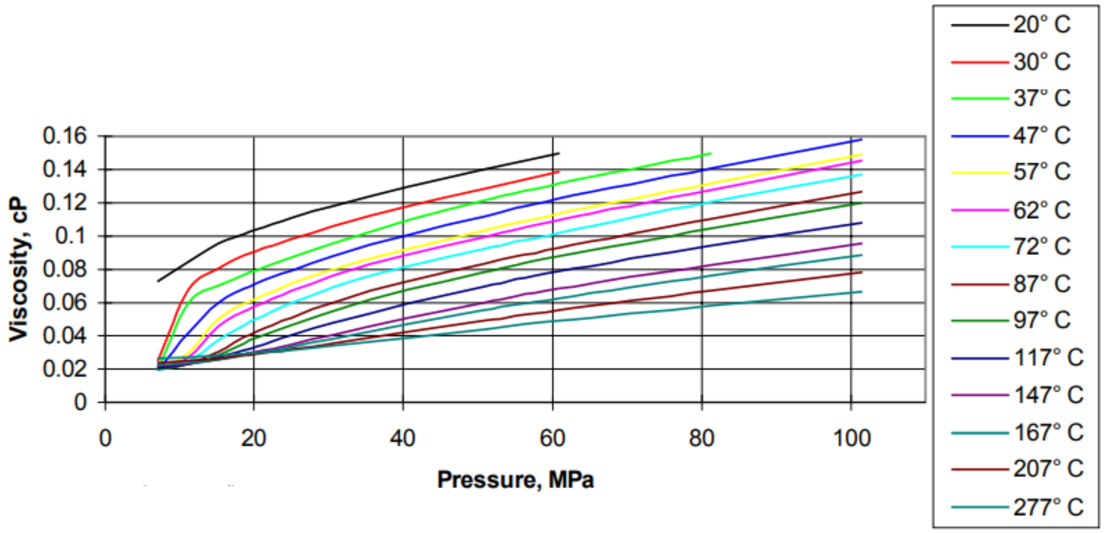

Figure 3-2. Viscosity of CO2 at different pressures(Gupta, 1998)

3.3 GOHFER Fracture design

Slickwater fracture design was base model which already had been validated and it was used for different scenarios by modifying pumping schedule. First case was hybrid CO_2 slickwater and second one was using pure CO_2 as a fracturing fluid.

3.3.1 Hybrid CO_2 slickwater scenario

In first case slickwater pumping schedule was modified by adding 100 m^3 of pure CO_2 right after acid stage which can be seen in table 3-1.

Table 3-1. Hybrid Slickwater CO2 pumping schedule

Stage #	Elapsed Time hh:mm:ss	Stage time mm:ss	Fluid	Proppant	Stage volume m3	Cum. Volume m3	Rate m3/min	Prop. Conc. kg/m3	Cum. Prop. Kg
1	0:00	10:00	HCL 15%	None	30	30	3	0	0
2	10:00	23:20	CO2 liquid	None	100	130	3	0	0
3	33:20	3:13	Slickwater	None	15	145	14	0	0
4	36:33	2:55	Slickwater	100 Mesh	40	185	14	50	2000
5	39:28	4:02	Slickwater	100 Mesh	55	240	14	75	6125
6	43:30	4:27	Slickwater	100 Mesh	60	300	14	100	12125
7	47:57	4:43	Slickwater	100 Mesh	63	363	14	125	20000
8	52:40	7:21	Slickwater	40/70 Badger	100	463	14	75	27500
9	1:00:00	9:16	Slickwater	40/70 Badger	125	588	14	100	40000
10	1:09:17	9:08	Slickwater	40/70 Badger	122	710	14	125	55250
11	1:18:24	9:04	Slickwater	40/70 Badger	120	830	14	150	73250
12	1:27:28	8:23	Slickwater	40/70 Badger	110	940	14	175	92500
13	1:35:51	7:41	Slickwater	40/70 Badger	100	1040	14	200	112500
14	1:43:32	7:45	Slickwater	40/70 Badger	100	1140	14	225	135000
15	1:51:17	3:43	Slickwater	40/70 CRC	50	1190	14	100	140000
16	1:55:00	2:51	Slickwater	40/70 CRC	38	1228	14	125	144750
17	1:57:51	2:39	Slickwater	40/70 CRC	35	1263	14	150	150000
18	2:00:30	4:09	Slickwater	None	58.08	1321	14	0	150000
19	2:04:38	10:00	Slickwater	None	0	1321	0	0	150000

In table 3-2 fracture parameters obtained with hybrid CO_2 slickwater were summarized. Average fracture lengths were longer for 5% which was 1166 m comparing to 1113m, average fracture height remained the same 16.6 m, average fracture width increased for 29% which was 4.2 mm comparing to 3 mm, however propped fracture length decreased for 11% which was 113 m comparing to 126 m.

Figure 3-3 shows the fracture width distribution along the length of the fracture. Slickwater width was very uniform along the all length of the fracture in Figure 2-13 however pumping just 100 m3 of pure CO_2 before main treatment increased maximum width of the fracture for 5 mm. Orange spots are 10-12 mm wide fractures and yellow ones 8-10 mm wide fracture sections.

Using CO_2 as a pad fluid is advantageous since low viscosity fluid has helped to have lower breakdown and extension pressures; moreover it helps to have a fracture complexity which has given more access to reservoir.

Table 3-2. Hybrid Slickwater CO2 fracture parameters

Fracture		Gross Frac Length.M	Proppant Cutoff Length.M	Fracture Height.M	Average Proppant Conc. kg/m²	Average Fracture Width. mm	Max Fracture Width. mm
1	Transverse 6	2051.9	243.8	24.0	3.4	6.0	16.9
	Transverse 5	890.4	111.9	12.0	1.0	3.2	8.5
	Transverse 4	1529.2	194.0	16.0	2.4	4.7	10.5
	Transverse 3	174.2	22.4	12.0	0.1	1.7	6.2
	Transverse 2	1819.6	211.4	20.0	3.0	5.5	12.0
	Transverse 1	19.4	2.5	4.0	0.2	1.9	2.2
2	Transverse 6	1800.2	206.5	12.0	3.5	5.5	10.6
	Transverse 5	987.2	124.4	12.0	1.4	3.6	6.2
	Transverse 4	1142.1	144.3	12.0	2.5	4.0	8.7
	Transverse 3	1045.3	131.8	12.0	1.4	3.6	6.2
	Transverse 2	1122.7	141.8	12.0	2.3	3.8	8.6
	Transverse 1	1567.9	179.1	12.0	3.4	5.1	12.4
3	Transverse 6	1858.3	218.9	20.0	3.1	5.7	11.4
	Transverse 5	813.0	102.0	4.0	1.5	3.3	7.1
	Transverse 4	1316.3	166.7	20.0	2.1	4.2	8.8
	Transverse 3	832.4	104.5	4.0	1.3	3.3	6.3
	Transverse 2	1084.0	131.8	4.0	2.3	3.9	8.3
	Transverse 1	1703.4	196.5	4.0	3.1	5.4	10.8
4	Transverse 6	425.9	2.5	0.0	0.0	2.0	2.5
	Transverse 5	1819.6	213.9	20.0	3.0	5.5	11.2
	Transverse 4	1238.9	156.7	16.0	1.9	3.9	8.8
	Transverse 3	851.7	102.0	4.0	1.4	3.4	6.7
	Transverse 2	1238.9	156.7	16.0	1.8	4.0	8.9
	Transverse 1	1587.3	186.6	4.0	2.8	5.1	11.9
5	Transverse 6	2129.3	256.2	32.0	2.8	5.9	14.2
	Transverse 5	677.5	87.1	16.0	0.2	2.1	5.1
	Transverse 4	696.9	89.5	16.0	0.2	2.3	5.1
	Transverse 3	174.2	2.5	0.0	0.0	1.7	2.2
	Transverse 2	154.9	2.5	0.0	0.0	1.6	2.2
	Transverse 1	2032.5	243.8	4.0	2.5	5.8	11.2
6	Transverse 3	2322.8	296.0	40.0	1.6	5.6	11.5
	Transverse 2	793.6	67.2	24.0	0.1	2.0	4.3
	Transverse 1	1838.9	213.9	44.0	4.2	6.2	18.1
7	Transverse 6	1780.8	194.0	28.0	3.2	5.9	17.6
	Transverse 5	1238.9	151.7	24.0	2.5	5.0	19.4
	Transverse 4	1006.6	104.5	12.0	2.0	3.7	11.2
	Transverse 3	1374.4	141.8	12.0	3.2	5.1	16.1
	Transverse 2	174.2	19.9	12.0	0.5	1.1	3.6
	Transverse 1	19.4	2.5	4.0	0.2	1.9	2.2
8	Transverse 6	1606.6	27.4	24.0	10.9	4.5	23.3
	Transverse 5	1045.3	17.4	24.0	11.7	4.4	22.3
	Transverse 4	1025.9	29.8	24.0	9.5	5.0	21.6
	Transverse 3	1142.1	32.3	28.0	11.4	5.7	26.6
	Transverse 2	967.9	104.5	24.0	4.8	4.7	13.2
	Transverse 1	1413.1	32.3	28.0	10.3	5.6	24.5
9	Transverse 6	1645.4	22.4	28.0	10.6	4.7	24.2
	Transverse 5	1045.3	22.4	28.0	9.9	4.6	20.6
	Transverse 4	1238.9	64.7	28.0	6.5	5.1	23.2
	Transverse 3	987.2	24.9	24.0	10.3	4.3	20.5
	Transverse 2	967.9	84.6	28.0	6.3	5.7	14.5
	Transverse 1	1509.8	29.8	40.0	9.7	5.5	22.3
10	Transverse 6	1761.5	181.6	28.0	3.7	6.0	18.0
	Transverse 5	754.9	72.1	8.0	2.1	3.6	13.3
	Transverse 4	154.9	12.4	8.0	0.8	1.7	7.6
	Transverse 3	1335.6	136.8	8.0	2.8	4.4	14.1
	Transverse 2	948.5	107.0	8.0	2.3	3.7	12.2
	Transverse 1	1587.3	134.3	12.0	4.1	5.3	17.0
Average		**1166.2**	**113.4**	**16.56**	**3.50**	**4.19**	**12.18**

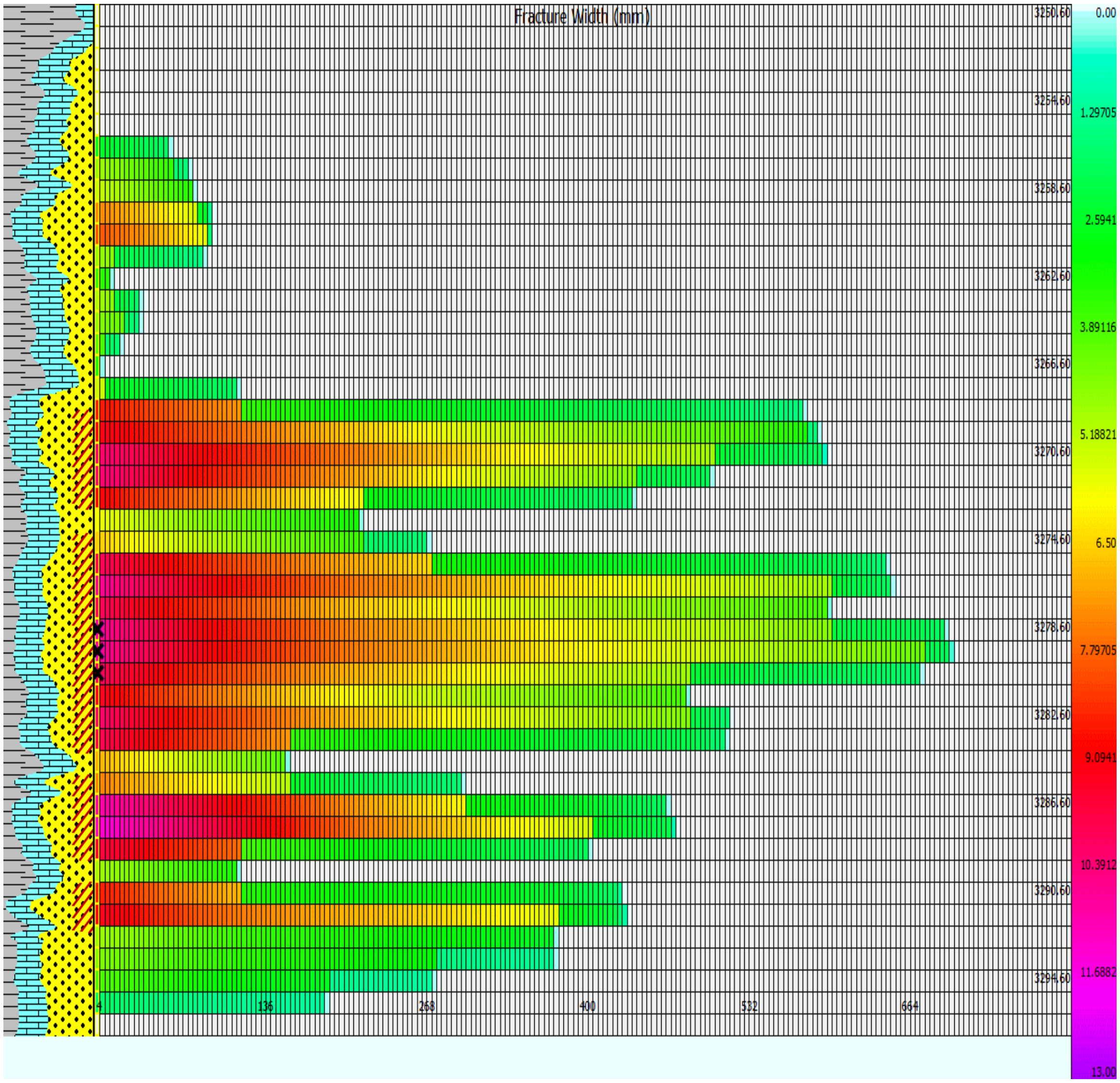

Figure 3-3. Fracture width of slickwater CO2 hybrid

3.3.2 Pure CO2 scenario

Previous section discussed how 100m3 of pure CO2 gave us longer and wider fractures and in this section pumping schedules were modified so all stages were pure CO2. Table 3-3 shows modified pumping schedule.

Table 3-4 shows all fracture parameters created with liquid CO2. CO2 as expected gave the longest average fracture length which his equal to 1311 m comparing to 1113 which is 15% more than slickwater. As discussed earlier one of the issue of CO2 is carrying proppant limitation which showed as 44% decrease in propped fracture length from 126 to 80 m.

Table 3-3. Liquid CO_2 pumping schedule

Stage #	Elapsed Time hh:mm:ss	Stage time mm:ss	Fluid	Proppant	Stage volume m3	Cum. Volume m3	Rate m3/min	Prop. Conc. kg/m3	Cum. Prop. Kg
1	0:00	10:00	HCL 15%	None	30	30	3	0	0
2	10:00	23:20	CO2 liquid	None	70	100	3	0	0
3	33:20	3:13	CO2 liquid	None	45	145	14	0	0
4	36:33	2:55	CO2 liquid	100 Mesh	40	185	14	50	2000
5	39:28	4:02	CO2 liquid	100 Mesh	55	240	14	75	6125
6	43:30	4:27	CO2 liquid	100 Mesh	60	300	14	100	12125
7	47:57	4:43	CO2 liquid	100 Mesh	63	363	14	125	20000
8	52:40	7:21	CO2 liquid	40/70 Badger	100	463	14	75	27500
9	1:00:00	9:16	CO2 liquid	40/70 Badger	125	588	14	100	40000
10	1:09:17	9:08	CO2 liquid	40/70 Badger	122	710	14	125	55250
11	1:18:24	9:04	CO2 liquid	40/70 Badger	120	830	14	150	73250
12	1:27:28	8:23	CO2 liquid	40/70 Badger	110	940	14	175	92500
13	1:35:51	7:41	CO2 liquid	40/70 Badger	100	1040	14	200	112500
14	1:43:32	7:45	CO2 liquid	40/70 Badger	100	1140	14	225	135000
15	1:51:17	3:43	CO2 liquid	40/70 CRC	50	1190	14	100	140000
16	1:55:00	2:51	CO2 liquid	40/70 CRC	38	1228	14	125	144750
17	1:57:51	2:39	CO2 liquid	40/70 CRC	35	1263	14	150	150000
18	2:00:30	4:09	CO2 liquid	None	58.08	1321	14	0	150000
19	2:04:38	10:00	Slickwater	None	0	1321	0	0	150000

Table 3-4. Pure CO2 fracture parameters

Fracture		Gross Frac Length M	Proppant Cutoff Length M	Fracture Height M	Average Proppant Conc. kg/m²	Average Fracture Width mm	Max Fracture Width mm
1	Transverse 6	2306.9	171.3	12.6	9.1	4.9	12.5
	Transverse 5	1001.1	78.7	6.3	2.8	2.6	6.3
	Transverse 4	1719.3	136.3	8.4	6.4	3.8	7.8
	Transverse 3	195.9	15.7	6.3	0.2	1.4	4.6
	Transverse 2	2045.7	148.6	10.5	8.2	4.5	8.9
	Transverse 1	21.8	1.7	2.1	0.5	1.5	1.7
2	Transverse 6	2024.0	145.1	6.3	9.4	4.5	7.8
	Transverse 5	1109.9	87.4	6.3	3.8	2.9	4.6
	Transverse 4	1284.0	101.4	6.3	6.6	3.2	6.4
	Transverse 3	1175.2	92.6	6.3	3.8	2.9	4.6
	Transverse 2	1262.3	99.6	6.3	6.3	3.1	6.4
	Transverse 1	1762.8	125.8	6.3	9.1	4.2	9.2
3	Transverse 6	2089.2	153.8	10.5	8.3	4.7	8.4
	Transverse 5	914.0	71.7	2.1	4.0	2.7	5.3
	Transverse 4	1479.9	117.1	10.5	5.8	3.4	6.5
	Transverse 3	935.8	73.4	2.1	3.5	2.7	4.7
	Transverse 2	1218.7	92.6	2.1	6.2	3.1	6.2
	Transverse 1	1915.2	138.1	2.1	8.5	4.4	8.0
4	Transverse 6	478.8	1.7	0.0	0.0	1.7	1.8
	Transverse 5	2045.7	150.3	10.5	8.0	4.5	8.3
	Transverse 4	1392.8	110.1	8.4	5.1	3.2	6.5
	Transverse 3	957.6	71.7	2.1	3.8	2.7	4.9
	Transverse 2	1392.8	110.1	8.4	4.8	3.2	6.6
	Transverse 1	1784.6	131.1	2.1	7.6	4.2	8.8
5	Transverse 6	2393.9	180.0	16.8	7.6	4.8	10.5
	Transverse 5	761.7	61.2	8.4	0.4	1.7	3.8
	Transverse 4	783.5	62.9	8.4	0.5	1.9	3.7
	Transverse 3	195.9	1.7	0.0	0.0	1.4	1.7
	Transverse 2	174.1	1.7	0.0	0.0	1.3	1.7
	Transverse 1	2285.1	171.3	2.1	6.7	4.7	8.3
6	Transverse 3	2611.6	208.0	21.0	4.3	4.6	8.5
	Transverse 2	892.3	47.2	12.6	0.2	1.6	3.2
	Transverse 1	2067.5	150.3	23.1	11.4	5.1	13.4
7	Transverse 6	2002.2	136.3	14.7	8.7	4.8	13.0
	Transverse 5	1392.8	106.6	12.6	6.7	4.1	14.4
	Transverse 4	1131.7	73.4	6.3	5.5	3.0	8.3
	Transverse 3	1545.2	99.6	6.3	8.5	4.2	11.9
	Transverse 2	195.9	14.0	6.3	1.4	0.9	2.7
	Transverse 1	21.8	1.7	2.1	0.5	1.5	1.7
8	Transverse 6	1806.3	19.2	12.6	29.3	3.7	17.2
	Transverse 5	1175.2	12.2	12.6	31.5	3.6	16.5
	Transverse 4	1153.4	21.0	12.6	25.7	4.1	16.0
	Transverse 3	1284.0	22.7	14.7	30.8	4.6	19.7
	Transverse 2	1088.2	73.4	12.6	12.8	3.9	9.7
	Transverse 1	1588.7	22.7	14.7	27.9	4.6	18.1
9	Transverse 6	1849.9	15.7	14.7	28.7	3.9	17.9
	Transverse 5	1175.2	15.7	14.7	26.7	3.8	15.2
	Transverse 4	1392.8	45.4	14.7	17.7	4.1	17.2
	Transverse 3	1109.9	17.5	12.6	27.7	3.5	15.2
	Transverse 2	1088.2	59.4	14.7	17.1	4.7	10.7
	Transverse 1	1697.5	21.0	21.0	26.2	4.5	16.5
10	Transverse 6	1980.4	127.6	14.7	9.9	4.9	13.3
	Transverse 5	848.8	50.7	4.2	5.6	2.9	9.8
	Transverse 4	174.1	8.7	4.2	2.2	1.4	5.6
	Transverse 3	1501.7	96.1	4.2	7.6	3.6	10.4
	Transverse 2	1066.4	75.2	4.2	6.3	3.0	9.0
	Transverse 1	1784.6	94.4	6.3	11.0	4.3	12.6
Average		**1311.1**	**79.7**	**8.69**	**9.46**	**3.41**	**9.02**

Figure 3-4 shows fracture width and length after hydraulic fracturing was performed with CO_2 as a fracturing fluid. Average fracture width was 3.4 mm comparing to slickwater's 3 mm which was 13% more. Since propped fractures were shorter than slickwater, average proppant concentration was higher per fracture rising up to 9.5 kg/m3 comparing to 2.8 kg/m3 of slickwater. Figure 3-5 shows proppant concentration along the fracture.

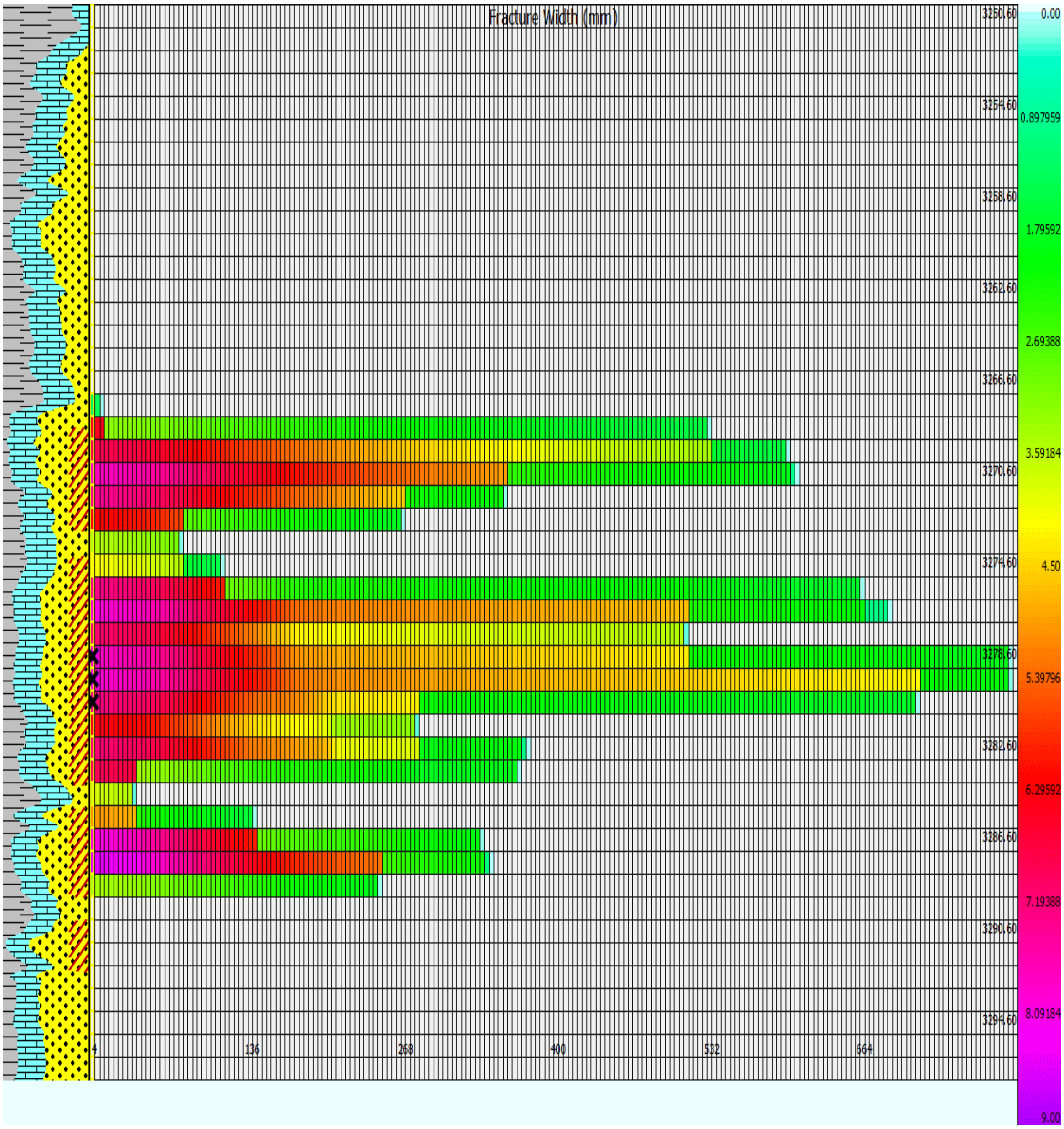

Figure 3-4. Fracture width of pure CO2 model

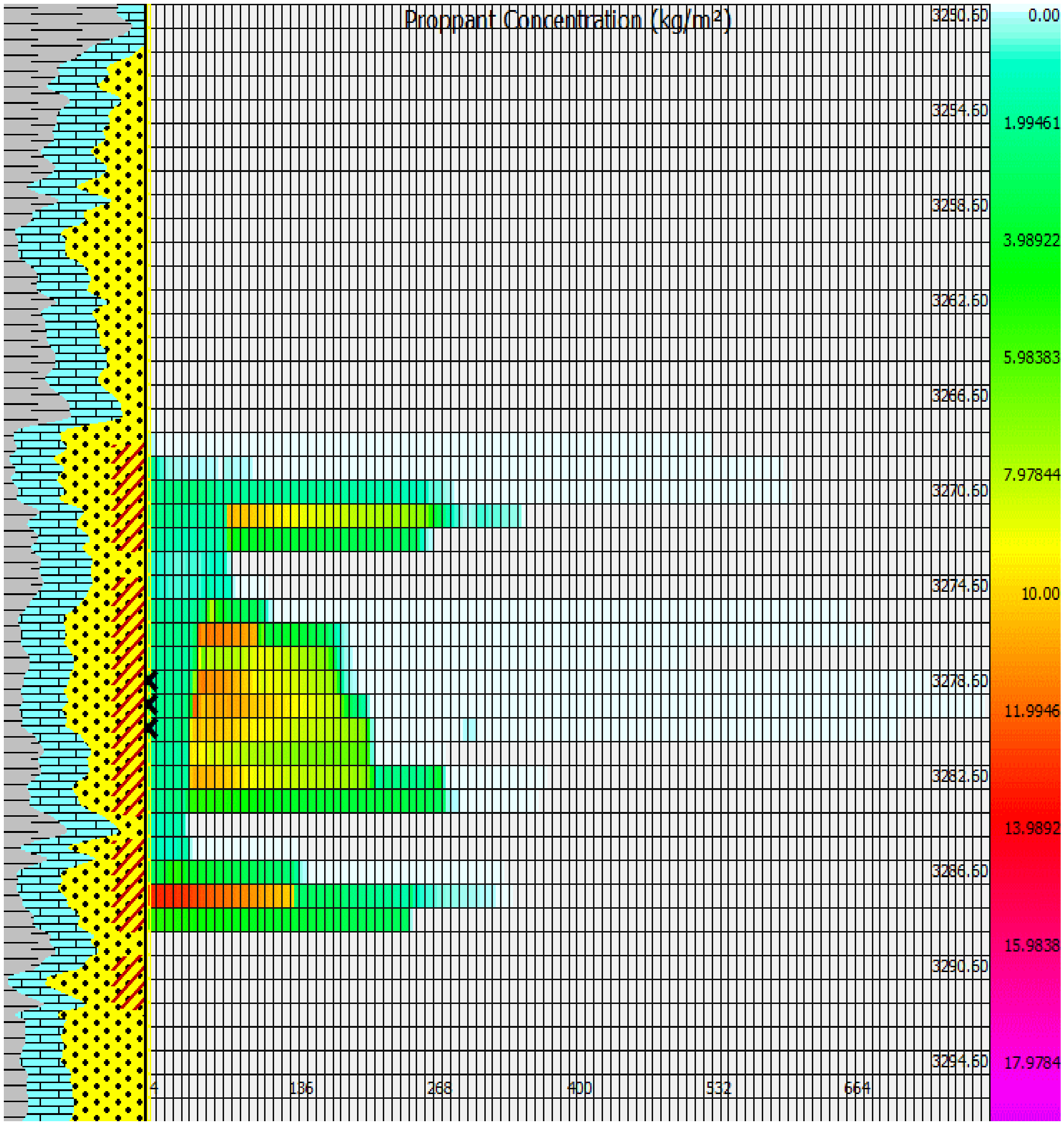

Figure 3-5. Propped fracture length of pure CO2 model

3.3.3 CO2 sensitivity analysis with proppant amount

CO2 has big advantage as non-damaging and fracture length and width increasing fluid, but CO2 has a disadvantage limited proppant carrying capacity due to low viscosity. Sensitivity analysis was conducted with different amount of proppant but the same volume of CO2. Our case analyzed total of 100, 150, 200 and 250 tons of proppant. Figure 3-6 shows gross fracture length for different proppant tonnages. Gross fracture length is stayed constant except little decrease at 200 and 25o tons of proppant.

Next parameter to analyze is length of propped fracture. Figure 3-7 shows how proppant cutoff length reaches maximum of 90 m at 200 tons, but drops 86 m for 250 tons fracture. Figure 3-8 shows that maximum and average fracture width reach maximum of 11 mm and 3.7 mm respectively at 250 tons of proppant.

Moreover simulation results show that pumping schedule can be more optimized by decreasing amount of fluid or increasing maximum proppant concentrations, however it is always good to keep in mind that simulation results may not work with real pumping operations in the field due to equipment, water, types of chemical being pumped and even operator of the equipment.

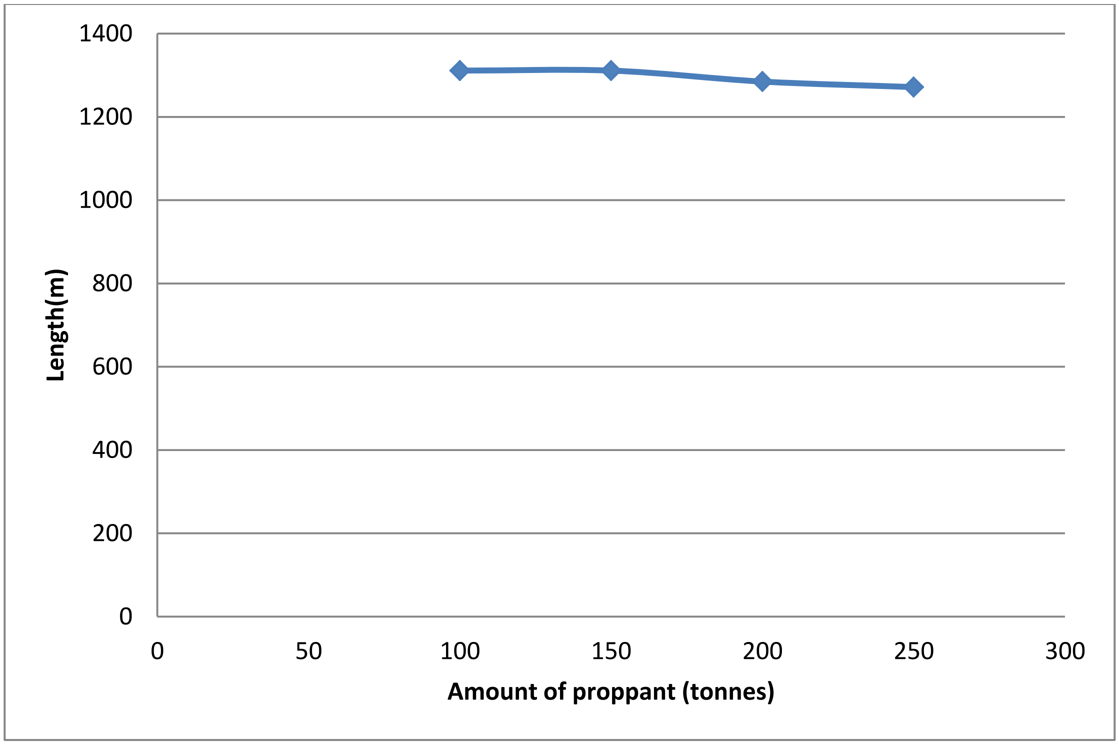

Figure 3-6. Gross fracture length for different proppant tonnage – Pure CO2

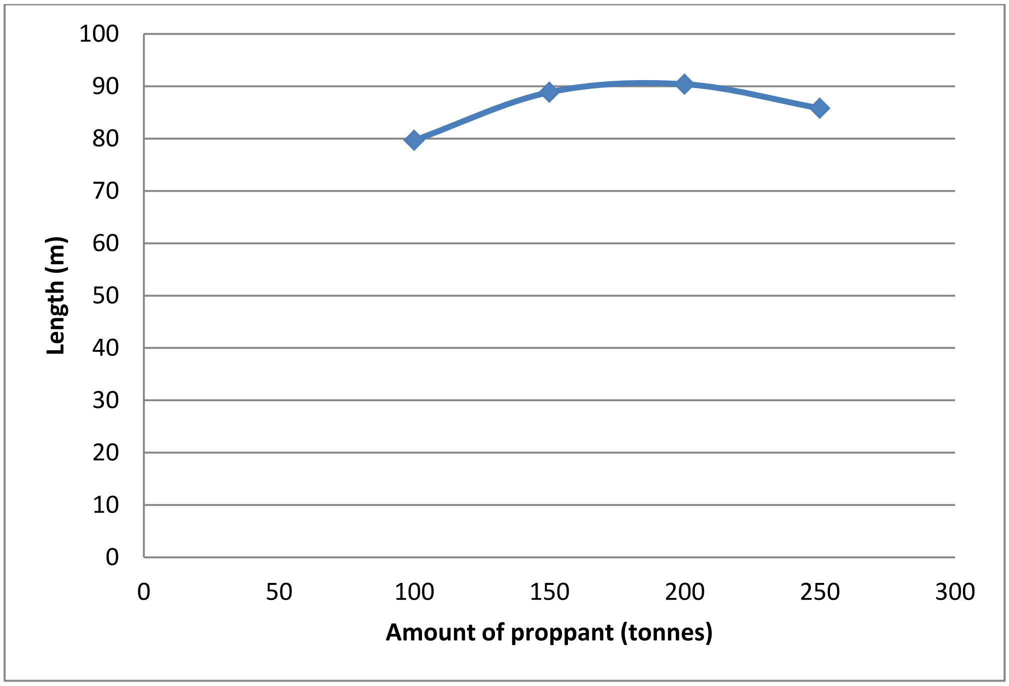

Figure 3-7. Proppant cutoff length for different proppant tonnage – Pure CO2

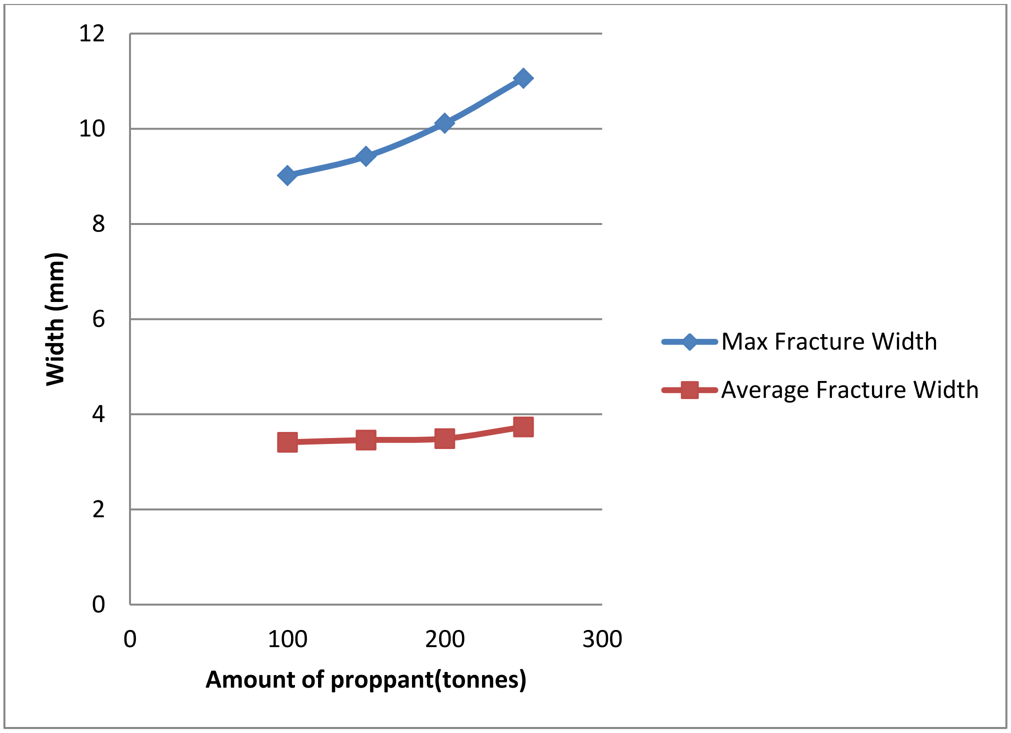

Figure 3-8. Maximum and average fracture width for different proppant tonnage – Pure CO2

3.3.4 Results

In summary, three case scenarios using slickwater, hybrid CO2 and pure CO2 as a fracturing fluid were modeled using GOHFER simulator. Longest fractures were obtained with pure CO2 which due to low viscosity of CO2. Low viscosity helps to enter smaller fractures of rock and connect them, also it helps pressure to be distributed evenly along the fracture. Fluid with low viscosity extended fractures easier. Table 3-5 shows summarized table of all 3 case scenarios with all fracture parameters. Figure 3-9 show how fractures obtained with CO2 were highest but propped fracture length was lowest.

Low viscosity of CO2 affects proppant ability of fracturing fluid to carry the proppant deeper to formation. Table 3-6 shows summarized table of fracture parameters of different proppant amount but the same amount of fluid. As earlier mentioned using CO2 as a fracturing fluid gave the longest fracture but the least propped fracture length. Liquid CO2

Table 3-5. Summary of fracture parameters

Frac. Fluid type	Gross Frac Length.M	Proppant Cutoff Length.M	Fracture Height.M	Average Proppant Conc.kg/m²	Average Fracture Width.mm	Max Fracture Width.mm
Slickwater	1114	126	17	2.8	3.0	7.0
Hybrid	1166	113	17	3.5	4.2	12
Pure CO2	1311	80	8.7	9.5	3.4	9.0

Table 3-6. Fracture parameters for different proppant tonnages – Pure CO_2

Amount of proppant (tonnes)	Gross Frac Length.M	Proppant Cutoff Length.M	Fracture Height. M	Average Proppant Conc.kg/ m^2	Average Fracture Width	Max Fracture Width
250	1272	86	8.7	14.9	3.7	11.0
200	1285	90	8.7	12.7	3.5	10.1
150	1311	89	8.7	11.4	3.5	9.4
100	1311	80	8.7	9.5	3.4	9.0

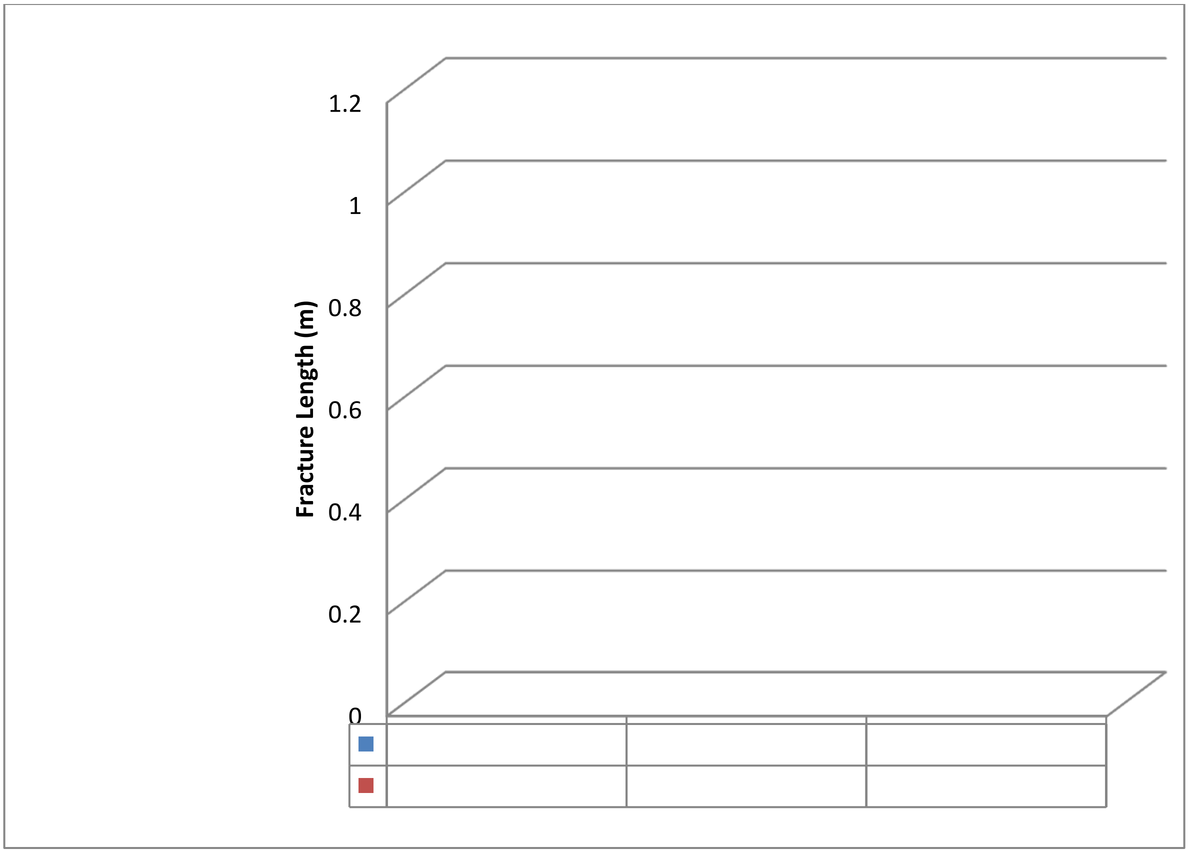

Figure 3-9. Fracture length and propped fracture length of different fluid

3.4 Numerical simulation with CMG

Once GOHFER hydraulic fracture model with pure CO_2 and hybrid CO_2 were created, those models for each 10 stages were imported into the CMG GEM model. Reason for switching from IMEX to GEM was ability of GEM inject CO_2. Model dimensions were the same as slickwater model 3050 x 1050 x 30 m. Reservoir properties were taken from table 2-2 from previous section. CMG model had regular Cartesian grid system which can be discretized into 61*50 m for I direction, 21*50 m for J direction and 1*30 m for K direction as shown in Figure 2-15.

Once fractures were imported to CMG, simulations were run for 3000 days. Figure 3-10 shows cumulative methane production. Methane comparison was chosen in order to eliminate CO_2 that was being produced at the same time. Slickwater case had cumulative production of $1.02\text{x}10^7$ kg of methane, hybrid case had $2.09\text{x}10^7$ kg of methane which is double comparing to slickwater and pure CO_2 case had $4.77\text{x}10^7$ kg of methane which is 4.7 times more than slickwater. This can be explained that water has damaging effect due to high capillary pressure. This proves that using CO_2 as a fracturing fluid proves it is better hydraulic fracturing fluid than slickwater

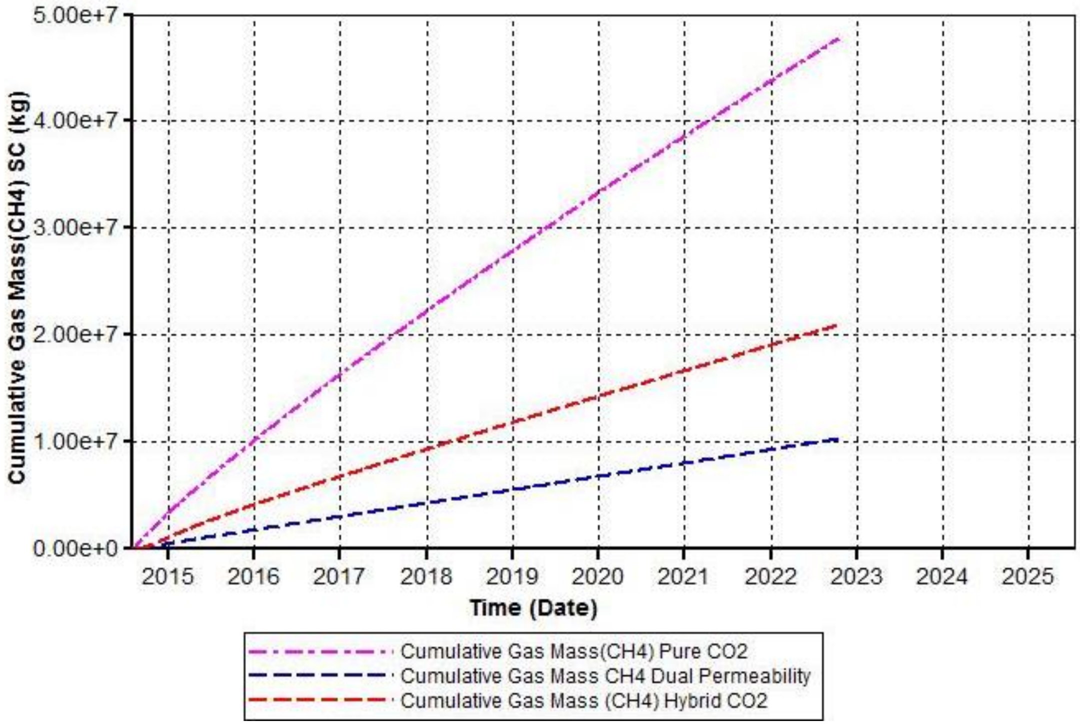

Figure 3-10. Cumulative methane production

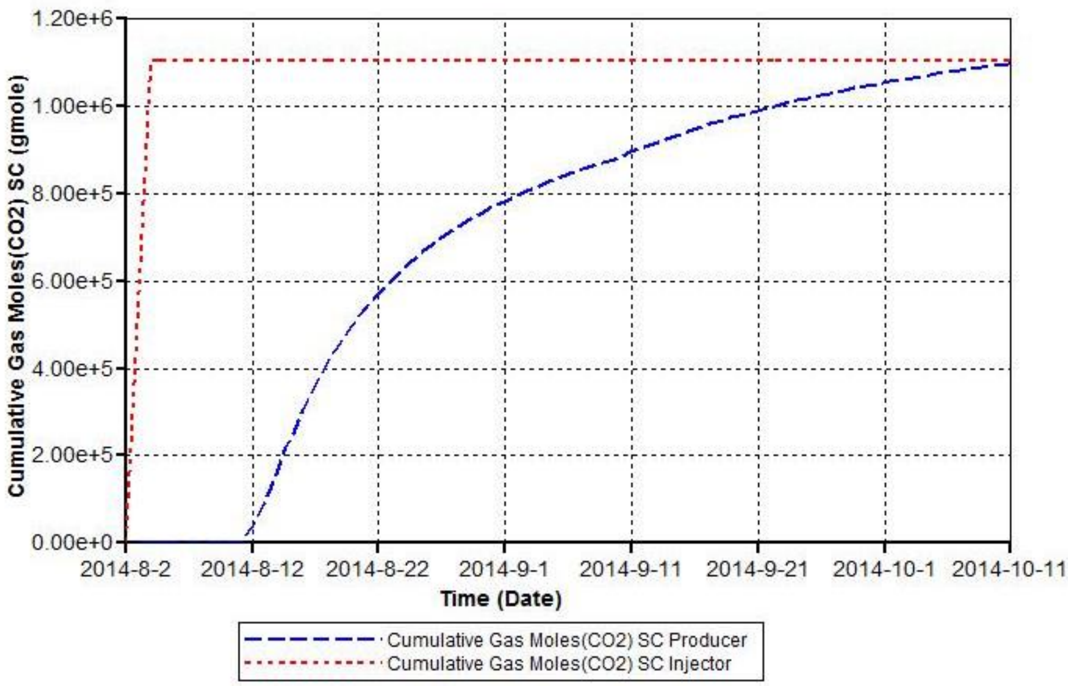

Figure 3-11. CO2 recovery from pure CO2 case

Figure 3-11 shows injected amount of CO_2 and CO_2 production from pure CO_2 case. All CO_2 was recovered from well in 70 days, so it means it can be captured and reused for further fracturing operations. Cryogenic carbon capture technology was developed in 2008 which uses external cooling loop and it can be used at the wellsite to capture CO_2 (Sayre, 2017). Lastly, Figure 3-12 shows water production comparison of slickwater case and hybrid case. Faster water recovery can be explained by CO_2 acting as energizing fluid and helping by pushing water bch to the wellbore.

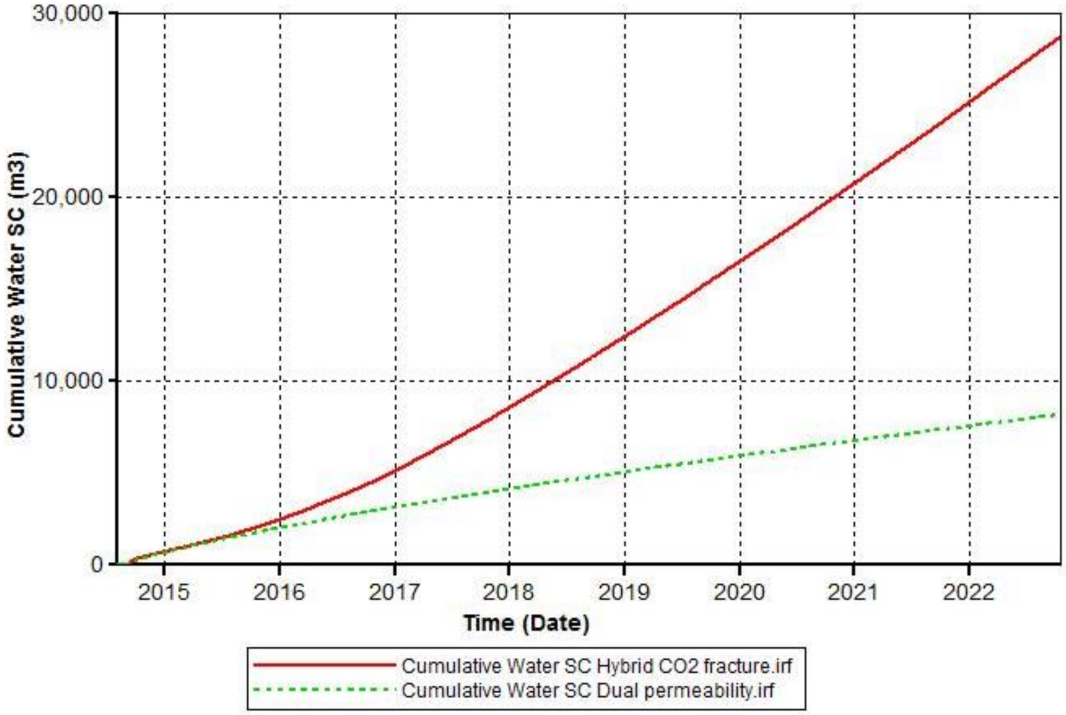

Figure 3-12. Water production comparison

CHAPTER 4: Summary and future work

4.1 Summary of completed research

The major conclusions and findings of this thesis:

(1) Hydraulic fracturing where fracturing fluid was water, water with CO2 pad and CO2 models were created in GOHFER. Hybrid CO2 case's fracture length were longer for 5%, average fracture height remained the same 16.56m, average fracture width increased for 29%, however propped fracture length decreased for 11% comparing to water case. Pure CO2 case gave the longest average fracture length 15% more than slickwater, however there was 44% decrease in propped fracture length due to low viscosity of CO2.

(2) Sensitivity analyses were performed on pure CO2 case with different amount of proppant. By increasing proppant amount, increase in length wasn't achieved, however there was a strong correlation of proppant amount and fracture width. Maximum and average fracture width increased by amount of proppant increase.

(3) Cumulative methane production was compared slickwater case to hybrid and pure CO2 cases and production significantly showed improvement with CO2 cases. Hybrid CO2 case cumulative methane production had 2 times increase in production and pure CO2 had 4.7 times more production comparing to slickwater case.

(4) Cumulative water production was analyzed for slickwater and hybrid CO2 cases. Water recovery of slickwater case is only 50% after 3000 days of production, whereas hybrid CO2 recovered all water after 1800 days.

(5) Lastly CO_2 production from pure CO_2 case was analyzed and all fracturing CO_2 was recovered after 70 days.

4.2 Future work

In this thesis all fracture parameters were obtained are limited to tight gas formation Duvernay. Different formation may result in different results due to different rock properties. Economic analysis weren't performed and methods of CO_2 capture and reuse wasn't part of this thesis.

(1) Investigate the effect of CO_2 as a hydraulic fracturing for other formations of WCSB like Montney and Cardium

(2) CO_2 might affect wettability of rock and it can be researched for further production analysis

(3) Economic analysis can be performed for capturing and reuse of CO_2

List of References

AER (2015). Alberta's Energy Reserves 2014 and Supply/Demand Outlook 2015-2024. Calgary: Alberta Energy Regulator. Retrieved from http://www.aer.ca/documents/sts/ST98/ST98-2015.pdf

AER (2016). Duvernay Reserves and Resources Report: A Comprehensive Analysis of Alberta’s Foremost Liquids-Rich Shale Resource. Retrieved from https://aer.ca/documents/reports/DuvernayReserves_2016.pdf

AER (2017). Hydrocarbon Resource Potential of the Duvernay Formation in Alberta – Update. Retrieved from http://ags.aer.ca/document/OFR/OFR_2017_02.pdf

Alberta Oil & Gas Industry (2017). All About Alberta’s Oil & Gas Industry. Retrieved from http://www.albertacanada.com/files/albertacanada/OilGas_QuarterlyUpdate_Spring2017.pdf

Akuanyionwu, O.C., Elghanduri, K., Mokdad, B. et al. (2012) Examination of Hydraulic Fracture Production Modeling Techniques. Presented at the SPE International Production and Operations Conference & Exhibition, Doha, Qatar, May 14—16, 2012.

Broacha, E. (2009). Conversation, Bill Barrett Corp., November 2009 and January 2010.

Byrnes, P.A., Chesapeake Energy Corp. (2011). Role of Induced and Natural Imbibition in Frac Fluid transport and Fate in Gas Shales. Paper presented at US EPA Conference, Virginia, Arlington, USA, March 28-29.

Chemical disclosure registry (CDR). 2012. What is hydraulic fracturing. Retrieved from http://fracfocus.ca/hydraulic-fracturing-process/what-hydraulic-fracturing

Clifton, R. J., and Abou-Sayed, A.S. (1979). On the computation of three-dimensional geometry of hydraulic fractures. Paper SPE 7943 presented at the Symposium on Low Permeability Gas Reservoirs, Denver, CO, USA, 20-22 May.

Dunn, L., Shmidt, G., Hammermaster, K., Brown, M., Bernard, R., Wen, E., Befus, R., and Gardiner, S. (2012). The Duvernay Formation (Devonian): Sedimentology and Reservoir Characterization of a Shale Gas/Liquids play in Alberta, Canada. Paper 280 presented on GeoConvention, Calgary, AB, Canada, May 14-18.

Economides, M.J., and T. Martin. (2008). Modern Fracturing – Enhancing Natural Gas Production, 1st Edition. Energy Tribune Publishing Inc., January 1.

Ehrl, E. and Schueler, S.K. (2000). Simulation of a Tight-gas Reservoir with

Horizontal Multifractured Wells. Paper SPE 651108-MS presented at the SPE EUROPEC, Paris, October 24-25.

Enick, R.M., Olsen, D.K., et al (2012). Mobility and Conformance Control for CO2 EOR via Thickeners, Foams, and Gels – A Literature Review of 40 Years of Research and Pilot Tests. Paper SPE 154122 presented at the SPE Improved Oil Recovery Symposium, Tulsa, Oklahoma, 14-18 April.

ERCB (2012). Summary of Alberta's Shale- and Siltstone – Hosted hydrocarbon Resource Potential. Retrieved from http://ags.aer.ca/document/OFR/OFR_2012_06.pdf

Fan, L., Thompson, J. W., Robinson, J. R. (2010). Understanding Gas Production Mechanism and Effectiveness of Well Stimulation in the Haynesville Shale Through Reservoir Simulation, SPE paper 136696, presented in Canadian Unconventional Resources and International Petroleum Conference, Calgary, Alberta, Canada.

Fang, C., Chen, W., and Amro, M., TU Bergakademie Freiburg (2014). Simulation Study of Hydraulic Fracturing Using Super Critical CO2 in Shale. Paper SPE 172110-MS presented at the Abu Dabi International Petroleum Exhibition and Conference, Abu Dhabi, UAE, November 10-13.

Farinas, M., and Fonseca, E. (2013). Hydraulic Fracturing Simulation Case Study and Post Frac Analysis in the Haynesville Shale: SPE Paper No 163847, Presented at the SPE Hydraulic Fracturing Technology Conference held in the Woodlands, Texas, USA, 4-6 February.

Gadde, P.b., Liu, Y., et al etc. (2014) Modeling Proppant Settling in Water-Fracs: SPE Paper No 89875, Presented at the SPE Annual Technical Conference and Exhibition held in Houston, Texas, USA, 26-29 September.

Gidley, J.L., Holditch, S.A., Nierode, D.E. et al. (1989). Three-Dimensional Fracture-Propagation Models. In Recent Advances in Hydraulic Fracturing, 12. Chap. 5, 95. Richardson, Texas: Monograph Series, SPE.

Gidley, J.L., Holditch, S.A., Nierode, D.E. et al. (1989). Two-Dimensional Fracture-Propagation Models. In Recent Advances in Hydraulic Fracturing, 12. Chap. 4, 81. Richardson, Texas: Monograph Series, SPE.

Geertsma, J. and Haafkens, R. (1979). Comparison of the theories for predicting width and extent of vertical hydraulically induced fractures. *Journal of Energy Resource Technology* , 101 (1): 8-19.

GEM User's Guide. (2017). Computer Modelling Group Ltd., Calgary, AB, Canada.

Gupta, D.V.S. and Bobier D.M. (1998). The History and Success of Liquid CO2 and CO2/N2 Fracturing System. Paper SPE 40016 presented at the SPE Gas Technology Symposium, Calgary, Canada, 15-18 March.

GOHFER User Manual. (2015). Barree & Associates LLC., Lakewood, CO, USA.

Hadley, G.F., and Handy, L.L. (1956). A Theoretical and Experimental Study of the Steady State Capillary End Effect. Paper SPE 707-G presented at the SPE 31st Annual Meeting, Los Angeles, October 14-17.

Halliburton. (2006). Salt Tolerant, CO2 Compatible and Cold Temperature Capable Fluid System Helps Prevent Clay Swelling and Fines Migration. Retrieved from http://www.halliburton.com/public/pe/contents/Data_sheets/web/H/H05001.pdf

Heffernan, K. (2010). An Overview of Canada's Natural Gas Resources. Canadian Society for Uncoventional Gas. Retrieved from http://www.csug.ca/images/news/2011/Natural_Gas_in_Canada_final.pdf

Hegre, T.M. (1996). Hydraulically Fractured Horizontal Well Stimulaton. Paper SPE 35506 presented at European 3-D Reservoir Modelling Conference, Stavanger, Norway,

IMEX User's Guide. (2017). Computer Modelling Group Ltd., Calgary, AB, Canada.

Karcher, B.J., Giger, F.M., and Combe, J. (1986). Some Practical Formulas to Predict Horizontal Well Behavior. Paper SPE 15430 presented at the SPE Annual Technical Conference and Exhibition, New Orleans, October 5-8.

Ketter, A., Daniels, J., Heinze, J., & Waters, G. (2006). A field study optimizing completion strategies for fracture initiation in Barnett shale horizontal wells. In SPE Annual Technical Conference and Exhibition.

King, G.E. (2010). Thirty years of gas shale fracturing: what have we learned?. In SPE Annual Technical Conference and Exhibition.

King, G. E., & Corporation, A. (2012). SPE 152596 Hydraulic Fracturing 101 : What Every Representative , Environmentalist , Regulator , Reporter , Investor , University Researcher , Neighbor and Engineer Should Know About Estimating Frac Risk and Improving Frac Performance in Unconventional Ga (pp. 1–80).

King, G.R., Haile, L. Shuss, J, Dobkins, T.A. (2008). Increasing Fracture Path Complexity and Controlling Downward Fracture Growth in the Barnett Shale. Paper SPE 119896, Presented at the 2008 SPE Shale Gas Production Conference, Fort Worth, TX, 16-18 November.

Li, J., Hamid, S., and Oneal, D. (2005). Prediction of Tool Erosion in Gravel-Pack and Frack-Pack Applications Using Computational Fluid Dynamics(CFD) Simulation: OTC Paper No 17452, Presented at the 2005 Offshore Technology Conference held in Houston, TX, USA, 2-5 May.

Lillies, A.T. and King S.R. (1982). Sand Fracturing with Liquid Carbon Dioxide. Paper SPE 11341 presented at the SPE Production Technology Symposium, Hobbs, New Mexico, 8-9 November.

Mayerhofer, M.J., Economides, M.J., Nolte, K.G. (1991). An Experimental and Fundamental Interpretation of Filtercake Fracturing Fluid Loss. Paper SPE 22873.

Mazza, R. (2001). Liquid-Free CO2/Sand Stimulations: AN overlooked Technology – Production Update. Paper SPE 72383 presented at the SPE Eastern Regional Meeting, Canton, Ohio, 17-19 October.

Makhanov, K. (2013). An Experimental Study of Spontaneous Imbibition in Horn River Shales. University of Alberta, Edmonton, Alberta, Canada.

Moneim, S.S.A., Rabee, R., Shehata, A.M. et al. (2012) Modeling hydraulic fractures in finite difference simulators using amalgam LGR (Local Grid Refinement). Presented at the North Africa Technical Conference and Exhibition, Cairo, Egypt, February 20—22.

NEB. (2011). Tight Oil Developments in the Western Canada Sedimentary Basin. National Energy Board. Retrieved from https://www.neb-one.gc.ca/nrg/sttstc/crdlndptrlmprdct/rprt/tghtdvlpmntwcsb2011/tghtdvlpmntwcsb2011-eng.pdf

NEB. (2015). Exploitation and Production of Shale and Tight Resources. Retrieved from http://www.nrcan.gc.ca/energy/sources/shale-tight-resources/17677

NEB. (2017). Duvernay Resources Assessment. Retrieved from https://www.neb-one.gc.ca/nrg/sttstc/crdlndptrlmprdct/rprt/2017dvrn/index-eng.html

Patel, P.S., Robart, C.J., Ruegamer. M., and Yang, A. (2014). Analysis of US Hydraulic Fracturing Fluid System and Proppant Trends. Paper SPE 168645 presented at the Hydraulic Fracturing Technology Conference, The Woodlands, Texas, Feb 4-6.

Pope, C.D., Wiles, T.J., and Pierce, B.R. (1987). Curable Resin Coated Sand Control Proppant Flowback. Paper SPE 16209 presented at the SPE Production Operations Symposium, Oklahoma city, March 8-10.

Reynolds, M. M., Bachman, R. C., Reservoir, T., Peters, W. E. (2014). SPE 168632, A

Comparison of the Effectiveness of Various Fracture Fluid Systems Used in Multi-Stage Fractured Horizontal Wells : Montney Formation, Unconventional Gas, (2010), 1–21.

Ribeiro, L.H. and Sharma, M.M. 2013. Fluid selection for Energized Fracture Treatments. Paper SPE 163867 presented at the hydraulic Fracturing Technology Conference, The Woodlnads, Texas, Feb 4-6.

Ribeiro, L.H. (2013). *Design of Energized Hydraulic Fractures.* PhD Dissertation, The University of Texas at Austin, Austin, Texas.

Sayre, A., Frankman, D., Baxter, L.L., Stitt, K. (2017) Field Testing of Cryogenic Carbon Capture. CMTC 486652-MS presented at the Carbon Management Technology Conference held I nHouston ,TX, USA. 17-20 July, 2017.

Settari, A., Bachman, R.C., and Morrison, D.C. (1987). Numerical simulation of hydraulic fracturing treatments with low-viscosity fluids: PETSOC Paper No 87-05-02, *Journal of Canadian Petroleum Technology*, September-October, Montreal.

Shmidt, K. K.(2008). What is Hydraulic Fracturing? ProPublica. Retrieved from https://www.propublica.org/article/hydraulic-fracturing-national

Sinal, M.L. and Lancaster, G. (1987). Liquid CO2 Fracturing: Advantages and

Limitations. J Cdn. Pet. Tech 26(5):26-30.

Smith, B.M. (2016). Fracture Modeling: fracture Models Everywhere – Wat To Do? Presentation presented at SPE Asia Pacific Hydraulic Fracturing Conference, Beijing, China 24-26 August.

STIM-LAB. (2003). Fracturing Fluid Cleanup, July 10-11.

Taylor, R. S., Stobo, B., Niebergall, G., Aguilera, R., Walter, J., Hards, E. (2014). Optimization of Duvernay Fracturing Treatment Design Using Fully Compositional Dual Permeability Numeric Reservoir Simulation. Paper SPE 171602 presented at the SPE/CSUR Unconventional Resources Conferences in Calgary, AB, Canada on 30 September – 2 October, 2014.

Taylor, R., Hards, E., Fyten, G., Hoch, O., Storozhenko, K., Stobo, B., Niebergall, G. (2013). Optimization of Duvernay Fracture Design Workflow. Paper SPE 167238 presented at SPE Unconventional Resources Conference in Calgary 5-6 November.

Tudor, R., Vozniak, C., Peters, W., and Banks, M.-L. (1994). Technical Advances in Liquid CO2 Fracturing. Paper 94-36 presented at the Annual Technical Meeting, Calgary, Canada, June 12-15.

Warren, J.E., and Root, P.J. (1963). The Behaviour of Naturally Fractured Reservoirs, SPE J., 3(3): 245-255. Paper SPE 426-PA.

Appendix A

Fracture geometries generated by GOHFER and imported into CMG

```
RESULTS PLNRTEMPLATE NAME 'Template (F34 - GFrac - Stage 10.cmg)'
RESULTS PLNRTEMPLATE PRIMFRACWIDTH 4
RESULTS PLNRTEMPLATE PRIMFRACPERM 7.24852
RESULTS PLNRTEMPLATE PRIMFRACTIP 0.0724853
RESULTS PLNRTEMPLATE ORIGINALREFINEINTO 5 5 3
RESULTS PLNRTEMPLATE ORIGINALHALFLENGTH 44
RESULTS PLNRTEMPLATE END
*PLNRFRAC_TEMPLATE 'Template (F34 - GFrac - Stage 10.cmg)'
  *PLNR_REFINE *INTO  5 5 3
    *BWHLEN 44
    *JDIR
    *INNERWIDTH 0.6096
    *LAYERSUP 0
    *LAYERSDOWN 0
  *PERMI MATRIX *FZ 47.5625 0.475625
  *PERMJ MATRIX *FZ 47.5625 0.475625
  *PERMK MATRIX *FZ 47.5625 0.475625
*END_TEMPLATE
** Please don't remove these RESULTS PLNRTEMPLATE keywords.
RESULTS PLNRTEMPLATE NAME 'Template (Injector - GFrac - Stage 2.cmg)'
RESULTS PLNRTEMPLATE PRIMFRACWIDTH 4
RESULTS PLNRTEMPLATE PRIMFRACPERM 7.77593
RESULTS PLNRTEMPLATE PRIMFRACTIP 0.0777593
RESULTS PLNRTEMPLATE ORIGINALREFINEINTO 5 5 3
RESULTS PLNRTEMPLATE ORIGINALHALFLENGTH 52
RESULTS PLNRTEMPLATE END
*PLNRFRAC_TEMPLATE 'Template (Injector - GFrac - Stage 2.cmg)'
  *PLNR_REFINE *INTO  5 5 3
    *BWHLEN 52
    *JDIR
    *INNERWIDTH 0.6096
    *LAYERSUP 0
    *LAYERSDOWN 0
  *PERMI MATRIX *FZ 51.0232 0.510232
  *PERMJ MATRIX *FZ 51.0232 0.510232
  *PERMK MATRIX *FZ 51.0232 0.510232
*END_TEMPLATE
** Please don't remove these RESULTS PLNRTEMPLATE keywords.
RESULTS PLNRTEMPLATE NAME 'Template (F34 - GFrac - Stage 2.cmg)'
RESULTS PLNRTEMPLATE PRIMFRACWIDTH 4
RESULTS PLNRTEMPLATE PRIMFRACPERM 7.77593
RESULTS PLNRTEMPLATE PRIMFRACTIP 0.0777593
RESULTS PLNRTEMPLATE ORIGINALREFINEINTO 5 5 3
RESULTS PLNRTEMPLATE ORIGINALHALFLENGTH 52
```

```
RESULTS PLNRTEMPLATE END
*PLNRFRAC_TEMPLATE 'Template (F34 - GFrac - Stage 2.cmg)'
  *PLNR_REFINE *INTO  5 5 3
    *BWHLEN 52
    *JDIR
    *INNERWIDTH 0.6096
    *LAYERSUP 0
    *LAYERSDOWN 0
  *PERMI MATRIX *FZ 51.0232 0.510232
  *PERMJ MATRIX *FZ 51.0232 0.510232
  *PERMK MATRIX *FZ 51.0232 0.510232
*END_TEMPLATE
** Please don't remove these RESULTS PLNRTEMPLATE keywords.
RESULTS PLNRTEMPLATE NAME 'Template (F34 - GFrac - Stage 7.cmg)'
RESULTS PLNRTEMPLATE PRIMFRACWIDTH 4
RESULTS PLNRTEMPLATE PRIMFRACPERM 1.38032
RESULTS PLNRTEMPLATE PRIMFRACTIP 0.0138032
RESULTS PLNRTEMPLATE ORIGINALREFINEINTO 5 5 3
RESULTS PLNRTEMPLATE ORIGINALHALFLENGTH 124
RESULTS PLNRTEMPLATE END
*PLNRFRAC_TEMPLATE 'Template (F34 - GFrac - Stage 7.cmg)'
  *PLNR_REFINE *INTO  5 5 3
    *BWHLEN 124
    *JDIR
    *INNERWIDTH 0.6096
    *LAYERSUP 0
    *LAYERSDOWN 0
  *PERMI MATRIX *FZ 9.05722 0.0905722
  *PERMJ MATRIX *FZ 9.05722 0.0905722
  *PERMK MATRIX *FZ 9.05722 0.0905722
*END_TEMPLATE
** Please don't remove these RESULTS PLNRTEMPLATE keywords.
RESULTS PLNRTEMPLATE NAME 'Template (F34 - GFrac - Stage 8.cmg)'
RESULTS PLNRTEMPLATE PRIMFRACWIDTH 4
RESULTS PLNRTEMPLATE PRIMFRACPERM 10.4257
RESULTS PLNRTEMPLATE PRIMFRACTIP 0.104257
RESULTS PLNRTEMPLATE ORIGINALREFINEINTO 5 5 3
RESULTS PLNRTEMPLATE ORIGINALHALFLENGTH 70
RESULTS PLNRTEMPLATE END
*PLNRFRAC_TEMPLATE 'Template (F34 - GFrac - Stage 8.cmg)'
  *PLNR_REFINE *INTO  5 5 3
    *BWHLEN 70
    *JDIR
    *INNERWIDTH 0.6096
    *LAYERSUP 0
    *LAYERSDOWN 0
  *PERMI MATRIX *FZ 68.4101 0.684101
  *PERMJ MATRIX *FZ 68.4101 0.684101
```

```
  *PERMK MATRIX *FZ 68.4101 0.684101
*END_TEMPLATE
** Please don't remove these RESULTS PLNRTEMPLATE keywords.
RESULTS PLNRTEMPLATE NAME 'Template (F34 - GFrac - Stage 3.cmg)'
RESULTS PLNRTEMPLATE PRIMFRACWIDTH 4
RESULTS PLNRTEMPLATE PRIMFRACPERM 1.54313
RESULTS PLNRTEMPLATE PRIMFRACTIP 0.0154313
RESULTS PLNRTEMPLATE ORIGINALREFINEINTO 5 5 3
RESULTS PLNRTEMPLATE ORIGINALHALFLENGTH 94
RESULTS PLNRTEMPLATE END
*PLNRFRAC_TEMPLATE 'Template (F34 - GFrac - Stage 3.cmg)'
  *PLNR_REFINE *INTO  5 5 3
    *BWHLEN 94
    *JDIR
    *INNERWIDTH 0.6096
    *LAYERSUP 0
    *LAYERSDOWN 0
  *PERMI MATRIX *FZ 10.1255 0.101255
  *PERMJ MATRIX *FZ 10.1255 0.101255
  *PERMK MATRIX *FZ 10.1255 0.101255
*END_TEMPLATE
** Please don't remove these RESULTS PLNRTEMPLATE keywords.
RESULTS PLNRTEMPLATE NAME 'Template (F34 - GFrac - Stage 9.cmg)'
RESULTS PLNRTEMPLATE PRIMFRACWIDTH 4
RESULTS PLNRTEMPLATE PRIMFRACPERM 8.64405
RESULTS PLNRTEMPLATE PRIMFRACTIP 0.0864405
RESULTS PLNRTEMPLATE ORIGINALREFINEINTO 5 5 3
RESULTS PLNRTEMPLATE ORIGINALHALFLENGTH 56
RESULTS PLNRTEMPLATE END
*PLNRFRAC_TEMPLATE 'Template (F34 - GFrac - Stage 9.cmg)'
  *PLNR_REFINE *INTO  5 5 3
    *BWHLEN 56
    *JDIR
    *INNERWIDTH 0.6096
    *LAYERSUP 0
    *LAYERSDOWN 0
  *PERMI MATRIX *FZ 56.7195 0.567195
  *PERMJ MATRIX *FZ 56.7195 0.567195
  *PERMK MATRIX *FZ 56.7195 0.567195
*END_TEMPLATE
** Please don't remove these RESULTS PLNRTEMPLATE keywords.
RESULTS PLNRTEMPLATE NAME 'Template (F34 - GFrac - Stage 4.cmg)'
RESULTS PLNRTEMPLATE PRIMFRACWIDTH 4
RESULTS PLNRTEMPLATE PRIMFRACPERM 1.25642
RESULTS PLNRTEMPLATE PRIMFRACTIP 0.0125642
RESULTS PLNRTEMPLATE ORIGINALREFINEINTO 5 5 3
RESULTS PLNRTEMPLATE ORIGINALHALFLENGTH 100
RESULTS PLNRTEMPLATE END
```

```
*PLNRFRAC_TEMPLATE 'Template (F34 - GFrac - Stage 4.cmg)'
  *PLNR_REFINE *INTO  5 5 3
    *BWHLEN 100
    *JDIR
    *INNERWIDTH 0.6096
    *LAYERSUP 0
    *LAYERSDOWN 0
  *PERMI MATRIX *FZ 8.24423 0.0824423
  *PERMJ MATRIX *FZ 8.24423 0.0824423
  *PERMK MATRIX *FZ 8.24423 0.0824423
*END_TEMPLATE
** Please don't remove these RESULTS PLNRTEMPLATE keywords.
RESULTS PLNRTEMPLATE NAME 'Template (F34 - GFrac - Stage 1 _1 Copy.cmg)'
RESULTS PLNRTEMPLATE PRIMFRACWIDTH 4
RESULTS PLNRTEMPLATE PRIMFRACPERM 11.3378
RESULTS PLNRTEMPLATE PRIMFRACTIP 0.113378
RESULTS PLNRTEMPLATE ORIGINALREFINEINTO 5 5 3
RESULTS PLNRTEMPLATE ORIGINALHALFLENGTH 58
RESULTS PLNRTEMPLATE END
*PLNRFRAC_TEMPLATE 'Template (F34 - GFrac - Stage 1 _1 Copy.cmg)'
  *PLNR_REFINE *INTO  5 5 3
    *BWHLEN 58
    *JDIR
    *INNERWIDTH 0.6096
    *LAYERSUP 0
    *LAYERSDOWN 0
  *PERMI MATRIX *FZ 74.395 0.74395
  *PERMJ MATRIX *FZ 74.395 0.74395
  *PERMK MATRIX *FZ 74.395 0.74395
*END_TEMPLATE
** Please don't remove these RESULTS PLNRTEMPLATE keywords.
RESULTS PLNRTEMPLATE NAME 'Template (F34 - GFrac - Stage 6.cmg)'
RESULTS PLNRTEMPLATE PRIMFRACWIDTH 4
RESULTS PLNRTEMPLATE PRIMFRACPERM 0.979325
RESULTS PLNRTEMPLATE PRIMFRACTIP 0.00979325
RESULTS PLNRTEMPLATE ORIGINALREFINEINTO 5 5 3
RESULTS PLNRTEMPLATE ORIGINALHALFLENGTH 126
RESULTS PLNRTEMPLATE END
*PLNRFRAC_TEMPLATE 'Template (F34 - GFrac - Stage 6.cmg)'
  *PLNR_REFINE *INTO  5 5 3
    *BWHLEN 126
    *JDIR
    *INNERWIDTH 0.6096
    *LAYERSUP 0
    *LAYERSDOWN 0
  *PERMI MATRIX *FZ 6.42602 0.0642602
  *PERMJ MATRIX *FZ 6.42602 0.0642602
  *PERMK MATRIX *FZ 6.42602 0.0642602
```

```
*END_TEMPLATE
** Please don't remove these RESULTS PLNRTEMPLATE keywords.
RESULTS PLNRTEMPLATE NAME 'Template (F34 - GFrac - Stage 5.cmg)'
RESULTS PLNRTEMPLATE PRIMFRACWIDTH 4
RESULTS PLNRTEMPLATE PRIMFRACPERM 0.568468
RESULTS PLNRTEMPLATE PRIMFRACTIP 0.00568468
RESULTS PLNRTEMPLATE ORIGINALREFINEINTO 5 5 3
RESULTS PLNRTEMPLATE ORIGINALHALFLENGTH 150
RESULTS PLNRTEMPLATE END
*PLNRFRAC_TEMPLATE 'Template (F34 - GFrac - Stage 5.cmg)'
  *PLNR_REFINE *INTO  5 5 3
    *BWHLEN 150
    *JDIR
    *INNERWIDTH 0.6096
    *LAYERSUP 0
    *LAYERSDOWN 0
  *PERMI MATRIX *FZ 3.7301 0.037301
  *PERMJ MATRIX *FZ 3.7301 0.037301
  *PERMK MATRIX *FZ 3.7301 0.037301
*END_TEMPLATE
** Please don't remove these RESULTS PLNRTEMPLATE keywords.
RESULTS PLNRTEMPLATE NAME 'Template (Injector - GFrac - Stage 1 _1 Copy.cmg)'
RESULTS PLNRTEMPLATE PRIMFRACWIDTH 4
RESULTS PLNRTEMPLATE PRIMFRACPERM 11.3378
RESULTS PLNRTEMPLATE PRIMFRACTIP 0.113378
RESULTS PLNRTEMPLATE ORIGINALREFINEINTO 5 5 3
RESULTS PLNRTEMPLATE ORIGINALHALFLENGTH 58
RESULTS PLNRTEMPLATE END
*PLNRFRAC_TEMPLATE 'Template (Injector - GFrac - Stage 1 _1 Copy.cmg)'
  *PLNR_REFINE *INTO  5 5 3
    *BWHLEN 58
    *JDIR
    *INNERWIDTH 0.6096
    *LAYERSUP 0
    *LAYERSDOWN 0
  *PERMI MATRIX *FZ 74.395 0.74395
  *PERMJ MATRIX *FZ 74.395 0.74395
  *PERMK MATRIX *FZ 74.395 0.74395
*END_TEMPLATE
** Please don't remove these RESULTS PLNRSTAGE keywords.
RESULTS PLNRSTAGE NAME 'Planar Stage 1'
RESULTS PLNRSTAGE WELL 'Injector'
RESULTS PLNRSTAGE DATE 2014-08-02
RESULTS PLNRSTAGE BASENAME 'Injector - GFrac'
RESULTS PLNRSTAGE FRACS 'Injector - GFrac_1'
RESULTS PLNRSTAGE SLABS '22'
RESULTS PLNRSTAGE PERFOPTION 1
RESULTS PLNRSTAGE LAYERMIN 1
```

```
RESULTS PLNRSTAGE LAYERMAX 1
RESULTS PLNRSTAGE END
*PLNRFRAC 'Template (F34 - GFrac - Stage 1 _1 Copy.cmg)' 13,11,1 *BG_NAME 'Injector - GFrac_1'
** Please don't remove these RESULTS PLNRSTAGE keywords.
RESULTS PLNRSTAGE NAME 'Planar Stage 2'
RESULTS PLNRSTAGE WELL 'Injector'
RESULTS PLNRSTAGE DATE 2014-08-02
RESULTS PLNRSTAGE BASENAME 'Injector - GFrac'
RESULTS PLNRSTAGE FRACS 'Injector - GFrac_2'
RESULTS PLNRSTAGE SLABS '26'
RESULTS PLNRSTAGE PERFOPTION 1
RESULTS PLNRSTAGE LAYERMIN 1
RESULTS PLNRSTAGE LAYERMAX 1
RESULTS PLNRSTAGE END
*PLNRFRAC 'Template (F34 - GFrac - Stage 2.cmg)' 17,11,1 *BG_NAME 'Injector - GFrac_2'
** Please don't remove these RESULTS PLNRSTAGE keywords.
RESULTS PLNRSTAGE NAME 'Planar Stage 3'
RESULTS PLNRSTAGE WELL 'Injector'
RESULTS PLNRSTAGE DATE 2014-08-02
RESULTS PLNRSTAGE BASENAME 'Injector - Frac'
RESULTS PLNRSTAGE FRACS 'Injector - Frac_1'
RESULTS PLNRSTAGE SLABS '30'
RESULTS PLNRSTAGE PERFOPTION 1
RESULTS PLNRSTAGE LAYERMIN 1
RESULTS PLNRSTAGE LAYERMAX 1
RESULTS PLNRSTAGE END
*PLNRFRAC 'Template (F34 - GFrac - Stage 3.cmg)' 21,11,1 *BG_NAME 'Injector - Frac_1'
** Please don't remove these RESULTS PLNRSTAGE keywords.
RESULTS PLNRSTAGE NAME 'Planar Stage 4'
RESULTS PLNRSTAGE WELL 'Injector'
RESULTS PLNRSTAGE DATE 2014-08-02
RESULTS PLNRSTAGE BASENAME 'Injector - Frac'
RESULTS PLNRSTAGE FRACS 'Injector - Frac_2'
RESULTS PLNRSTAGE SLABS '34'
RESULTS PLNRSTAGE PERFOPTION 1
RESULTS PLNRSTAGE LAYERMIN 1
RESULTS PLNRSTAGE LAYERMAX 1
RESULTS PLNRSTAGE END
*PLNRFRAC 'Template (F34 - GFrac - Stage 4.cmg)' 25,11,1 *BG_NAME 'Injector - Frac_2'
** Please don't remove these RESULTS PLNRSTAGE keywords.
RESULTS PLNRSTAGE NAME 'Planar Stage 5'
RESULTS PLNRSTAGE WELL 'Injector'
RESULTS PLNRSTAGE DATE 2014-08-02
RESULTS PLNRSTAGE BASENAME 'Injector - Frac'
RESULTS PLNRSTAGE FRACS 'Injector - Frac_3'
RESULTS PLNRSTAGE SLABS '38'
RESULTS PLNRSTAGE PERFOPTION 1
```

```
RESULTS PLNRSTAGE LAYERMIN 1
RESULTS PLNRSTAGE LAYERMAX 1
RESULTS PLNRSTAGE END
*PLNRFRAC 'Template (F34 - GFrac - Stage 5.cmg)' 29,11,1 *BG_NAME 'Injector - Frac_3'
** Please don't remove these RESULTS PLNRSTAGE keywords.
RESULTS PLNRSTAGE NAME 'Planar Stage 6'
RESULTS PLNRSTAGE WELL 'Injector'
RESULTS PLNRSTAGE DATE 2014-08-02
RESULTS PLNRSTAGE BASENAME 'Injector - Frac'
RESULTS PLNRSTAGE FRACS 'Injector - Frac_4'
RESULTS PLNRSTAGE SLABS '42'
RESULTS PLNRSTAGE PERFOPTION 1
RESULTS PLNRSTAGE LAYERMIN 1
RESULTS PLNRSTAGE LAYERMAX 1
RESULTS PLNRSTAGE END
*PLNRFRAC 'Template (F34 - GFrac - Stage 6.cmg)' 33,11,1 *BG_NAME 'Injector - Frac_4'
** Please don't remove these RESULTS PLNRSTAGE keywords.
RESULTS PLNRSTAGE NAME 'Planar Stage 7'
RESULTS PLNRSTAGE WELL 'Injector'
RESULTS PLNRSTAGE DATE 2014-08-02
RESULTS PLNRSTAGE BASENAME 'Injector - Frac'
RESULTS PLNRSTAGE FRACS 'Injector - Frac_5'
RESULTS PLNRSTAGE SLABS '46'
RESULTS PLNRSTAGE PERFOPTION 1
RESULTS PLNRSTAGE LAYERMIN 1
RESULTS PLNRSTAGE LAYERMAX 1
RESULTS PLNRSTAGE END
*PLNRFRAC 'Template (F34 - GFrac - Stage 7.cmg)' 37,11,1 *BG_NAME 'Injector - Frac_5'
** Please don't remove these RESULTS PLNRSTAGE keywords.
RESULTS PLNRSTAGE NAME 'Planar Stage 8'
RESULTS PLNRSTAGE WELL 'Injector'
RESULTS PLNRSTAGE DATE 2014-08-02
RESULTS PLNRSTAGE BASENAME 'Injector - Frac'
RESULTS PLNRSTAGE FRACS 'Injector - Frac_6'
RESULTS PLNRSTAGE SLABS '50'
RESULTS PLNRSTAGE PERFOPTION 1
RESULTS PLNRSTAGE LAYERMIN 1
RESULTS PLNRSTAGE LAYERMAX 1
RESULTS PLNRSTAGE END
*PLNRFRAC 'Template (F34 - GFrac - Stage 8.cmg)' 41,11,1 *BG_NAME 'Injector - Frac_6'
** Please don't remove these RESULTS PLNRSTAGE keywords.
RESULTS PLNRSTAGE NAME 'Planar Stage 9'
RESULTS PLNRSTAGE WELL 'Injector'
RESULTS PLNRSTAGE DATE 2014-08-02
RESULTS PLNRSTAGE BASENAME 'Injector - Frac'
RESULTS PLNRSTAGE FRACS 'Injector - Frac_7'
RESULTS PLNRSTAGE SLABS '54'
RESULTS PLNRSTAGE PERFOPTION 1
```

```
RESULTS PLNRSTAGE LAYERMIN 1
RESULTS PLNRSTAGE LAYERMAX 1
RESULTS PLNRSTAGE END
*PLNRFRAC 'Template (F34 - GFrac - Stage 9.cmg)' 45,11,1 *BG_NAME 'Injector - Frac_7'
** Please don't remove these RESULTS PLNRSTAGE keywords.
RESULTS PLNRSTAGE NAME 'Planar Stage 10'
RESULTS PLNRSTAGE WELL 'Injector'
RESULTS PLNRSTAGE DATE 2014-08-02
RESULTS PLNRSTAGE BASENAME 'Injector - Frac'
RESULTS PLNRSTAGE FRACS 'Injector - Frac_8'
RESULTS PLNRSTAGE SLABS '58'
RESULTS PLNRSTAGE PERFOPTION 1
RESULTS PLNRSTAGE LAYERMIN 1
RESULTS PLNRSTAGE LAYERMAX 1
RESULTS PLNRSTAGE END
*PLNRFRAC 'Template (F34 - GFrac - Stage 10.cmg)' 49,11,1 *BG_NAME 'Injector - Frac_8'
```

Appendix B

Fracture geometries generated by GOHFER for different proppant amount for Pure CO_2:

a) 150 tons of proppant

Fracture		Gross Frac Length.M	Proppant Cutoff Length.M	Fracture Height.M	Average Proppant Conc.kg/m²	Average Fracture Width.mm	Max Fracture Width.mm
1	Transverse 6	2306.9	191.1	12.6	11.0	5.0	13.1
	Transverse 5	1001.1	87.7	6.3	3.4	2.7	6.5
	Transverse 4	1719.3	152.1	8.4	7.8	3.8	8.1
	Transverse 3	195.9	17.5	6.3	0.2	1.4	4.8
	Transverse 2	2045.7	165.7	10.5	9.9	4.5	9.3
	Transverse 1	21.8	1.9	2.1	0.6	1.5	1.7
2	Transverse 6	2024.0	161.8	6.3	11.4	4.5	8.2
	Transverse 5	1109.9	97.5	6.3	4.7	3.0	4.8
	Transverse 4	1284.0	113.1	6.3	8.0	3.3	6.7
	Transverse 3	1175.2	103.3	6.3	4.6	3.0	4.8
	Transverse 2	1262.3	111.1	6.3	7.6	3.2	6.6
	Transverse 1	1762.8	140.4	6.3	11.0	4.2	9.6
3	Transverse 6	2089.2	171.6	10.5	10.0	4.7	8.8
	Transverse 5	914.0	79.9	2.1	4.8	2.7	5.5
	Transverse 4	1479.9	130.6	10.5	7.0	3.4	6.8
	Transverse 3	935.8	81.9	2.1	4.3	2.7	4.9
	Transverse 2	1218.7	103.3	2.1	7.5	3.2	6.4
	Transverse 1	1915.2	154.0	2.1	10.2	4.5	8.3
4	Transverse 6	478.8	1.9	0.0	0.0	1.7	1.9
	Transverse 5	2045.7	167.7	10.5	9.7	4.5	8.7
	Transverse 4	1392.8	122.8	8.4	6.2	3.2	6.8
	Transverse 3	957.6	79.9	2.1	4.6	2.8	5.2
	Transverse 2	1392.8	122.8	8.4	5.9	3.3	6.8
	Transverse 1	1784.6	146.2	2.1	9.2	4.2	9.2
5	Transverse 6	2393.9	200.8	16.8	9.2	4.9	11.0
	Transverse 5	761.7	68.2	8.4	0.5	1.7	4.0
	Transverse 4	783.5	70.2	8.4	0.6	1.9	3.9
	Transverse 3	195.9	1.9	0.0	0.0	1.4	1.7
	Transverse 2	174.1	1.9	0.0	0.0	1.3	1.7
	Transverse 1	2285.1	191.1	2.1	8.1	4.8	8.7
6	Transverse 3	2611.6	232.0	21.0	5.2	4.6	8.9
	Transverse 2	892.3	52.6	12.6	0.3	1.7	3.3
	Transverse 1	2067.5	167.7	23.1	13.8	5.1	14.0
7	Transverse 6	2002.2	152.1	14.7	10.6	4.9	13.6
	Transverse 5	1392.8	118.9	12.6	8.1	4.1	15.0
	Transverse 4	1131.7	81.9	6.3	6.6	3.0	8.7
	Transverse 3	1545.2	111.1	6.3	10.3	4.2	12.5
	Transverse 2	195.9	15.6	6.3	1.7	0.9	2.8
	Transverse 1	21.8	1.9	2.1	0.6	1.5	1.7
8	Transverse 6	1806.3	21.4	12.6	35.5	3.7	18.0
	Transverse 5	1175.2	13.6	12.6	38.1	3.6	17.2
	Transverse 4	1153.4	23.4	12.6	31.1	4.1	16.7
	Transverse 3	1284.0	25.3	14.7	37.3	4.7	20.6
	Transverse 2	1088.2	81.9	12.6	15.5	3.9	10.2
	Transverse 1	1588.7	25.3	14.7	33.7	4.6	18.9
9	Transverse 6	1849.9	17.5	14.7	34.7	3.9	18.7
	Transverse 5	1175.2	17.5	14.7	32.4	3.8	15.9
	Transverse 4	1392.8	50.7	14.7	21.4	4.2	18.0
	Transverse 3	1109.9	19.5	12.6	33.5	3.6	15.9
	Transverse 2	1088.2	66.3	14.7	20.7	4.7	11.2
	Transverse 1	1697.5	23.4	21.0	31.7	4.6	17.2
10	Transverse 6	1980.4	142.3	14.7	12.0	4.9	13.9
	Transverse 5	848.8	56.5	4.2	6.7	3.0	10.3
	Transverse 4	174.1	9.7	4.2	2.7	1.4	5.9
	Transverse 3	1501.7	107.2	4.2	9.2	3.6	10.9
	Transverse 2	1066.4	83.8	4.2	7.6	3.1	9.4
	Transverse 1	1784.6	105.3	6.3	13.3	4.4	13.1
Average		1311.1	88.9	8.69	11.44	3.46	9.42

b) 200 tons of proppant

Fracture		Gross Frac Length.M	Proppant Cutoff Length.M	Fracture Height.M	Average Proppant Conc.kg/m²	Average Fracture Width.mm	Max Fracture Width.mm
1	Transverse 6	2260.5	194.4	12.6	12.2	5.0	14.0
	Transverse 5	981.0	89.2	6.3	3.7	2.7	7.0
	Transverse 4	1684.7	154.7	8.4	8.6	3.9	8.7
	Transverse 3	191.9	17.8	6.3	0.3	1.4	5.1
	Transverse 2	2004.6	168.6	10.5	10.9	4.6	10.0
	Transverse 1	21.3	2.0	2.1	0.7	1.5	1.9
2	Transverse 6	1983.3	164.6	6.3	12.7	4.6	8.8
	Transverse 5	1087.6	99.2	6.3	5.2	3.0	5.1
	Transverse 4	1258.2	115.0	6.3	8.9	3.3	7.2
	Transverse 3	1151.6	105.1	6.3	5.1	3.0	5.1
	Transverse 2	1236.9	113.0	6.3	8.4	3.2	7.1
	Transverse 1	1727.4	142.8	6.3	12.1	4.3	10.3
3	Transverse 6	2047.2	174.5	10.5	11.1	4.8	9.4
	Transverse 5	895.7	81.3	2.1	5.3	2.7	5.9
	Transverse 4	1450.1	132.9	10.5	7.8	3.5	7.3
	Transverse 3	917.0	83.3	2.1	4.7	2.7	5.2
	Transverse 2	1194.2	105.1	2.1	8.3	3.2	6.9
	Transverse 1	1876.7	156.7	2.1	11.3	4.5	9.0
4	Transverse 6	469.2	2.0	0.0	0.0	1.7	2.1
	Transverse 5	2004.6	170.6	10.5	10.7	4.6	9.3
	Transverse 4	1364.8	124.9	8.4	6.8	3.2	7.3
	Transverse 3	938.3	81.3	2.1	5.1	2.8	5.5
	Transverse 2	1364.8	124.9	8.4	6.5	3.3	7.4
	Transverse 1	1748.7	148.7	2.1	10.2	4.2	9.9
5	Transverse 6	2345.8	204.3	16.8	10.2	4.9	11.8
	Transverse 5	746.4	69.4	8.4	0.6	1.8	4.3
	Transverse 4	767.7	71.4	8.4	0.7	2.0	4.2
	Transverse 3	191.9	2.0	0.0	0.0	1.4	1.9
	Transverse 2	170.6	2.0	0.0	0.0	1.3	1.9
	Transverse 1	2239.2	194.4	2.1	8.9	4.9	9.3
6	Transverse 3	2559.1	236.0	21.0	5.8	4.7	9.6
	Transverse 2	874.3	53.5	12.6	0.3	1.7	3.5
	Transverse 1	2025.9	170.6	23.1	15.2	5.2	15.0
7	Transverse 6	1962.0	154.7	14.7	11.7	5.0	14.6
	Transverse 5	1364.8	121.0	12.6	9.0	4.2	16.1
	Transverse 4	1108.9	83.3	6.3	7.4	3.1	9.3
	Transverse 3	1514.1	113.0	6.3	11.5	4.3	13.4
	Transverse 2	191.9	15.9	6.3	1.9	0.9	3.0
	Transverse 1	21.3	2.0	2.1	0.7	1.5	1.9
8	Transverse 6	1770.0	21.8	12.6	39.3	3.8	19.3
	Transverse 5	1151.6	13.9	12.6	42.2	3.7	18.5
	Transverse 4	1130.3	23.8	12.6	34.4	4.1	17.9
	Transverse 3	1258.2	25.8	14.7	41.3	4.7	22.1
	Transverse 2	1066.3	83.3	12.6	17.2	4.0	10.9
	Transverse 1	1556.8	25.8	14.7	37.4	4.7	20.3
9	Transverse 6	1812.7	17.8	14.7	38.4	3.9	20.1
	Transverse 5	1151.6	17.8	14.7	35.8	3.9	17.1
	Transverse 4	1364.8	51.6	14.7	23.6	4.2	19.3
	Transverse 3	1087.6	19.8	12.6	37.1	3.6	17.0
	Transverse 2	1066.3	67.4	14.7	22.9	4.8	12.0
	Transverse 1	1663.4	23.8	21.0	35.1	4.6	18.5
10	Transverse 6	1940.6	144.8	14.7	13.3	5.0	14.9
	Transverse 5	831.7	57.5	4.2	7.4	3.0	11.0
	Transverse 4	170.6	9.9	4.2	2.9	1.4	6.3
	Transverse 3	1471.5	109.1	4.2	10.2	3.7	11.7
	Transverse 2	1045.0	85.3	4.2	8.4	3.1	10.1
	Transverse 1	1748.7	107.1	6.3	14.8	4.4	14.1
Average		1284.8	90.4	8.69	12.67	3.49	10.12

c) 250 tons of proppant

Fracture		Gross Frac Length.M	Proppant Cutoff Length.M	Fracture Height.M	Average Proppant Conc.kg/m²	Average Fracture Width.mm	Max Fracture Width.mm
1	Transverse 6	2237.3	184.5	12.6	14.3	5.4	15.4
	Transverse 5	970.9	84.7	6.3	4.4	2.9	7.7
	Transverse 4	1667.5	146.8	8.4	10.1	4.1	9.5
	Transverse 3	190.0	16.9	6.3	0.3	1.5	5.6
	Transverse 2	1984.1	160.0	10.5	12.8	4.9	10.9
	Transverse 1	21.1	1.9	2.1	0.8	1.7	2.0
2	Transverse 6	1962.9	156.2	6.3	14.9	4.9	9.6
	Transverse 5	1076.5	94.1	6.3	6.0	3.2	5.6
	Transverse 4	1245.3	109.2	6.3	10.4	3.5	7.9
	Transverse 3	1139.8	99.8	6.3	5.9	3.2	5.6
	Transverse 2	1224.2	107.3	6.3	9.8	3.4	7.8
	Transverse 1	1709.7	135.5	6.3	14.2	4.6	11.2
3	Transverse 6	2026.3	165.6	10.5	13.0	5.1	10.3
	Transverse 5	886.5	77.2	2.1	6.2	2.9	6.4
	Transverse 4	1435.3	126.1	10.5	9.1	3.7	8.0
	Transverse 3	907.6	79.1	2.1	5.6	2.9	5.7
	Transverse 2	1182.0	99.8	2.1	9.7	3.4	7.5
	Transverse 1	1857.4	148.7	2.1	13.3	4.9	9.8
4	Transverse 6	464.4	1.9	0.0	0.0	1.8	2.2
	Transverse 5	1984.1	161.9	10.5	12.6	4.9	10.2
	Transverse 4	1350.8	118.6	8.4	8.0	3.5	7.9
	Transverse 3	928.7	77.2	2.1	6.0	3.0	6.1
	Transverse 2	1350.8	118.6	8.4	7.6	3.5	8.0
	Transverse 1	1730.8	141.2	2.1	12.0	4.5	10.8
5	Transverse 6	2321.8	193.9	16.8	12.0	5.2	12.9
	Transverse 5	738.7	65.9	8.4	0.7	1.9	4.6
	Transverse 4	759.8	67.8	8.4	0.8	2.1	4.6
	Transverse 3	190.0	1.9	0.0	0.0	1.5	2.0
	Transverse 2	168.9	1.9	0.0	0.0	1.4	2.0
	Transverse 1	2216.2	184.5	2.1	10.5	5.2	10.2
6	Transverse 3	2532.8	224.0	21.0	6.8	5.0	10.5
	Transverse 2	865.4	50.8	12.6	0.3	1.8	3.9
	Transverse 1	2005.2	161.9	23.1	17.9	5.5	16.4
7	Transverse 6	1941.8	146.8	14.7	13.7	5.3	16.0
	Transverse 5	1350.8	114.8	12.6	10.5	4.5	17.6
	Transverse 4	1097.6	79.1	6.3	8.6	3.3	10.2
	Transverse 3	1498.6	107.3	6.3	13.4	4.6	14.6
	Transverse 2	190.0	15.1	6.3	2.2	1.0	3.3
	Transverse 1	21.1	1.9	2.1	0.8	1.7	2.0
8	Transverse 6	1751.9	20.7	12.6	46.1	4.0	21.1
	Transverse 5	1139.8	13.2	12.6	49.5	3.9	20.2
	Transverse 4	1118.7	22.6	12.6	40.3	4.4	19.6
	Transverse 3	1245.3	24.5	14.7	48.4	5.1	24.2
	Transverse 2	1055.3	79.1	12.6	20.2	4.2	11.9
	Transverse 1	1540.8	24.5	14.7	43.8	5.0	22.2
9	Transverse 6	1794.1	16.9	14.7	45.1	4.2	22.0
	Transverse 5	1139.8	16.9	14.7	42.0	4.1	18.7
	Transverse 4	1350.8	48.9	14.7	27.7	4.5	21.1
	Transverse 3	1076.5	18.8	12.6	43.6	3.9	18.6
	Transverse 2	1055.3	64.0	14.7	26.8	5.1	13.1
	Transverse 1	1646.3	22.6	21.0	41.2	4.9	20.2
10	Transverse 6	1920.7	137.4	14.7	15.6	5.3	16.3
	Transverse 5	823.2	54.6	4.2	8.7	3.2	12.1
	Transverse 4	168.9	9.4	4.2	3.5	1.5	6.9
	Transverse 3	1456.4	103.5	4.2	11.9	3.9	12.8
	Transverse 2	1034.2	80.9	4.2	9.9	3.3	11.0
	Transverse 1	1730.8	101.6	6.3	17.3	4.7	15.4
Average		1271.6	85.8	8.69	14.86	3.73	11.06